# Using Surfactants to Remobilize the Interface of a Rising Bubble A Theoretical and Experimental Study

**By**

**Ashish Taneja**

A Dissertation Submitted to the Graduate Faculty in Engineering in Partial Fulfillment of the Requirements for the Degree of Doctor of Philosophy
The City University of New York
2007



ProQuest Information and Learning Company
300 North Zeeb Road
P.O. Box 1346
Ann Arbor, MI 48106-1346

This manuscript has been read and accepted for the Graduate Faculty in Engineering in satisfaction of the dissertation requirement for the degree of Doctor of Philosophy.

Charles Maldarelli

Date: Chair of Examining Committee

Mumtaz K. Kassir

Date: Executive Officer

Alexander Couzis

Demetrios T. Papageorgiou

Morton Denn

Jeffrey Morris

Supervisory Committee

THE CITY UNIVERSITY OF NEW YORK

# ABSTRACT

## Using Surfactants to Remobilize the Interface of a Rising Bubble

## A Theoretical and Experimental Study

By

Ashish Taneja

Advisor: Professor Charles Maldarelli

Generally surfactants retard the terminal velocity and interfacial mobility of rising bubbles. Only remobilizing surfactants do not retard the motion and in this work, we studied the physicochemical regimes in which they do not retard the motion.

In the first regime, we study experimentally surfactants with rapid kinetic exchange which remain in monomeric form at high concentrations. At high bulk concentrations, the adsorption saturates causing the surface concentration distribution to become uniform and the Marangoni retarding force to tend to zero. The remobilizing surfactants chosen are intermediate chain length alcohols. We measure the rise velocity of nitrogen bubbles rising in either water or a 70:30 mixture of glycerol-water, each with dissolved alcohol. For the glycerol/water system rise velocities are reduced relative to bubble motion in water, and the kinetic desorption rate is of the order of or larger than the convective rate. Partial remobilization was observed. In the water system with dissolved alcohols, we find that the large velocities and hence greater convective rates do not permit remobilization due to a kinetic barrier.

In the second regime, we study theoretically remobilization for the case in which the remobilizing surfactant forms micellar aggregates at high concentrations. For bulk concentrations far from the bubble just below the critical concentration for aggregate formation (CMC), a micelle zone appears at the rear end of the bubble due to the elevated surfactant concentrations in the sublayer of liquid next to the bubble. We assume that the exchange of surfactant between micelle and monomer is infinitely fast relative to convective and diffusive rates so that the monomer concentration remains at the CMC. We also assume, as the case for a remobilizing surfactant, that the kinetic exchange is fast relative to surface convection. Hence the sublayer concentration of monomer in the micelle zone is constant, maintaining a uniform surface concentration along the interface adjoining the micelle-zone and is unretarded. As the bulk concentration exceeds the CMC, a micelle free zone appears at the front end of the bubble, and only this part of the surface remains retarded. We obtain numerical hydrodynamic solutions for this micelle-facilitated remobilization for a bubble translating with zero inertia and up to order one rates of diffusion in the bulk relative to convection.

# ACKNOWLEDGEMENTS

I take this opportunity to express my deepest appreciation to my advisors Professor Charles Maldarelli and Professor Demetrios Papageorgiou, who not only provided me with the resources and but also shared with me their invaluable insight and intuition, which helped me in my research. I was lucky, to have advisors like them. They were willing to spend countless hours working with me. They were hard when they needed to be and supportive when I needed it the most. Without their guidance, I would not have been able to clear many of the obstacles in my research.

I thank Professor Alexander Couzis also, who helped me a lot in my research. I thank him from my heart for all he did for me. He was a source of inspiration for some of the things that I did during my doctoral dissertation.

I would also like to thank my parents and my family for their love, support and their faith in me, which helped me in completing my PhD.

My thanks all goes to all my friends which helped me in my graduate study, with a special mention of John Singh, Rajesh Goyal and Andy Eng.

# CONTENTS

# List of Tables

# List of Figures

# CHAPTER 1

# Introduction

## 1.1 BACKGROUND

The motion of a bubble moving in a continuous phase can be retarded by the presence of surfactants dissolved in the liquid phase. The surfactants adsorb to the interface of the translating bubble and change the mobility of the interface. The interfacial mobility can range from complete stagnation to stress free motion. We begin by first describing qualitatively how the adsorption of surfactants onto the bubble interface alters the interfacial mobility in order to introduce the problems to be addressed in this thesis.

The adsorption of surfactant molecules onto a bubble interface changes the surface mobility as a result of gradients in the surface concentration which develop because of the convective flux of the surfactant along the surface. To understand this mechanism, consider first adsorption of surfactant onto an interface in the absence of bulk motion from a solution with bulk concentration $C_b$. When an air or vapor interface is created in a surfactant solution, surfactant initially adsorbs onto the interface from the sublayer of liquid near the surface by the process of kinetic adsorption (Figure 1.1, shown for a planar interface). Kinetic adsorption reduces the sublayer concentration relative to the bulk, creating a diffusive flux to the sublayer matching the kinetic adsorption. As the surface concentration increases, surfactant begins to desorbs from the surface and back into the sublayer, In general the net kinetic flux j is a function of the surface concentration $\Gamma$ and sublayer concentrations, $C_s$ i.e. $j(C_s,\Gamma)$. At a large enough surface concentration, an equilibrium is reached in which the adsorption rate is balanced by the desorption rate and the diffusive gradient disappears (Figure 1.1). A surface concentration $\Gamma_e$ in

equilibrium with the bulk concentration $C_b$ is achieved, and is described by the adsorption isotherm, $\Gamma_e(C_b)$ where $j(C_b,\Gamma_e)=0$. At dilute concentrations, the adsorption is linear, while as the bulk concentration increases, the equilibrium surface concentration also increases until the surface begins to saturate due to molecular crowding and approaches the maximum packing concentration $\Gamma_\infty$ (Fig 1.2). The linear adsorption at low bulk concentrations is given by $\Gamma_e = K\Gamma_\infty C_b$, where K is a Henry's law constant. The adsorption constant K can be used to scale the bulk concentration by defining a nondimensional concentration $k = KC_b$. The nondimensional adsorption isotherm can be formulated as $\frac{\Gamma_e}{\Gamma_\infty} = f(k)$, where as $k \to 0$, $f(k) \to k$.

The parameter K describes the surface activity, the larger K the more surface active the species. At high enough concentrations, $k \gg 1$, near the saturation, $f(k) \to 1$, the surfactant forms aggregates (micelles) in the bulk. The concentration at which this occurs is the critical micelle concentration ($C_{CMC}$). For concentrations larger than this value, the surface concentration no longer changes with bulk concentration ($\Gamma_e = \Gamma_{CMC} < \Gamma_\infty$), as surfactant added to the system is incorporated into the aggregates. The nondimensional critical micelle concentration is denoted as $k_{emc}=KC_{CMC}$. Surfactants which do not form micelles have an upper limit to solubility; for concentrations larger than this limit, large domains of insoluble surfactant form and the tension and surface concentration do not change with concentration.

The equilibrium adsorption reduces the surface tension of the interface from the clean value $\gamma_c$ as described by the equation of state $\gamma(\Gamma_e)$. The Gibbs-Duhem equation $d\gamma = -RT\Gamma_e(C_b)d\ln C_b$ provides a relationship between the bulk (or surface) concentration and the tension at equilibrium; in the regime of linear adsorption $\gamma(\Gamma_e) = \gamma_c - RT\Gamma_e;\quad \gamma(C_b) = \gamma_c - RT\Gamma_\infty KC_b$ the tension reduction is linear in the adsorption.

As the surface concentration increases, the tension reduction becomes larger and diverges at the maximum packing concentration. Adsorption models (Langmuir, Frumkin, etc.) provide explicit expressions for the kinetic fluxes, the adsorption isotherm and equation of state. Measurement of the equilibrium tension as a function of concentration, when compared to the predictions of theory for a particular model, provide values for the equilibrium model constants. The introductory analysis presented here however is independent of the adsorption model details, and their description is described in the individual analysis in the following chapters.

Consider next the case (Figure 1.3) of a bubble of radius *a* formed in a surfactant solution with an initially clean interface and with the bulk concentration of surfactant maintained at some value $C_o$ far from the bubble. The surface concentration in equilibrium with this farfield value is $\Gamma_o$. As the bubble begins to move with constant velocity U, surfactant adsorbs from the sublayer adjacent to the surface onto the bubble interface. This initially reduces the sublayer concentration uniformally around the bubble surface, and surfactant diffuses from the bulk to the bubble sublayer. Surfactant adsorbed onto the surface is convected to the stagnation pole at the bubble's trailing edge, where it accumulates and begins to desorb. The desorption eventually raises the sublayer concentration at the back end to values larger than the far field, and surfactant diffuses from the back sublayer into the bulk. A steady state (Figure 1.4) is eventually reached where at the front end the sublayer concentration ($C_f$) is less than the far field value $C_o$ by a value $\Delta C$ (>0), and surfactant steadily diffuses to the front end from the far field. The diffusion towards the bubble interface is balanced by kinetic adsorption at the front end. These rates are in turn balanced by convection along the bubble surface to the back end. At the back, the convection is balanced by desorption which in turn is balanced by diffusion back into the bulk from the sublayer whose concentration is larger than the far field value. Since the net flux of surfactant to

the bubble surface is equal to zero at steady state the concentration at the back end, $C_b$ is of order $C_o+\Delta C$ larger than $C_0$. Since at the front surfactant adsorbs to the surface from a sublayer whose concentration is less than the far field value, and at the back surfactant desorbs to a sublayer of concentration larger than the far field value, the surface concentration at the back is larger than that at the front. Thus while the average surface concentration is the value in equilibrium with $C_0$, i.e. $\Gamma_o$, the front end has a surface concentration $\Gamma_f = \Gamma_o - \Delta\Gamma$ ($\Delta\Gamma>0$) which is smaller than $\Gamma_o$, and the back end has a surface concentration $\Gamma_b = \Gamma_o + \Delta\Gamma$ larger than $\Gamma_o$ (Figure 1.2). Since the surface tension is a decreasing function of concentration of adsorbed surfactant, lower tensions develop in the regions where the surface flow converges and surfactant accumulates. The interface pulls towards areas of the interface with higher tensions, exerting a Marangoni stress that retards the surface flow (Figure 1.3). This mechanism of retardation was first recognized by [Frumkin & Levich (1947)].

The diffusive and kinetic transport rates of surfactant between the bulk and the surface, together with the Marangoni force, set the interfacial velocity and thereby the drag exerted by the continuous phase on the bubble surface. The balance of kinetic and diffusive fluxes at the interface assuming small departures from equilibrium to obtain scaling behavior is given by:

$$D\frac{\Delta C}{a} = -\left[\left[\frac{\partial j}{\partial \Gamma}\right]_{C_0,\Gamma_0}\Delta\Gamma - \left[\frac{\partial j}{\partial \Gamma}\right]_{C_0,\Gamma_0}\left[\frac{d\Gamma_e}{dC_b}\right]_{C_{0,}\Gamma_0}\Delta C\right]. \qquad (1.1)$$

In the above D is the diffusion coefficient of the surfactant and the diffusion length scale is taken as the bubble radius *a*; when convection effects dominate diffusion in the bulk and boundary layers develop the diffusion length scale can be changed accordingly. Solving for the sublayer concentration difference in terms of the surface concentration difference we obtain:

$$\frac{\Delta C}{C_0} = \frac{BiPe(f(k)/(k\chi))}{1 + BiPe(f'(k)/(\chi))}\frac{\Delta\Gamma}{\Gamma_0} \tag{1.2}$$

$$Bi' = -\left[\frac{\partial j}{\partial \Gamma}\right]_{C_0,\Gamma_0}\frac{a}{U} \tag{1.3}$$

where $Pe = \frac{Ua}{D}$, $\chi = \frac{a}{K\Gamma_\infty}$, $\frac{\Gamma_0}{\Gamma_\infty} = f(k)$ and $k = KC_0$. The Biot number, Bi', is the characteristic rate of desorption of surfactant off of the surface $-\left[\frac{\partial \mathrm{j}}{\partial \Gamma}\right]_{C_0,\Gamma_0} \mathrm{a}^2\Gamma_0$, to the rate of convection of surfactant along the surface $a\Gamma_o U_s$. The Peclet number, Pe, is the ratio of convective to diffusion rates of surfactant in the bulk. Equating the above diffusive and convective rates to the rate of surface convection, provides a scale for the interfacial velocity $U_s$.

$$aU_S\Gamma_0 = a^2\left[\frac{D\Delta C}{a}\right] \tag{1.4}$$

$$\frac{U}{U_S} = \left[\frac{\chi k}{Pe}\right]\left[\frac{1}{f(k)}\right]\left[\frac{\Delta C}{C_0}\right] \tag{1.5}$$

which, combining with the above, yields:

$$\frac{U}{U_S} = \left\{\frac{1}{\frac{1}{Bi} + \frac{Pef'(k)}{\chi}}\right\}\left[\frac{\Delta\Gamma}{\Gamma_0}\right] \tag{1.6}$$

The viscous drag exerted on the bubble surface, scaled as $\mu\frac{U - U_s}{a}$ (where μ is the viscosity of the continuous phase) is equated to the Marangoni force to obtain an expression for the interfacial velocity:

$$\mu\frac{U}{a}\left[1 - \frac{U_S}{U}\right] = \frac{1}{a}\left[-\frac{\partial\gamma}{\partial\Gamma}\right]_{\Gamma_0}\Delta\Gamma \tag{1.7}$$

$$\left[1-\frac{U_S}{U}\right]=Ma\left[\frac{f(k)}{RT\Gamma_\infty}\right]\left[-\frac{\partial\gamma}{\partial\Gamma}\right]_{\Gamma_0}\frac{\Delta\Gamma}{\Gamma_0} \tag{1.8}$$

$$1=\frac{U_S}{U}+Ma\left[-\frac{1}{RT}\frac{\partial\gamma}{\partial\Gamma}\right]_{\Gamma_0}\frac{\Delta\Gamma}{\Gamma_0}=\frac{U_S}{U_0}\left[1+Ma\left[-\frac{1}{RT}\frac{\partial\gamma}{\partial\Gamma}\right]_{\Gamma_0}\left\{\frac{1}{BI}+\frac{Pef'(k)}{\chi}\right\}\right] \tag{1.9}$$

$$\frac{U_S}{U}=\frac{1}{\left[1+Ma\left[-\frac{1}{RT}\frac{\partial\gamma}{\partial\Gamma}\right]_{\Gamma_0}\left[\frac{1}{Bi'}+\frac{Pef'(k)}{\chi}\right]\right]} \tag{1.10}$$

The Marangoni number Ma=$\frac{RT\Gamma_0}{\mu U}$, scales the ratio of the magnitudes of surface stresses due to tension gradients along the surface arising from surface concentration differences to viscous shear stresses exerted by the continuous phase on the interface. The latter equation demonstrates clearly that the retardation in surface velocity arises from kinetic $\frac{1}{Bi'}$ and diffusion $\frac{Pef'(k)}{\chi}$ barriers, and is proportional to the Marangoni number.

The above equation provides a uniform framework for interpreting the Marangoni retardation, and defining the scope of this work. The table below provides details on the magnitudes of the surfactant parameters, and typical values for the flow parameters and nondimensional groups. These values are for buoyancy and thermocapillary driven motions in aqueous phases as Marangoni retardation in these contexts provide the motivation for this study (see below). In the table, the surface activity parameter K and the maximum packing concentration $\Gamma_\infty$ are obtained from equilibrium tension measurements of the tension as a function of bulk concentration by fitting these measurements using a Langmuir adsorption isotherm. Values of the diffusion coefficients are obtained from dynamic tension measurements as surfactant equilibrates on a surface and the diffusion coefficient is inferred from the solution

of mass transfer models, or directly from light scattering or pulsed field gradient NMR measurements (see Chang and Frances, 1995).

| Flow | D x$10^6$ $cm^2$/sec | a cm | K $cm^3$/mole | $\Gamma_\infty$ x$10^{10}$ mole/$cm^2$ | U (cm/sec) | $\chi$ | Pe | Ma | $k_{cmc}$ |
|---|---|---|---|---|---|---|---|---|---|
| Buoyancy | 2-6 | $10^{-3}$-$10^{-1}$ | $10^3$-$10^{12}$ | 1-7 | $10^{-2}$-10 | $10^{-5}$ -$10^5$ | 10-$10^6$ | 1-$10^2$ | $10^2$-$10^3$ |
| Thermo-capillarity | 2-6 | $10^{-3}$-$10^{-1}$ | $10^3$-$10^{12}$ | 1-7 | $10^{-3}$-$10^{-1}$ | $10^{-5}$ -$10^5$ | 1-$10^4$ | 1-$10^3$ | $10^2$-$10^3$ |

From the table it is evident that Peclet numbers are typically large, as is usual for diffusion and convection in liquids, although for thermocapillary flows the values are not as large as for buoyancy driven motions. The surfactant parameters K and $\chi$ vary widely; the smallest values in the table arise for the most surface active species such as long hydrocarbon chain surfactants (which are nearly insoluble) and the largest values are for less surface active species such as very short chain alcohols. The nondimensional concentration at the CMC varies only within order of magnitude, primarily because as the surface activity increases, the surfactant is more hydrophobic and its critical micelle concentration decreases. Thus the nondimensionalization normalizes the large variations in CMC concentrations which are usually observed.

Most of the research (as outlined in the following chapter) on surfactant retardation in the motion of bubbles has focused on the regime in which the surfactant is present in the bulk in very dilute amounts, k<<1. In this limit, the surface velocity is given as

$$\frac{U_s}{U} = \frac{1}{\left[1 + Ma\left[\frac{1}{Bi'} + \frac{Pe}{\chi}\right]\right]} \tag{1.11}$$

Even in the absence of kinetic barriers, and for surfactants that are of average or above average surface activity (Table 1, $10^{-5} < \chi < 10^{o}$), because the Peclet number are typically large, $Pe / \chi$ is much greater than one and the interfacial velocity is near zero. Hence in the dilute limit the interface is immobile and the studies which have focused on this dilute limit have studied this complete stagnation. Some studies have examined the case of k of order one, where the same considerations apply as $f'(k)$ is of order one and the interface is immobile or partially mobile. This thesis will focus on the *remobilization regime*, in which at high concentrations the saturation in the adsorption relaxes the Marangoni stress and the interfacial mobility is restored.

## 1.2 SCOPE OF STUDY

This thesis is concerned with the remobilization limit, a regime in which even in the presence of appreciable surfactant adsorption, the bubble interface can remain stress-free. From the scaling expression given above, it is clear that to realize this situation, firstly, the kinetic barriers to transport have to be removed, i.e. the rate of desorption of surfactant must be larger than the rate of surface convection of surfactant along the interface ($Bi' >> 1$). Secondly, the diffusive barriers have to be eliminated. These barriers can be removed under conditions in which the farfield bulk concentration $C_o$ is large enough, i.e k>>1. When k>>1, the dependence of the equilibrium surface concentration on the bulk concentration saturates, $f'(k) \to 0, \quad k >> 1$. Physically, the concentration differences between the sublayer and the bulk phase can be sustained while still maintaining a large convective surface velocity because the surface concentration difference is negligibe from the top to the bottom of the bubble as a result of the saturation. Mathematically, the criteria for remobilization is k large enough such that:

$$Ma\left[-\frac{1}{RT}\frac{\partial\gamma}{\partial\Gamma}\right]_{\Gamma_0}\left[\frac{1}{Bi'}\right]<<1 \tag{1.12}$$

$$Ma\left[-\frac{1}{RT}\frac{\partial\gamma}{\partial\Gamma}\right]_{\Gamma_0}\left[\frac{Pef'(k)}{\chi}\right]<<1 \tag{1.13}$$

The importance of this regime lies not only in the fact that the regime provides a means for making translating bubble interfaces which have been retarded by surfactant adsorption mobile again. In addition, by varying the bulk concentration of surfactant up to the remobilization concentrations, the mobility of the interface can be systematically varied from immobile to stress free. The ability to "dial-up" the interfacial mobility has broad technological applications as we explain below.

Theoretical and experimental studies of the remobilization regime in the surfactant retardation of bubble motion have been few. We outline the literature in the following chapter, and provide a few notes here. In an early work, not connected with bubble motion, Lucassen *et al* were the first one to show experimentally that by increasing the bulk concentration of surfactant, bulk diffusion can be made to outscale surface convection and render an interface uniformly populated with surfactants. They studied the effect of surfactants on the propagation of longitudinal surface waves, which were created at the gas/liquid interface of a liquid film placed in a Langmuir trough by the in-surface periodic oscillations of opposing barriers positioned on the surface. This causes the periodic expansion and contraction of the surface ($\Delta A/A$). The bulk soluble surfactant present in the liquid film adsorbs onto the surface, and the periodic area change causes the surfactant to, alternately desorb and diffuse away from the surface or adsorb and diffuse towards the surface. The periodic oscillation in the surface concentration ($\Delta\Gamma$) causes an oscillation in the surface tension ($\Delta\gamma$). The periodic change in surface tension with change in area can be expressed as complex surface elasticity or modulus,$\varepsilon'=\partial\gamma/\partial\ln A$. They found that, for

a fixed oscillation frequency, as the bulk concentration is increased the surface elasticity goes through a maximum and then tends to zero. They argued that at these concentrations the kinetic exchange and bulk diffusion are fast enough to outscale surface convection and hence uniform surfactant concentration is established at the oscillating interface, which results in modulus to be zero. Another important result from their study was that uniform surface concentrations can be achieved at bulk concentrations above the critical aggregate concentration.

With regard to the remobilization regime in bubble motion, Wang *et al*. [Wang, Papageorgiou, & Maldarelli (1999 & 2001)] studied the case of a bubble moving in a surfactant solution for creeping and order one Reynolds number flows. They obtained numerical solutions for the drag, assuming that the kinetic exchange was infinite, for increasing bulk concentrations of surfactant and demonstrated that as k becomes large enough that the remobilization criteria is satisfied, the interface of the bubble does remobilize.

Experimental verification of the remobilization of an interface under the above criteria was first demonstrated by Stebe *et al* [Stebe, Lin & Maldarelli (1991&1994)]. These authors studied a three-phase periodic slug flow in a capillary tube in which a train of alternating air and aqueous segments containing surfactant Triton X-100 and Brij 35, move in a Teflon tube whose inner surface has been coated with a film of fluorocarbon oil. When the interface of these bubbles is immobile, the pressure gradient required to drive the slug train at a constant velocity is found to be higher than for a mobile interface. They found that at low concentrations of surfactant the pressure required to drive the slugs at constant velocity increases with increase in concentration. However at very high concentrations, above the critical micelle concentrations, the pressure relaxes, indicating remobilization.

Palaparthi *et al* [Palaparthi (2001)] designed a set of experiments to verify remobilization for bubbles rising in a continuous phase. The terminal velocity was measured for nitrogen bubbles rising in a glycerol-water mixture in the presence of the polyethoxylated surfactant surfactant $C_{10}E_{8,}$ dissolved in the bulk phase. The terminal velocity was measured as a function of the bulk concentration, Palaparthi *et al* observed that for the surfactant used, the remobilization criteria could not be satisfied because micelles began to form at a concentration for which the parameter $\left[-\frac{1}{RT}\frac{\partial\gamma}{\partial\Gamma}\right]_{\Gamma_0}\frac{Pef'(k)}{\chi} << 1$. When this parameter is order one. Palaparthi *et al* found that for increasing surfactant concentrations above the CAC, the interface did remobilize (the terminal velocity increased) suggesting, as with Stebe *et al* that micelles offer a route towards remobilization.

The above studies of remobilization have left open two important issues, whose solutions are the major objectives of this thesis.

i. An experimental validation of remobilization, for surfactant transport below the critical micelle concentration, has yet to be demonstrated. Our objective is to identify a surfactant system which can remobilize the interface of a moving bubble for concentrations below the critical micelle concentration in accordance with the criteria presented above and the theoretical frame work presented in Figure 1.4. This study is presented in Chapter 3 of this thesis.

ii. A theoretical explanation and model of the remobilization of a translating bubble interface above the CMC as observed by Stebe *et al* and Palaparthi *et al* has not been developed. Our objective is to formulate a theory for micellar remobilization, and determine the conditions at which the surface becomes remobilized. This study is presented in Chapter 4 of this thesis.

## 1.3 MOTIVATION

Understanding remobilization provides an avenue for using surfactants to control precisely interfacial mobility from stagnant to completely mobile, and as such has broad technological applications Three particular applications which provide the motivation for our research are the reduction in thermocapillary migration of bubbles and drops in a microgravity environment [Kim & Subramanian (1989a&b)], the reduction in interphase mass transfer efficiency in drop-wise or bubble-wise extraction [Elzinga & Banchero (1961)] & [Beitel & Heideger (1971)] and the stability of foams and emulsion [Nikolov & Wasan (1995)]. We review these below.

### Thermocapillary Migration

Fluid material processing in microgravity environment has applications in making high quality crystals, optical fibers and superconductive materials. Microgravity processes must rely on mechanisms other than buoyancy to move bubbles or droplets from one region to another in a continuous liquid phase. One suggested method is thermocapillary migration in which a temperature gradient is applied to the continuous phase, it causes the bubbles to migrate, mostly in the direction of increasing temperature (Figure 1.5). This migration is based on the change in surface tension with temperature. When a fluid particle contacts this gradient, one pole of the particle becomes warmer than the opposing pole. The interfacial tension between the drop or bubble phase and the continuous phase usually decreases with temperature. Thus the cooler pole is of higher interfacial tension than the warmer pole, and the interface is tugged in the direction of the cooler end. This thermocapillary or thermally induced Marangoni surface stress induces a

shear in the external fluid, propelling the fluid particle in the direction of the warmer fluid. (For a general discussion of thermocapillary driven motions of fluid particles and their relevance to microgravity processes, see for example the review article by Subramanian et al [Subramanian, Chhabra & DeKee (1992)]). The migrations of these translating bubbles and drops can be significantly retarded by the adsorption onto the fluid particle surface of surface active impurities dissolved in the continuous or (if the particle is a liquid) droplet phases [Kim & Subramanian (1989a&b)]. This arrests the thermocapillary migration and hampers the efficiency of the process, as the bubbles or drops present in the system are not removed from the system efficiently.

Most experimental evidence in tests both on earth and under microgravity conditions indicate that it is difficult to achieve significant thermocapillary migrations in agreement with the Young et al value, and many studies have attributed the reduced migrations to the retarding effect of surfactant impurities unavoidably present in the bulk phases (see for example Papazian and Wilcox [Papazia & Wilcox (1978)] and Nallani and Subramanian [Nallini & Subramanian (1993)]. In addition, Barton and Subramanian [Barton & Subramanian (1989)] demonstrated directly the retardation by the intentional addition of surfactant to a liquid phase in which droplets were moving by thermocapillarity. To date the problem of retardation of thermocapillary driven particle motion due to surfactant impurities remains unresolved. Significant thermocapillary motions can only be achieved in systems in which extreme precautions have been taken to remove impurities (as, for example, in Barton and Subramanian, experiments using ethyl salicylate drops in ethylene glycol, or in systems in which the fluid particle surface energy is low enough that surfactant impurities do not adsorb appreciably at the

interface (see Merritt and Subramanian [Merritt & Subramanian(1988)] for the migration of gas bubbles in silicone oil).

Remobilizing surfactants can be used to remove the retarding effect of a surfactant impurity on the thermocapillary migration. The adsoption of a remobilizing surfactant outscales the adsorption of the impurity since the remobilizing surfactant is present at very high concentrations. In effect the remobilizing surfactant maintains interfacial mobility and protects the interface from the unwanted adsorption of impurities.

## Efficiency of Bubble-wise or Drop-wise Extraction Processes

The reduced interfacial mobility is known to affect the inter phase mass transport processes too (refer Figure 1.5). Consider the case of a removal of ammonia from a mixture of ammonia and air by sparging the mixture through water. In particular we consider the simple case of a single bubble of air/ammonia mixture rising in water and ammonia dissolving in it simultaneously. Consider a bubble of radius $10^{-1}$cm, rising at a velocity of the order of 10 cm $s^{-1}$. The diffusion coefficients of gases in the liquids are of the order of $10^{-5}$ $cm^2s^{-1}$, thus the Peclet numbers will be of the order of $10^5$. At these high Peclet numbers, the mass transfer boundary layer surrounding the bubble has a thickness which scales as $aPe^{-1/2}$, assuming the bubble surface is stress free. But, because of the presence of surface active impurities, the bubble surface may get partially or completely immobilized. These impurities form a stagnant-cap on the surface, giving a no-slip condition on the surface. In which case, the mass transfer boundary layer surrounding the bubble has a thickness which scales as $aPe^{-1/3}$. For a Peclet number of $10^5$, this thickness is one order of magnitude larger and hence increases the resistance to mass transfer by one order of magnitude and thus reduces the coefficient of mass transfer.

Some examples of the reduction in interphase mass transfer are as follows. Mass transfer coefficient for gas–liquid mass transfer between a bubble and surrounding liquid, for a bubble with totally mobile interface, can be given by Higbie's equation [Bird et al (2001)]:

$$k_L^{mobile} = 1.13\sqrt{\frac{u}{d}}D^{1/2} \tag{1.14}$$

where $d$ is the bubble diameter, $u$ is the bubble–liquid relative velocity (slip velocity) and $D$ is the diffusivity. Lower values of mass transfer coefficient occur for a bubble with a totally rigid surface, for which its value may be predicted using an equation proposed by [Frössling (1938)] from the laminar boundary layer theory:

$$k_L^{rigid} = c\sqrt{\frac{u}{d}}D^{2/3}\nu^{-1/6} \tag{1.15}$$

where $c \approx 0.6$ and $\nu$ is the kinematic viscosity of the liquid.

Remobilizing surfactants added to the continuous phase can potentially increase the interphase transfer by increasing the mobility. The adsorbed monolayer can also potentially retard the interphase transfer by providing a physical obstacle to mass transfer of solute. However, the nature of the remobilized interface is such that the monolayer is mobile and in a liquid state, rather than immobile and condensed. Consequently the interphase transport of species should not be significantly retarded.

## Lifetime of Foams and Emulsions

A foam or an emulsion consists of bubbles or droplets dispersed in high volume fractions in a continuous phase. In the initial stages of foam or bubble breakdown, two drops or bubbles approach each other as a liquid film of the continuous phase between the liquid phase drains

down. The lifetime of the foam depends on the resistance provided to the two approaching drops or bubbles.

Consider two approaching bubbles in a foam, separated by a thin liquid lamella, as presented in figure 1.6. As the two bubbles approach and drains the liquid between the bubbles, the surfactants present on the interface of these bubbles are swept to the back-end of the approaching bubbles. This creates a surfactant concentration gradient on the surface of the bubble, which immobilizes the interface of the bubbles. When the interface of these bubbles is immobile the drainage of the liquid is slow and hence the film thins slowly as compared to when the interface is stress free. When the thickness of these films is less than 1000 $A^{o}$, less electric repulsion between interfaces and Van der Waal's interaction effects the final stages of drainage and determine whether the foam remains or ruptures A key thing to note is that the foams are generally unstable, but the time scale of the rupture of these films is different. The dispersed phase coalesces, first droplet by droplet, and subsequently aggregate by aggregate. Also the time scale for rupture is usually faster than the time scale that characterizes the thin film drainage as particles of dispersed phase approach each other. Thus the drainage rate of the thin film determines the life time of a breaking foam or an emulsion. Controlling the interfacial mobility using remobilizing surfactants can provide a paradigm for effectively controlling the lifetime of foams and emulsions,

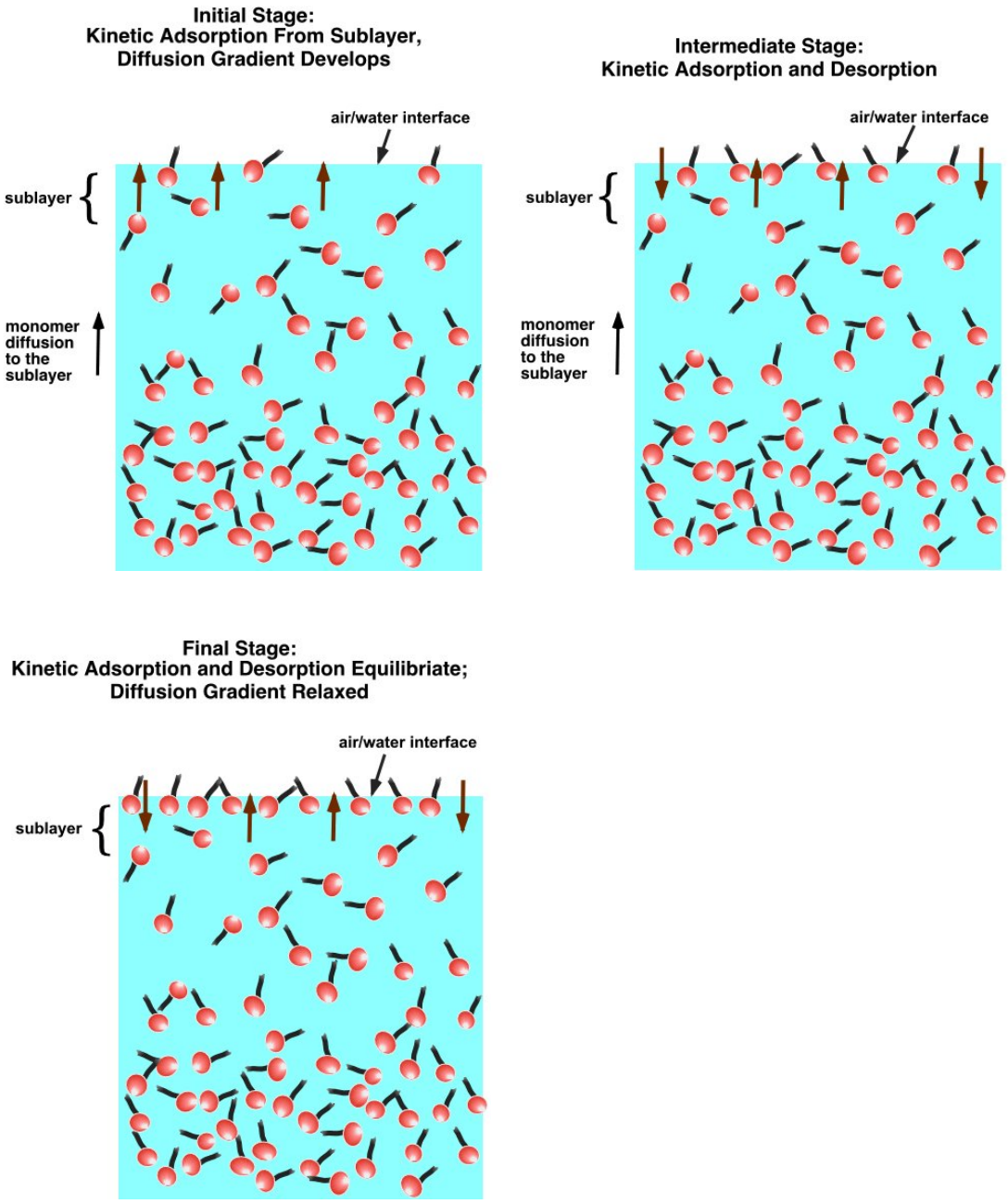


**Figure 1.1 Adsorption of surfactant onto an initially clean interface, and the kinetic and diffusive transport processes to equilibrium.**

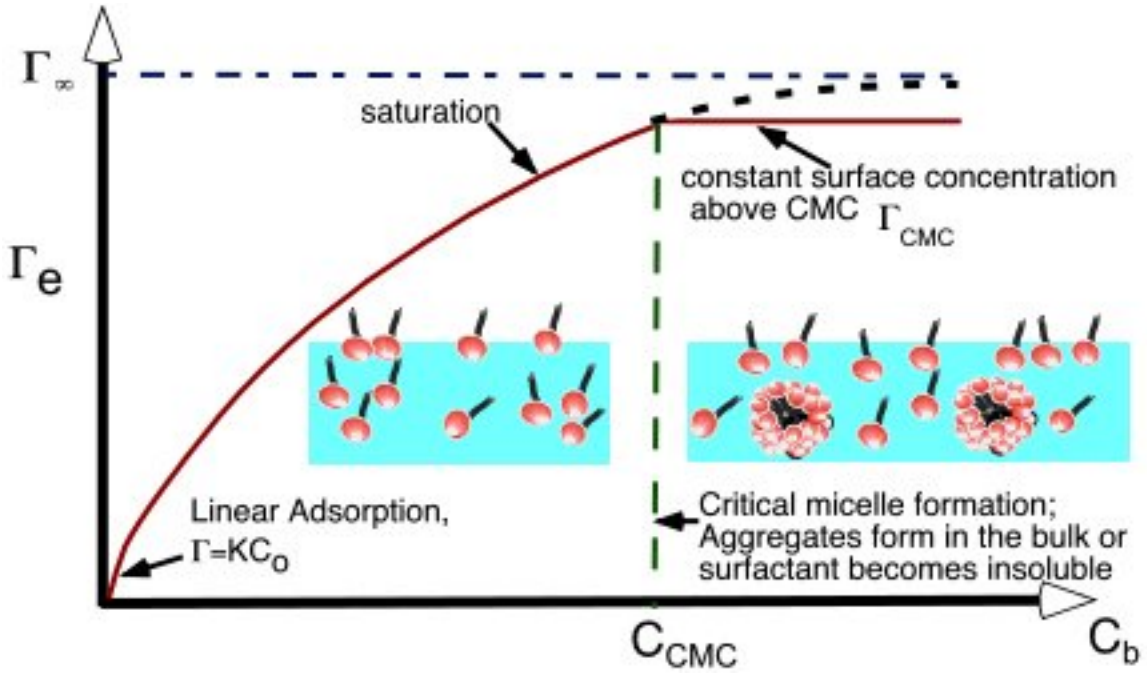


**Figure 1.2 Adsorption isotherm depicting the equilibrium surface concentration as a function of the bulk concentration of surfactant, and the demarcation of the critical micelle concentration**

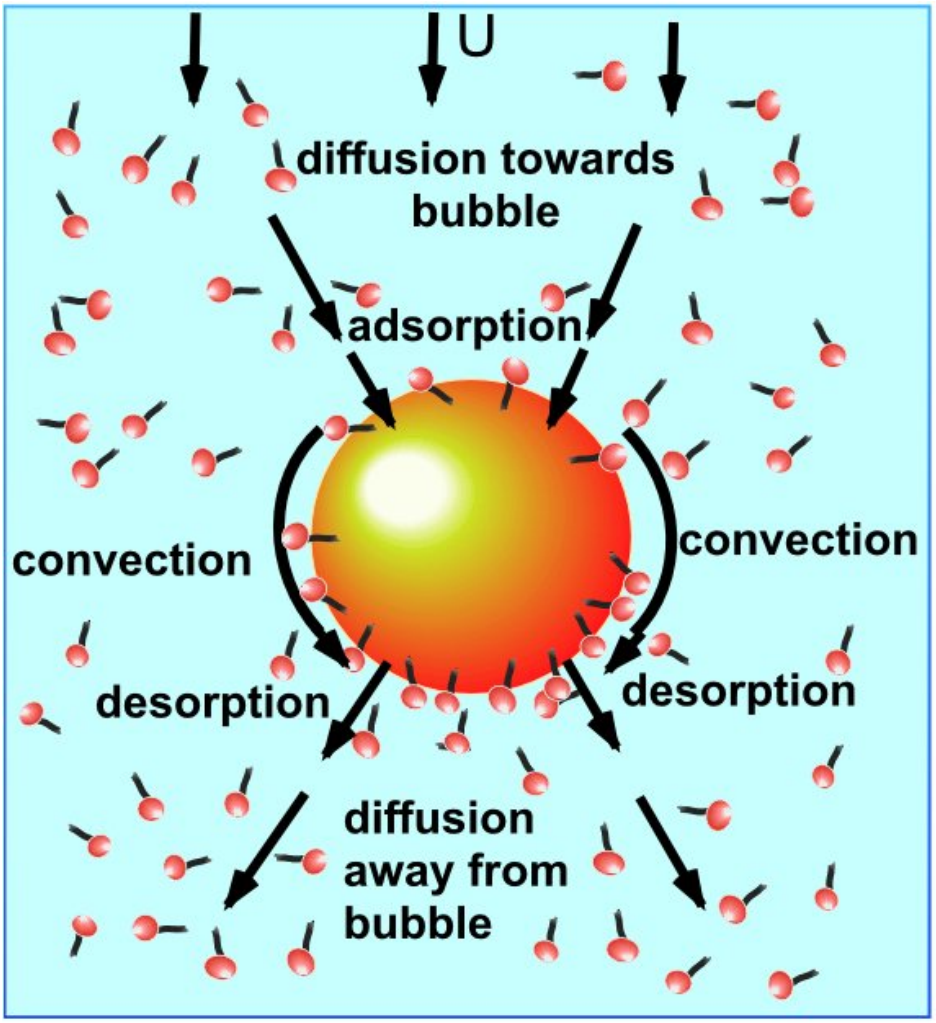


**Figure 1.3 Surfactant transport processes at a moving bubble interface; the bubble is viewed in a frame fixed to the bubble surface**

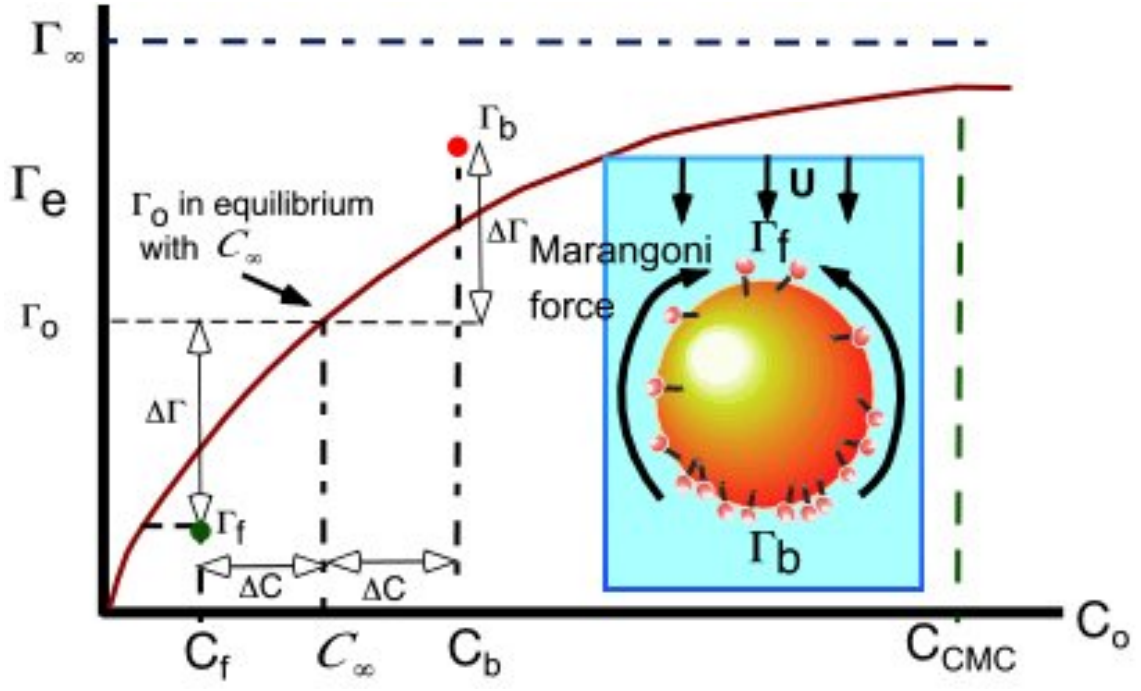


**Figure 1.4 Retarding Marangoni forces at the interface of a bubble**

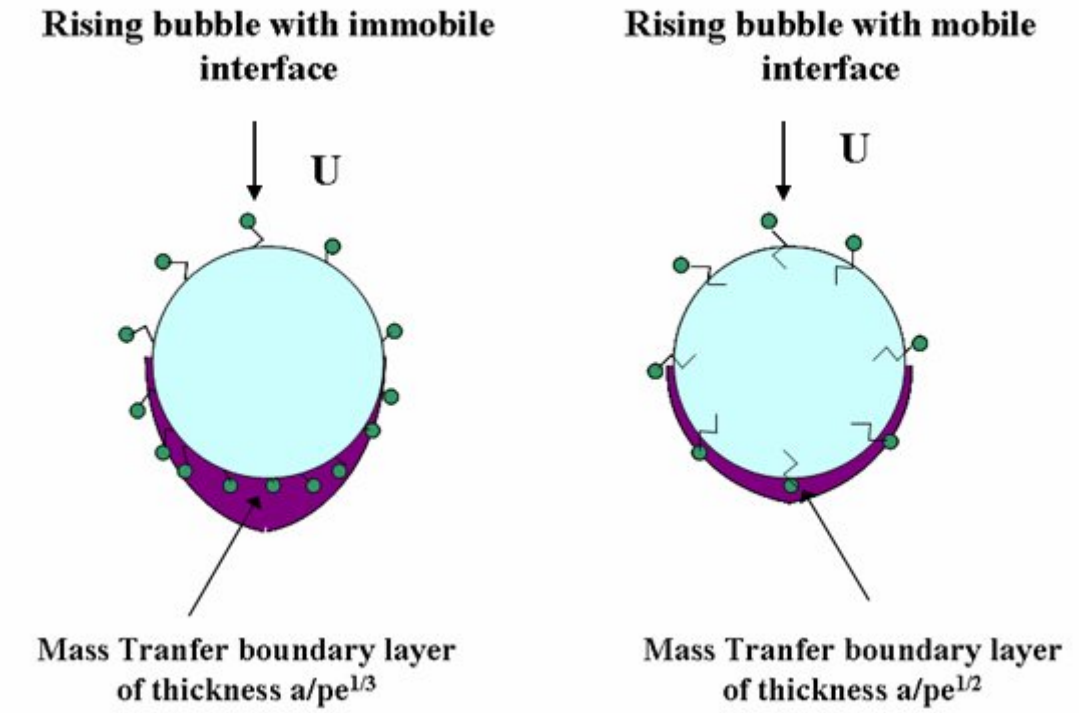


**Figure 1.5 Dependence of Efficiency of Bubble-Wise Extraction process on the Interfacial Mobility of Bubble**

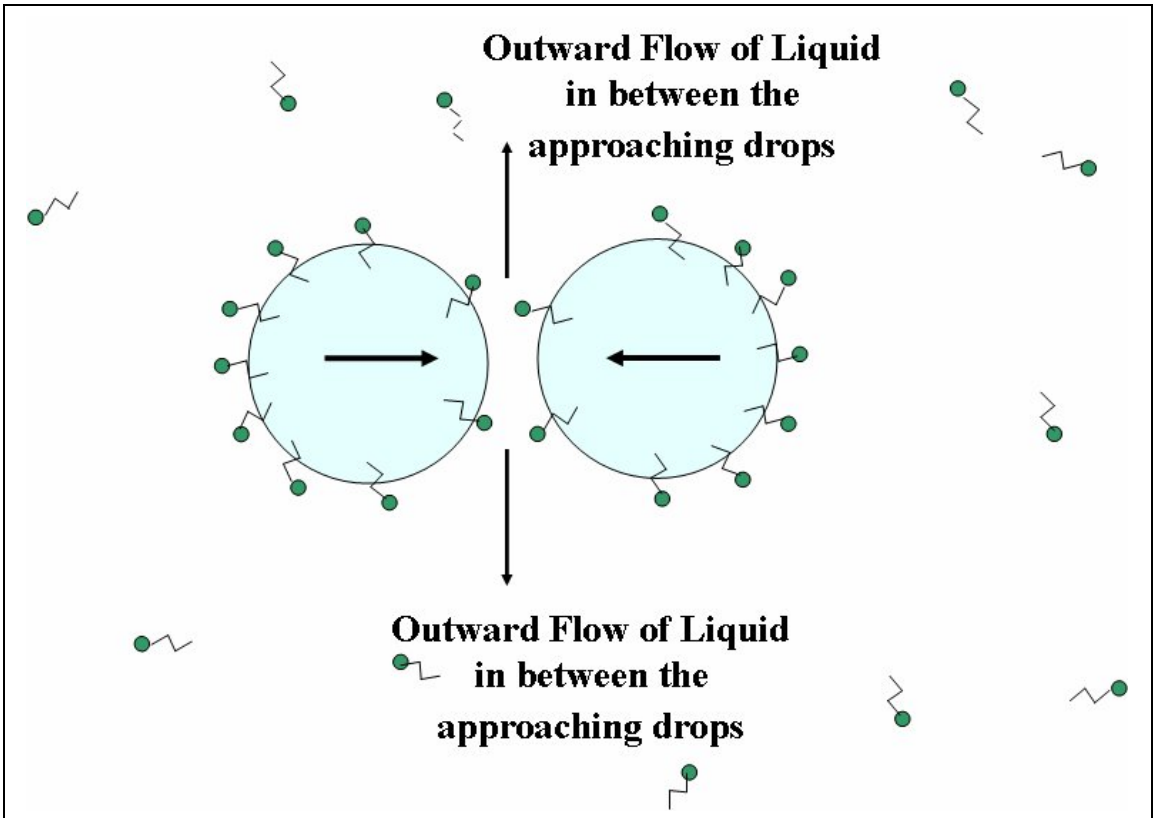


**Figure 1.6 Dependence of Stability of a Foam or a Bubble on the Interfacial mobility of these bubbles.**

# CHAPTER 2

## Literature Review

The aim of this chapter is to review the research undertaken on the effect of surfactant on the translation of a bubble in a continuous liquid phase, focusing on both theoretical and experimental studies. The buoyancy driven motion of small bubbles and drops in the absence of inertia (low Reynolds number) in a continuous liquid phase (and for fluids without surface active species) can be predicted by the theory developed independently by Hadamard [Hadamard (1911)] and Rybczynski [Rybczynski (1911)]. This theory shows that the interface of the bubble - because the gas inside the bubble does not exert a shear stress - is mobile and sustains a surface flow. In a frame of reference moving with the bubble, this flow is from the front or leading edge to the back or trailing end of the bubble, Bond and Newton [Bond & Newton (1928)] conducted experiments to measure the terminal velocities of bubbles and drops in the low Reynolds number regime, and found that they tend to move slower than the Hadamard-Rybczynski predicted values. While large bubbles and drops move according to the Hadamard-Rybczynski theory, small bubbles and drops move as if they were particles with a stagnant (rigid) interface, in accordance with Stokes law. Since these early measurements, many studies have confirmed this anomalous behavior where bubbles act as solid particles for small radii, both for inertialess and order one Reynlds numbers (for a review see Clift *et al* [Clift, Grace and Weber (1978)]). Frumkin and Levich [Frumkin and Levich (1947)] proposed a mechanism whereby interfacial tension gradients arrest the motion of the interface and hence causes this unusual behavior in the motion of bubbles. These interfacial tension gradients on the bubble surface are caused by dissolved surfactant impurities which are present inadvertently as a dilute contaminant (or added intentionally at a particular concentration) in the continuous phase.

Surfactants are adsorbed onto the interface of the bubble and are convected to and accumulate at the trailing edge to form a surface concentration gradient along the bubble surface increasing to the back end. The tension decreases with surface concentration, and hence the tension at the back end is lower than that at the front end. As a result, the front end tugs at the back, creating a Marangoni force which opposes the surface flow and immobilizes the interface. Frumkin and Levich calculated surface concentration and tension gradients which are smooth on the surface of the bubble, uniformally retarding the interface. The calculated terminal velocity of the bubble varied smoothly with the bubble radius from the velocity of a bubble with a fully mobile stress-free interface (Hadamard- Rybczynski) to the Stokes velocity of a bubble with a rigid (stagnant) interface. This model was criticized as it failed to predict the asymmetric flow patterns with a slow circulating region at the rear observed in flow visualizations of the motion of drops. Another drawback of the model was that the measured transition between stress free and immobile states with bubble radius is sharp, and not gradual. To explain the more abrupt shift observed experimentally, Savic [Savic (1953)], Griffith [Griffith (1962)], and Davis and Acrivos [Davis & Acrivos (1966)] detailed a stagnant cap model. This model also attributed the immobilization of the surface to surfactant induced interfacial tension gradients, but demonstrated the conditions under which surfactant collects in a stagnant cap at the trailing end of the bubble which leads to a step function change in the interfacial mobility with bubble radius. To understand the uniformly retarded and stagnant cap regimes, and the concept of the remobilization regime, we present scaling arguments of the surfactant transport.

A picture of the surfactant transport to the moving bubble is presented in Figure 2.1. Surfactant adsorbs onto the surface of a moving bubble and is convected by the surface flow from the front of the bubble to the trailing end, where the increase in surface concentration $\Gamma$

causes surfactant to kinetically desorb into the rear sublayer. This desorption locally raises the sublayer concentration, $C_s$, at the back above the bulk value $C_0$, far from the interface. The difference drives a diffusive flux away from the trailing end. Similarly at the front end, the reduction in surface concentration causes kinetic adsorption from the front sublayer onto the front of the bubble. The front sublayer concentration decreases, creating a diffusive flux from the bulk to the front end. Eventually a steady state develops: The surface concentration at the back end has increased by $\Delta\Gamma$ above the equilibrium value $\Gamma_e$ corresponding to $C_0$ (as given by adsorption isotherm $\Gamma_e$ ($C_0$) so that the desorption rate balances the convective rate. The back sublayer concentration has increased by $\Delta C$ above $C_0$ so that the diffusive flux away from the particle surface balances the kinetic desorption. At the front end, the surface concentration has decreased below $\Gamma_e$ so that kinetic adsorption balances convection, and the sublayer concentration is reduced below $C_0$ sufficiently so that the diffusion to the surface balances adsorption. Thus while the average concentration on the surface at steady state scales with $\Gamma_e$ ($C_0$), the surface concentration is considerably higher at the rear than at the front of the particle, and the interfacial tension($\gamma$) is lower at the back relative to the front. The interfacial tension difference creates a Marangoni stress along the surface which opposes the surface flow caused by the movement of the bubble, increases the drag and hence reduces the velocity of translation.

Kinetic exchange between the surface and the sublayer of liquid near the surface is described accurately using Frumkin kinetic scheme:

$$\frac{\partial \Gamma}{\partial t} = \beta \Gamma_\infty C_s (1 - \frac{\Gamma}{\Gamma_\infty}) - \alpha \Gamma e^{K\frac{\Gamma}{\Gamma_\infty}} \qquad (2.1)$$

where $\Gamma$ is the surface concentration, RT is the thermal energy, $\Gamma_\infty$ is the maximum packing density, $\alpha$ and $\beta$ are kinetic coefficients for desorption and adsorption, and $C_s$ is the

concentration of surfactant adjacent to the interface (i.e. sublayer concentration). For K<0, cohesive interactions between the hydrocarbon chains increase the activation energy for desorption and reduce desorption rate. When K>0, repulsive interactions between the head groups reduce the activation energy for desorption, and increase the desorption rate. From 2.1, we obtain the frumkin isotherm $\Gamma_e(C_b)$ by setting the kinetic rate equal to zero:

$$\frac{\Gamma_e}{\Gamma_\infty} = \frac{1}{1+\frac{\alpha}{\beta C_0} e^{K\frac{\Gamma_e}{\Gamma_\infty}}} = \frac{k}{k+e^{K\frac{\Gamma_e}{\Gamma_\infty}}} \qquad (2.2)$$

where the parameter $k= \beta C_0/\alpha$ scales or nondimensionalizes the bulk concentration. The ratio $\alpha/\beta$, the interaction parameter K and the maximum packing concentration $\Gamma_\infty$ are determined from equilibrium measurements of tension as a function of the bulk concentration; typical values of $\beta/\alpha$ for fairly aqueous soluble surfactants at air/water interface ranging from $10^3$ $cm^3$/mole for the least surface active alcohols like hexanol to $10^{12}$ $cm^{3/}$/mole for very surface active surfactants. Typical values for the maximum packing concentration are $1\text{-}7X10^{-10}$ mole/$m^2$ and the values of K are of the order one. Values for the kinetic rate constants are obtained from the measurements of the relaxation in surface tension as surfactant adsorbs onto a clean interface; the kinetic constants are not as well established as the equilibrium ratio, but values reported for $\alpha$ are in the range of $10^{-4}$-$10^2$ $s^{-1}$ and values of $\beta$ are obtained from the equilibrium ratio.

The above description of kinetic exchange is valid for the bulk concentrations up to the point of insolubility of the surfactant (in the case of alcohols), or, for the very surface active surfactants, up to the critical micelle concentration (CMC) or $C_{CMC}$ at which point surfactant molecules begin to aggregate in the bulk. For surfactant (monomer) concentrations $C_b$ greater than $C_{CMC}$, at equilibrium, the concentration of the un-aggregated surfactant in the bulk is observed to remain constant and approximately equal to the $C_{CMC}$, and the remainder of

surfactant in the bulk exists in aggregated form. The equilibrium partitioning is maintained by a balance between a micellar breakdown and re-aggregation which follows the chemical potential of the surfactant molecule to be equal in the aggregated and re-aggregated forms. Because the bulk concentration of the monomeric form remains constant for $C_0>C_{CMC}$, the chemical potential of the surfactant molecule to be equal in the aggregated and the unaggregated forms. Because the bulk concentration of the monomeric form remains constant for $C_0>C_{CMC}$, the chemical potential of the surfactant molecule remains approximately constant. With the constant chemical potential in the bulk maintain the surface concentration at the value achieved at the CMC:

$$\frac{\Gamma_{e,CMC}}{\Gamma_\infty} = \frac{1}{1+\frac{\alpha}{\beta C_{CMC}} e^{K\frac{\Gamma_{e,CMC}}{\Gamma_\infty}}} = \frac{k_{CMC}}{k_{CMC}+e^{K\frac{\Gamma_{e,CMC}}{\Gamma_\infty}}} \qquad (2.3)$$

where $k_{CMC}= \beta C_{CMC}/\alpha$. In aqueous media, the more surface active the surfactant, the lower is the CMC, and thus the maximum value of k which is approximately equal to $k_{CMC}$ is of the order $10^2$-$10^3$.

For a bubble with radius a moving with velocity U in a continuous phase containing the surfactant with the bulk concentration $C_0$, the convective transport scales as $\Gamma_e Ua$. From 2.1, we note that the scale for the maximum rate of kinetic adsorption (per unit area) is $\beta\Gamma_\infty C_0$ or $\left(\beta C_0 + \alpha e^{K\frac{\Gamma_e}{\Gamma_\infty}}\right)\Gamma_e$, so the ratio of maximum adsorption rate to the characteristic convective scale is $Bi\left(k+e^{K\frac{\Gamma_e}{\Gamma_\infty}}\right)$, where Bi= $\alpha a/U$. If $Bi\left(k+e^{K\frac{\Gamma_e}{\Gamma_\infty}}\right)$ <<1, then the front end is swept clean of surfactant as convection out scales diffusion and surfactant collects at the back. However if

$Bi\left( k + e^{K\frac{\Gamma_e}{\Gamma_\infty}} \right)$ is order one or larger, then kinetic exchange can balance surface convection. As this parameter becomes much greater than one, the surface and sublayer approach equilibrium, with the surface concentration perturbed from the equilibrium value corresponding to the local sublayer concentration. The rate of diffusive mass transfer to the front end of the bubble depends on the balance between convective and diffusive transport of surfactant in the continuous phase. This balance is described by Peclet number, Pe= Ua/D, where D is the bulk diffusion coefficient and is of the order of $10^{-6}$ $cm^2/s$. Computations of the mass transfer of the solute from uniform far field to the surface of a moving bubble for which the solute concentration is zero, show that when the Peclet number is order one or smaller, diffusive gradients adjacent to the bubble surface are of the order of the radius. Thus the diffusive flux scales as $DC_0/a$, where $C_0$ is the far field bulk concentration, a is the radius of the bubble and D is the coefficient of diffusion of the surfactant in the liquid. Consider an air bubble of diameter 1mm, rising by buoyancy at 10 cm/s, Pe = $O(10^6)$ >>1. When the Peclet number is large, diffusive gradients develop only in the boundary adjacent to the bubble surface, with the remainder of the continuous phase at uniform concentration. The size of the boundary scales as $aPe^{-1/2}$, and the diffusive flux scales as $DC_0Pe^{1/2}/a$. For scaling purposes we assume that Peclet number is large. For large Peclet number the ratio of the diffusive transport to the front end of the bubble to the convective flux along the bubble surface ($\Gamma_e U/a$) is $\chi(k + e^{K\frac{\Gamma_{ee}}{\Gamma_\infty}})/Pe^{\frac{1}{2}}$, where $\chi=\alpha a/(\beta\Gamma_\infty)$. A typical value of $\chi$ for a bubble of radius 0.5mm, $\beta/\alpha$ between $10^9$ to $10^{11}$ $cm^3$/mole and $\Gamma_\infty$ of $10^{-10}$ mole/$cm^2$, $\chi$ ranges between from $10^{-2}$ to 1.

## 2.1 STAGNANT CAP REGIME

The stagnant cap regime is the regime which is realized usually in the case of fluid particles buoyantly moving in an aqueous system containing surface active impurities. In this regime the maximum rate of either the diffusive or kinetic fluxes of surfactant to the surface is much smaller than surface convection i.e. either $\chi(k+e^{K\frac{\Gamma_{ee}}{\Gamma_\infty}})/Pe^{\frac{1}{2}}$ <<1 or/both $Bi\left(k+e^{K\frac{\Gamma_e}{\Gamma_\infty}}\right)$ <<1. As a result, to leading order, adsorbed surfactant behaves as if it is insoluble, and is swept to the back end of the particle. If in addition the surface Peclet number is large, then surfactant is swept to a stagnant cap with zero interfacial velocity at the back end since the adsorbed molecules cannot diffuse back to the front. At the front end the surface is clean of surfactant and stress free as shown in Figure 2.2. It has been studied extensively theoretically (Savic [Savic (1953)], Griffith [Griffith (1962)], Davis and Acrivos [Davis & Acrivos (1966)], Sadhal and Johnson [Sadhal and Johnson (1982)], and Palaparthi *et al* [Palaparthi, Papageorgiou and Maldarelli, 2006]). A few comparisons have been made between measurements of terminal velocities in the stagnant cap regime and theoretical computations. Savic [Savic (1953)] and Horton *et al* [Horton, Fritsch & Kintner(1965)] among others have showed the shift in the center of the circulation vortex to the leading edge, reflecting that a stagnant cap had formed on the surface of the drop. Aside from these qualitative observations, the first attempt at a quantitative comparison between a stagnant cap theory and experiment was Griffth's [Griffith (1962)] study of the motion of droplets with surfactants added to the system. Griffth interpreted his results in terms of the stagnant cap model, but the calculation of the cap angle as a function of the bulk concentration by solution of the surfactant transport equations were not undertaken. Duinveld [Duineveld (1994)] studied air bubbles rising in water with Triton X-100 as the surface active

agent. Duineveld conducted experiments to measure the reduction in terminal rise velocity of air bubbles in water as a function of increasing bulk concentration of surfactant and using scaling arguments verified that the bubbles were moving in stagnant cap regime. They compared these experimental results with theoretical calculations which solved surfactant transport equations but assumed only a kinetic limitation to the surfactant transfer. The simulations show qualitative agreement and with the experiments, in part due to the effects due to bulk diffusion were not included and in part due to the velocities may not have reached terminal values, as was pointed by Zhang *et al* [Zhang, McLaughlin, & Finch (2001)].

## 2.2 UNIFORMLY RETARTED REGIME

When the rates of bulk diffusion and surfactant kinetic exchange are not less than the rate of interfacial convection, the uniformly retarded regime is realized. Within the frame work of scale developed above, when $\chi(k+e^{K\frac{\Gamma_e}{\Gamma_\infty}})/Pe^{\frac{1}{2}}$ and $Bi(k+e^{K\frac{\Gamma_e}{\Gamma_\infty}})$ are not <<1 but either both of then or one of then is O(1). In this limit the bubble surface becomes more uniformly retarded rather than the case of stagnant cap, with a completely mobile front end and solid like back end. Figure 2.3 gives a schematic of this regime. Balancing of the diffusive rate with convective rate provides a scale for the difference between the bulk and sublayer concentrations ΔC:

$$\frac{D\Delta C}{aPe^{-\frac{1}{2}}} = O(\frac{\Gamma_e U}{a}) \tag{2.4}$$

or

$$\Delta C = O(\frac{\Gamma_e}{a}\frac{Ua}{D}Pe^{-\frac{1}{2}}) = O(\frac{\Gamma_e}{a}Pe^{\frac{1}{2}}) \tag{2.5}$$

but $$\Gamma_e = \Gamma_\infty \left( \frac{k}{k + e^{K\frac{\Gamma_e}{\Gamma_\infty}}} \right) \tag{2.6}$$

Using 2.5 and 2.6, we get

$$\Delta C = O(\frac{\Gamma_\infty}{a} \left( \frac{k}{k + e^{K\frac{\Gamma_e}{\Gamma_\infty}}} \right) Pe^{\frac{1}{2}}) \tag{2.7}$$

But $$\chi = \frac{\alpha a}{\beta \Gamma_\infty} = \frac{a C_0}{k \Gamma_\infty} \tag{2.8}$$

Using 2.7 and 2.8, we get

$$\frac{\Delta C}{C_0} = O(\frac{Pe^{\frac{1}{2}}}{\chi(1+k)}) \tag{2.9}$$

The balancing of the kinetic rate and the convective rate

$$\beta C_0 \left( \Gamma_\infty - \Gamma_e \right) - \alpha \Gamma_e e^{K\frac{\Gamma_e}{\Gamma_\infty}} = O(\frac{\Gamma_e U}{a}) \tag{2.10}$$

provides a scale for $\Delta\Gamma$:

$$\frac{\Delta\Gamma}{\Gamma_\infty} = O\left( \frac{1}{Bi(k + e^{K\frac{\Gamma_0}{\Gamma_\infty}})} + \frac{Pe^{1/2}}{\chi(k + + e^{K\frac{\Gamma_0}{\Gamma_\infty}})^2} \right) \tag{2.11}$$

The scale of the retarding Marangoni force ($\tau_m$) is given by

$$\tau_m = \frac{tension\ gradient}{viscous\ gradient} = O\left\{ \frac{1}{\mu U} \left[ \frac{\partial \gamma}{\partial \Gamma} \right]_{\Gamma_e} \Delta\Gamma \right\} \tag{2.12}$$

where $\mu$ is viscosity of the continuous phase.

The equation of state for Frumkin adsorption is given by

$$\gamma(\Gamma) = \gamma_c + RT\Gamma_\infty \left[ \ln\left\{1 - \frac{\Gamma}{\Gamma_\infty}\right\} - \frac{1}{2} K \left[\frac{\Gamma}{\Gamma_\infty}\right]^2 \right] \tag{2.13}$$

Therefore $$\left.\frac{\partial \gamma}{\partial \Gamma}\right|_{\Gamma_e} = -RT \left[ \frac{1}{1 - \frac{\Gamma_e}{\Gamma_\infty}} + K \frac{\Gamma_e}{\Gamma_\infty} \right] \tag{2.14}$$

Equations (2.12) and (2.14) gives

$$\tau_m = O\left[ Ma \left\{ \frac{k}{Bi(k + e^{K\frac{\Gamma_0}{\Gamma_\infty}})} + \frac{kPe^{1/2}}{\chi(k + e^{K\frac{\Gamma_0}{\Gamma_\infty}})^2} \right\} \right] \tag{2.15}$$

where Marangoni number, Ma = RTΓ∞/μU

In the creeping flow limit and for surfactant concentrations (k<1), this case has been studied by several authors. Levich [Levich (1962)], Harper [Harper (1974 & 1982)] and Saville [Saville (1973)], studied the regime for low surfactant concentration (k<1) for both kinetic and diffusion limited transport. Levich [Levich (1962)] studied the uniformly retarded regime, finding the reduction in terminal velocity when the surface tension was perturbed from its equilibrium value. The case was examined by Wasserman and Slattery [Wasserman & Slattery (1969)], who considered trace quantities of a diffusion controlled surfactant. Levan and Newman [Levan & Newman (1976)] derived equations for the terminal velocity and the interfacial velocity for a droplet with arbitrary surface tension gradient. These equations were solved for the case of an extremely dilute surfactant whose transport is bulk diffusion controlled. This work was extended by Holbrook and Levan [Holbrook & Levan (1983a&b)]. They derived the asymptotic solutions for both the stagnant cap and the uniform retarded regimes, for the surfactant being present either in the drop or external phase, while treating all the surfactant mass

transfer mechanism simultaneously. They also studied the limiting cases for mass transport mechanisms to achieve stagnant cap or uniformly retarded regime. Chen and Stebe [Chen & Stebe (1996 & 1997)] and Ybert and Megilo [Ybert & Megilo (2000)] also studied this regime at order one values of k and for kinetically limited transport.

## 2.3 REMOBILIZATION REGIME

In the limit, when the bulk concentration is high, k>>1 with diffusion $\chi(k+e^{K\frac{\Gamma_{ee}}{\Gamma_\infty}})/Pe^{\frac{1}{2}}=$ O( $\chi k/Pe^{\frac{1}{2}}$)>>1 and kinetic exchange outscaling convection $Bi\left(k+e^{K\frac{\Gamma_e}{\Gamma_\infty}}\right)=O(Bik)>>1$. Figure 2.4 provides a schematic of this regime, for concentrations less than the critical micelle concentration or CMC. In this limit of fast kinetic and diffusive transport to convection, the sublayer concentration is only slightly changed from $C_0$ (by amount $\Delta C$; negative at front and positive at back) and the surface concentration only slightly changed from the equilibrium value $\Gamma_e$ (by amount $\Delta\Gamma$). Balancing of the diffusive rate with convective rate provides a scale for the difference between the bulk and sublayer concentrations $\Delta C$ gives:

$$\frac{\Delta C}{C_0}=O(\frac{Pe^{\frac{1}{2}}}{\chi k})<<1 \qquad (2.16)$$

Since the kinetic rate is much faster than the convective rate, the surface and sublayer are in equilibrium so that the variation in the surface concentration from the equilibrium $\Delta\Gamma$ is small and can be related to the small variation in $\Delta C$:

$$\frac{\Delta\Gamma}{\Gamma_\infty}=O(\frac{Pe^{\frac{1}{2}}}{\chi k^2})<<1 \qquad (2.17)$$

The scale of the retarding Marangoni force ($\tau_m$) is given by

$$\tau_m = O\left[ Ma\left\{ \frac{1}{Bie^K} + \frac{Pe^{1/2}}{k\chi} \right\} \right] \tag{2.18}$$

Therefore, for remobilization $\tau_m$ must tend to zero, which can be achieved by high concentration (k>>1), large diffusive rate relative to convection ($\frac{k\chi}{Pe^{1/2}}$ >>1) and rapid kinetic exchange. Our assumption of rapid kinetic exchange only required kBi>>1, which can be satisfied even if $Bie^K$ is small as long as k is large enough. However in order to have remobilization, $Bie^K$ must also be large. Thus the conditions for remobilization are:

1) k>>1 (high bulk concentration)

2) kBi>>1 and $Bie^K$>>1 (rapid kinetic exchange relative to convection)

3) $\frac{\chi k}{Pe^{1/2}}$ >>1 (rapid diffusive exchange relative to convection)

These criteria for remobilization are for the case when the surfactant is in the unaggregated or monomer form and has been investigated and the concenpts verified theoretically for the case of diffusion-limited transport of the surfactant (i.e. Bi $\rightarrow \infty$, and $\frac{\chi k}{Pe^{1/2}}$ = O(1)), by Wang *et al* [Wang, Papageorgiou, & Maldarelli (1999)] for Re<<1, and for Re=O(1) by Wang *et al* [Wang, Papageorgiou, & Maldarelli (2001)] and Takemura [Takemura (2005)].

The experimental verification of remobilization has been undertaken in two studies. Stebe *et al* [Stebe, Lin & Maldarelli (1991&1994)] studied a three-phase periodic slug flow in a capillary tube in which a train of alternating air and aqueous segments containing surfactant Triton X-100 and Brij 35, move in a Teflon tube whose inner surface has been coated with a film of fluorocarbon oil. When the interface of these bubbles is immobile, the pressure gradient

required to drive the slug train at a constant velocity is found to be higher than for a mobile interface. They found that at low concentrations of surfactant the pressure required to drive the slugs at constant velocity increases with increase in concentration. However at very high concentrations, above the critical micelle concentration, the pressure relaxes, indicating remobilization.

Palaparthi *et al* [Palaparthi (2001)] designed a set of experiments to verify remobilization for bubbles rising in a continuous phase. The terminal velocity was measured for nitrogen bubbles rising in a glycerol-water mixture in the presence of the polyethoxylated surfactant surfactant $C_{10}E_{8,}$ dissolved in the bulk phase. The terminal velocity was measured as a function of the bulk concentration, Palaparthi *et al* observed that for the surfactant used, the remobilization criteria could not be satisfied because micelles began to form at a concentration for which the parameter $\frac{\chi k}{Pe^{1/2}}$ was only order one. Palaparthi *et al* found that for increasing surfactant concentrations above the CAC, the interface did remobilize (the terminal velocity increased) suggesting, as with Stebe *et al* that micelles offer a route towards remobilization.

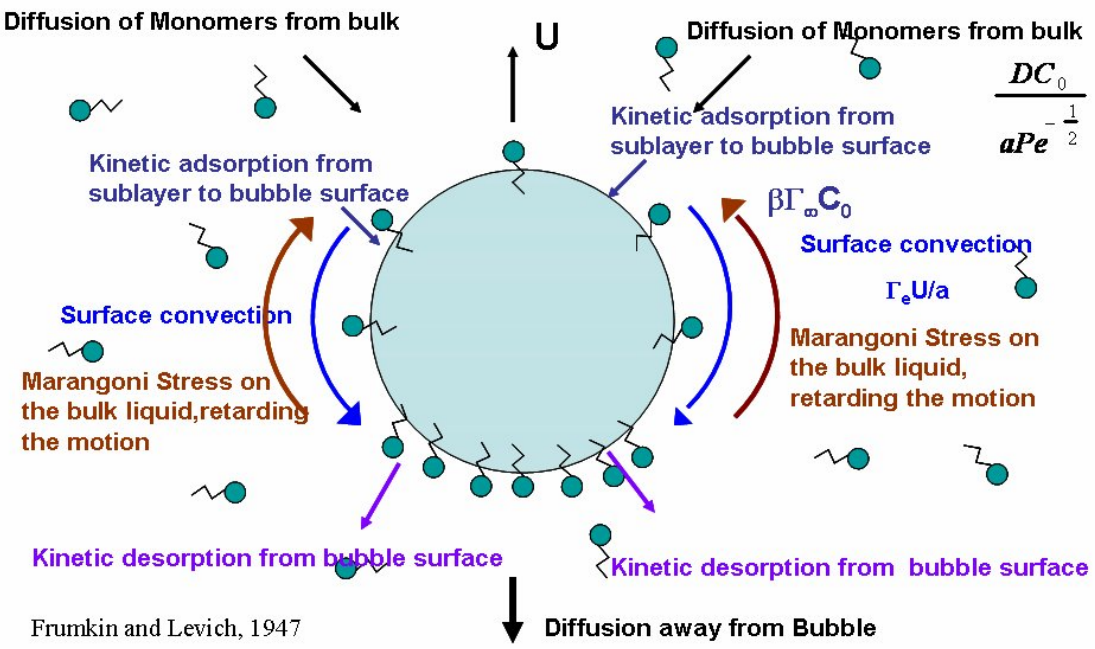


**Figure 2.1 Surfactant transport mechanism to the surface of a moving bubble.**

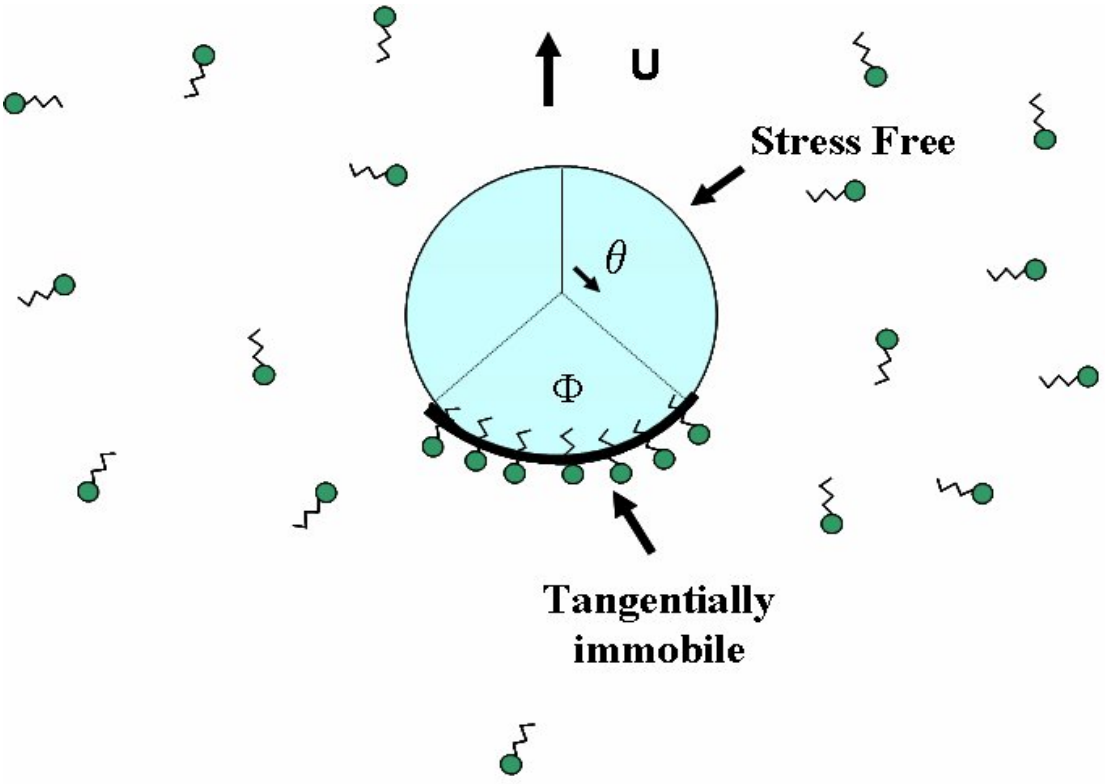


**Figure 2.2 Stagnant Cap Regime**

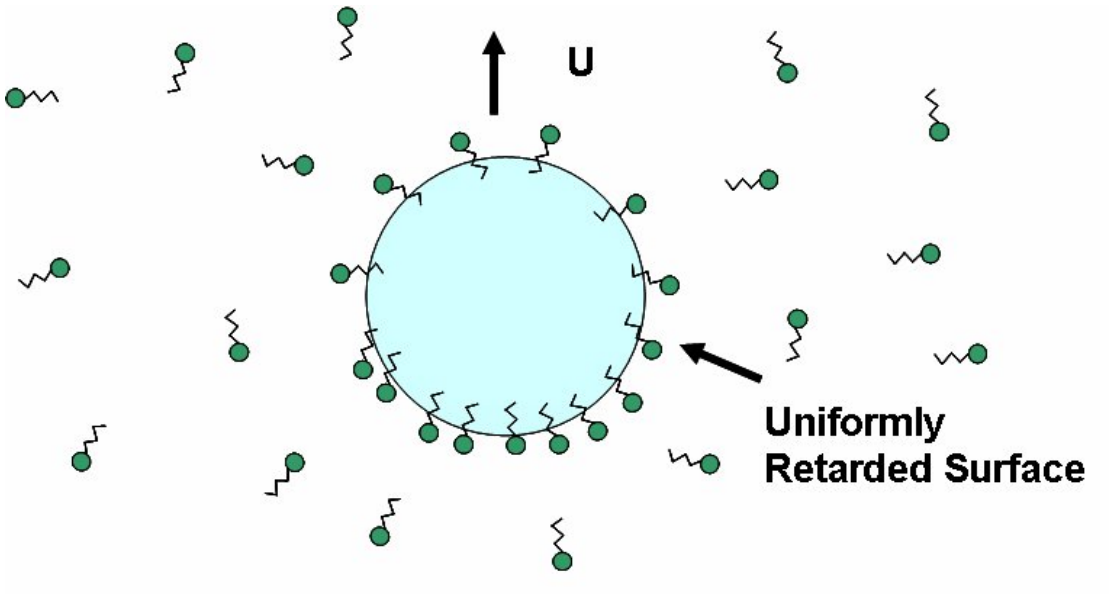


**Figure 2.3 Uniformly Retarded Regime**

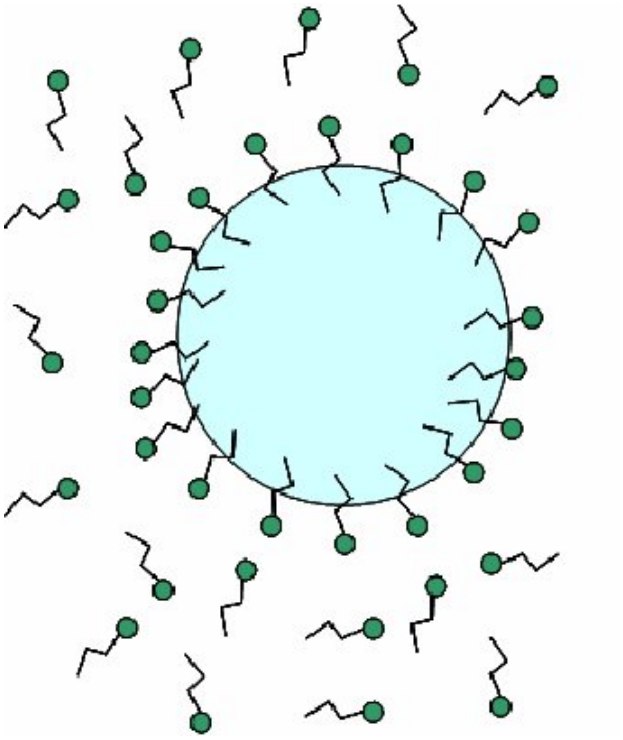

**Figure 2.4 Remobilization Regime at Concentrations less than the critical micelle concentration or CMC**

# CHAPTER 3

# Remobilization of the Surfactant-Retarded Interface of a Moving Bubble At High Bulk Surfactant Concentrations For an Amphiphile Which Remains Monomeric in the High Concentration Limit

## 3.1 INTRODUCTION

The aim of this chapter is to demonstrate experimentally the remobilization of the surfactant-retarded interface of a moving bubble at high surfactant concentrations for the case in which the surfactant remains in monomeric form in the high concentration limit. Remobilization is possible when the kinetic and diffusive barriers which give rise to the surface concentration/interfacial tension gradients that retard the interface motion are removed. In Chapters 1 and 2 we formulated the diffusive, kinetic and convective transport scales at the interface of a moving bubble, and arrived at criteria for remobilization. We review this analysis briefly below, before detailing the surfactant systems and experiments to verify this remobilization.

With regard to Figure 2.1, the diffusive flux to the interface of a bubble moving with velocity U, when the Peclet number (Pe=Ua/D) is of order one or smaller, scales as $DC_0/a$, where $C_0$ is the far field bulk concentration, a is the radius of the bubble, U is the bubble rise velocity and D is the coefficient of diffusion of the surfactant in the liquid. However, when the Peclet number is large, diffusive gradients develop only in the boundary adjacent to the bubble surface, with the remainder of the continuous phase at uniform concentration. The size of the boundary scales as $aPe^{-1/2}$, and the diffusive flux scales as $DC_0Pe^{1/2}/a$. For scaling purposes (with a view to

the applications in Chapter 1 and the remobilization experiments of buoyantly rising bubbles to follow) we assume that the Peclet number is large. If the Peclet number is order 1, then the arguments can easily be changed and the factor $Pe^{1/2}$ can be replaced by Pe. To describe the kinetic exchange, we will use the Langmuir isotherm which will prove sufficient for the monomeric surfactants considered in this part of the research. For Langmuir kinetics, $\frac{\partial \Gamma}{\partial t} = \beta \Gamma_\infty C_s - (\beta \Gamma_\infty C_s + \alpha)\Gamma$, where $C_s$ is the sublayer concentration, $\Gamma$ is the surface concentration, $\alpha$ is the coefficient of desorption, $\beta$ is the coefficient of adsorption and $\Gamma_\infty$ is the maximum packing density of surfactant at the interface. The scale for the rate of kinetic adsorption (per unit area) is $\beta\Gamma_\infty C_0$. The scale of transport due to surface convection is $\Gamma_0 U/a$, where U is the rising velocity of the bubble and $\Gamma_0$ is the characteristic surface concentration in equilibrium with the far field concentration $C_o$ as given by $\frac{\Gamma_o}{\Gamma_\infty} = \frac{k}{1+k} = \frac{\frac{\beta C_o}{\alpha}}{\frac{\beta C_o}{\alpha}+1}$, k is the non-dimensional concentration $k = \frac{\beta C_o}{\alpha}$. So the ratio of the characteristic diffusion rate to the rate of surface convection is given by $\chi(k+1)/Pe^{1/2}$, where $\chi$ is given by $\alpha a/(\beta\Gamma_\infty)$ and is equal to $\beta C_0/\alpha$. The ratio of the scale of the rate of adsorption to the characteristic rate of surface convection is given by Bi(k+1), where Bi is the Biot number given by $\alpha a/U$.

When the rates of bulk diffusion and the surfactant kinetic exchange are large enough to be of the same order of magnitude as the surface convection i.e. Bi(k+1) =O(1) and $\chi(k+1)/Pe^{1/2}$= O(1), then the surface of the bubble becomes uniformly retarded rather than forming stagnant caps. The balancing of the diffusive rate with the convective rate provides a scale for the difference between the bulk and sublayer concentrations $\Delta C$.

$$\frac{a^2 D\Delta C}{aPe^{-1/2}} = O(\Gamma_0 Ua) \tag{3.1}$$

or

$$\frac{\Delta C}{C_0} = O\left(\frac{Pe^{1/2}}{\chi(1+k)}\right) \tag{3.2}$$

The balancing of the kinetic rate to the convective rate provides a scale for $\Delta\Gamma$.

$$\mathrm{Bi}(1+\mathrm{k})\left(\frac{\Delta\Gamma}{\Gamma_0} - \frac{\Delta \mathrm{C}}{(1+\mathrm{k})\mathrm{C}_0}\right) = \mathrm{O}(1) \tag{3.3}$$

or

$$\frac{\Delta\Gamma}{\Gamma_0} = \frac{1}{Bi(k+1)} + \frac{\Delta C}{(1+k)C_0} \tag{3.4}$$

and therefore

$$\frac{\Delta\Gamma}{\Gamma_0} = \frac{1}{Bi(k+1)} + \frac{Pe^{1/2}}{\chi(1+k)^2} \tag{3.5}$$

The Marangoni force non-dimensionalized by viscous stress is given by

$$\tau_m = O\left\{\left[\frac{1}{\mu U}\right]\left[\frac{\partial\gamma}{\partial\Gamma}\right]_{\Gamma_o}\Delta\Gamma\right\} \tag{3.6}$$

where $\mu$ is the viscosity of the continuous phase. Using the fact that the derivative of the equation of state for Langmuir adsorption

$$\gamma - \gamma_c = RT\Gamma_\infty \ln\left(1 - \frac{\Gamma}{\Gamma_\infty}\right) = -RT\Gamma_\infty \ln\left(1 + \frac{\beta C_0}{\alpha}\right)$$

is:

$$\left[\frac{\partial\gamma}{\partial\Gamma}\right]_{\Gamma_o} = -\frac{RT}{1 - \frac{\Gamma_o}{\Gamma_\infty}} \tag{3.7}$$

we get

$$\tau_m = O\left\{Ma\left\{\frac{k}{Bi(k+1)} + \frac{kPe^{1/2}}{\chi(1+k)^2}\right\}\right\} \tag{3.8}$$

where Ma =$RT\Gamma_\infty/(\mu U)$.

In the limit in which the bulk concentration is large k>>1 and the kinetic and diffusive exchange are fast relative to convection ($\chi(k+1)/Pe^{1/2}>>1$ and $Bi(1+k)>>1$), the difference between the bulk and sublayer concentrations become small relative to $C_0$

$$\frac{\Delta C}{C_0} = \frac{Pe^{1/2}}{\chi(1+k)} << 1 \qquad (3.9)$$

Since the kinetic rate is much faster than the convective rate, the surface and the sublayer are in the equilibrium so that the variation in the sublayer concentration from the equilibrium $\Delta\Gamma$ is small and can be related to the small variation in $\Delta C$:

$$\frac{\Delta\Gamma}{\Gamma_\infty} = \frac{kPe^{1/2}}{\chi(1+k)^3} \qquad (3.10)$$

Therefore the Marangoni stress can be given by:

$$\tau_m = O\left\{Ma\left\{\frac{1}{Bi} + \frac{Pe^{1/2}}{k\chi}\right\}\right\} \qquad (3.11)$$

For remobilization of the surface, the Marangoni stress must tend to zero. On the assumption of large diffusive rate relative to convection ($\chi(k+1)/Pe^{1/2}>>1$) and high concentration (k>>1), the diffusive term in equation 3.11 tends to zero. The assumption of rapid kinetic exchange requires Bi(1+k)>>1, which could be satisfied by a small Bi and a large enough k. However in order to have remobilization, Bi must also be large .

Summarizing, the three conditions to achieve remobilization are:

a) High bulk concentration (k>>1)

b) Rapid kinetic exchange relative to convection, (kBi>>1 and Bi >>1)

c) Rapid diffusive exchange relative to convection, ($\chi(k+1)/Pe^{1/2}>>1$).

We note finally that these arguments are valid only when the surfactant exists as a monomer in the bulk phase; a theory for micelle-facilitated remobilization will be presented in Chapter 4

From the above criteria it is clear that a remobilizing surfactant must first be selected such that it exhibits rapid kinetic exchange, Bi>>1. We discuss this point first. As we have noted in Chapter 1 and 2, the kinetic parameters are measured in experiments in which the equilibrium and dynamic surface tensions are measured as a function of the bulk concentration of surfactant. Past studies have used two types of experiments to measure the surfactant diffusion coefficients and kinetic rate constants. These are:

(i) *Clean Interface Adsorption:* A fresh interface is created in a surfactant solution, and the relaxation in surface tension is measured as surfactant molecules adsorb from solution onto a static interface (the Wilhelmy plate or ring method and the pendant bubble technique) or a continuously deforming or flowing interface (oscillating jet, inclined plane, maximum bubble pressure, growing drop, and drop weight methods).

(ii) *Re-equilibration:* An equilibrium monolayer is perturbed either with small amplitude periodic oscillations (Langmuir trough and oscillating bubble methods) or large amplitude area changes (programmed area changes by an elastic ring or float on the air/water surface of a Langmuir trough as in the peak tensiometry, a reversed funnel, pulsating bubble and shrinking or expanding pendant bubble techniques), and the tension oscillation or relaxation as the interface re-equilibrates is measured.

For clean interface adsorption and re-equilibration, by modeling the kinetic exchange and the bulk diffusive and convective transport with the convective-diffusion equation, the surface concentration $\Gamma(t)$ can be predicted as a function of the surfactant transport parameters. From the equilibrium adsorption equation ($\Gamma_e(C_0)$) and the Gibbs-Duhem equation for the surface or

interfacial tension ($d\gamma = -RT\Gamma d\ln C_0$), an equation of state relating the surface tension $\gamma$ to the surface concentration can be obtained ($\gamma(\Gamma)$). (For example, for the Langmuir kinetic scheme for adsorption , the kinetic exchange is given by the following equation $\frac{\partial \Gamma}{\partial t} = \beta \Gamma_\infty C_s - (\beta \Gamma_\infty C_s + \alpha)\Gamma$ and the equilibrium adsorption and equation of state are $\frac{\Gamma_e}{\Gamma_\infty} = \frac{\beta C_0}{\alpha} / \left[1 + \frac{\beta C_0}{\alpha}\right]$; $\gamma - \gamma_c = -RT\Gamma_\infty \ln\left(1 + \frac{\beta C_0}{\alpha}\right)$ where $\gamma_c$ is the tension of the clean surface and $\alpha$, $\beta$, and $\Gamma_\infty$ are defined above.) From the equation of state the model prediction of the tension relaxation can be computed, and from a comparison of the model with the experimental results, ideally, the kinetic constants and the diffusion coefficient can be inferred. Equilibrium measurements of the tension as a function of the bulk concentration, when fitted to the equation of state, provide inter-relationships between the kinetic constants, and these facilitate the determination of the kinetic constants from the dynamic tension data. For example for Langmuir kinetics, the equation of state as a function of bulk concentration is $\gamma - \gamma_c = -RT\Gamma_\infty \ln\left(1 + \frac{\beta C_0}{\alpha}\right)$ , and fitting this curve to equilibrium data provides the ratio $\alpha/\beta$.

For air/aqueous surfaces, dynamic tension studies have shown that the more surface active surfactants with large hydrophobic chain lengths (8-16 methylene units) have relatively small desorption rate constants, $\alpha$, while the less surface active, intermediate length surfactants (3-7 methylene units) have larger desorption rate constants. This difference has been attributed to the fact that the longer the chain length, the greater is the activation energy required to desorb the long hydrocarbon chain into the aqueous phase and the smaller is $\alpha$. In particular for the intermediate chain length normal alcohols ($CH_3(CH_2)_{n-1}OH$), n=3-7, the kinetic desorption rate constant has been measured to be of order $10^2$ $sec^{-1}$, which is three or four orders of magnitude

larger than the desorption rate constants for the very surface active surfactants such as the $C_iE_j$ surfactants ($CH_3(CH_2)_{i-1}(CH_2)_jOH$, i=8-16.and j=2-8). Thus for aqueous systems the intermediate chain length alcohols are excellent remobilizing candidates.

The second requirement for remobilization is that the bulk concentration be large enough such that for k>>1, $\chi(k+1)/Pe^{1/2} \approx \chi k/Pe^{1/2} >> 1$. Careful examination of these criteria reveals that the condition is independent of the surface activity parameter $\alpha/\beta$, and can be written simply as $\frac{aC_o}{\Gamma_\infty Pe^{1/2}} >> 1$. Thus the higher the solubility of the surfactant, the greater is the potential for the surfactant near its solubility limit to remobilize the interface, even with Peclet numbers much greater than one. In this study we require that at the solubility limit, the surfactant does not aggregate into micelles but remains in monomeric form to illustrate remobilization in the absence of micellization. The intermediate chain length alcohols, suggested above as remobilization candidates in aqueous systems because of their large kinetic desorption rate constants, are also ideal for the satisfaction of this second criteria because they are very soluble in an aqueous phase and they do not form micelles. So we have selected these for study. To establish their remobilizing ability, we will measure the rise velocity of gas bubbles of the order of 100 μm – 1mm in radius in an aqueous phase, and a glycerol/water mixture. In an aqueous phase, for this size range of bubbles, the bubble rise velocity is too large, and the remobilizing requirement of Bi>>1 cannot be satisfied even for the relatively large values of desorption rate constants. For this reason, experiments are also undertaken with a 70:30 glycerol-water mixture as the continuous phase. The larger viscosity of this phase results in reduced velocities which allow for larger Biot numbers. The terminal velocity measurements are first undertaken in water with the four carbon alcohol butanol as a continuous phase to provide a reference for no

remobilization due to a reduced Biot number, and then in the glycerol-water mixture with the six carbon alcohol hexanol to demonstrate remobilization. Correct interpretation of remobilization for bubbles moving in the glycerol-water mixture containing alcohols necessitates measurement of the kinetic rate constants of the alcohol at the air/ glycerol-water mixture interface. These are undertaken first, using the pendant bubble technique to measure dynamic tensions, and are followed by the terminal velocity measurements.

## 3.2 MATRIALS AND METHODS EXPERIMENTAL SECTION

### 3.2.1 Materials

The study is carried out by measuring the terminal velocities of nitrogen bubbles rising either in water or in a 70:30 mixture by volume of glycerol-water. Medium chain alcohols, are used as the surface-active species. In preparing the continuous phase, the water used was purified from tap water using a Millipore Q System (Millipore, MA) with a specific resistance greater than 15 M ohm-cm. The glycerol was obtained from Fisher Scientific (ACS reagent, Cat. No. G33-4) and was used without any modification. Medium chain alcohols were used as the surface-active agents. For experiments in water, n-butyl alcohol was used, while n-hexyl alcohol was used with the mixture of glycerol/water. Butanol was obtained from Fisher Scientific (ACS reagent, Cat. No. A399-1), while hexanol (98% pure, Cat. No. 120799910) was obtained from Acros Organics.

### 3.2.2 Measurement of Dynamic and Equilibrium Surface Tension

The pendant bubble technique is used to measure the dynamic and equilibrium surface tensions. Fig. 3.1 presents a schematic diagram of the apparatus, which was developed in-house. A light beam produced by a lamp is collimated by passing through a series of lenses and a pinhole. A transparent quartz cell (2.5x4x4 cm) is filled with the surfactant solution and placed in the path of the collimated beam. An inverted stainless steel needle is immersed in the surfactant solution. A Cavro digital syringe pump is connected to the inverted needle through a three-way valve. A pendant bubble is formed rapidly (<200ms) on the edge of the needle by pushing air through the valve, tubing and the inverted needle. The collimated light forms a silhouette on the CCD array of the video camera (Kodak Ektapro fast motion video analyzer), placed on the other side of the quartz cell. The images of the bubble are captured and recorded sequentially in time. In the present study the images were captured at the maximum rate of 500 frames per second. Using Scion imaging software, the profile of the bubble is obtained. The surface tension is obtained by integrating the Young-Laplace equations and fitting the resulting numerical profile to the bubble profiles.

Two types of dynamic tension experiments are undertaken. In the first, clean interface adsorption experiment, a bubble is formed rapidly (<200 ms) on the tip of the inverted needle submerged in the surfactant solution of a known concentration. Surfactant adsorbs to the freshly formed interface, reducing the surface tension and elongating the bubble. The images of the bubble are captured sequentially with time until equilibrium is achieved. From the equilibrium data, the tension as a function of bulk concentration is obtained. In the second kind of experiment, after the surface concentration of the monolayer on the surface of the bubble has reached an equilibrium, the surface area of the equilibrium monolayer is changed, by sucking the

air out and contracting the bubble rapidly, causing a kinetic exchange with the sublayer and consequently with the bulk. The rate of compression of the bubble is chosen such that there are no hydrodynamic effects large enough to alter the shape of the bubble (as we explain below . Using the high speed camera, the image of the bubble during compression is recorded at the rate of 500 frames per second to probe the early time re-equilibration dynamics. These images are analyzed to measure the surface tension during compression.

We carried out clean interface adsorption to equilibration and re-equilibration dynamic surface tension measurements to measure the kinetic rate constants for the exchange of hexanol to the air/glycerol-water interface only. As the kinetic constants for the exchange of butanol to the air/water interface has been studied previously by Joos and Serrien [Joos & Serrien (1989)], no such attempt is made in the present study. The surface tension experiments for the adsorption of hexanol to the air/glycerol-water interface were done at relatively high bulk concentrations (2-8mM) of hexanol in glycerol-water mixture. These experiments were done at these high concentrations of hexanol so as to observe an appreciable amount of drop in surface tension (>1.5 dynes/cm) from the clean value, which is not obtained from concentrations of 1 mM or less, (also refer Figure 3.3). This is necessary as the error in measurements of surface tension from the following technique can be as high as 0.5 dynes/cm.

### 3.2.3 Measurements of Terminal Velocities of Rising Bubbles in Surfactant Solutions

In the present study, the mobility of the gas/liquid interface of a rising bubble is determined by measuring the terminal velocities of these rising bubbles. A schematic diagram of the experimental apparatus designed to measure their terminal velocities is presented in Figure

3.2. The apparatus consists of two parts, one horizontal capillary tube, in which bubble is created and second is the vertical chamber filled with the continuous liquid phase and connected to the capillary tube, in which the bubble rises and their velocities and shape are measured by video recording. A train of nitrogen bubbles is created in the horizontal precision bore borosilicate capillary tube of 0.254 mm inner diameter (Wilmad Glass, NJ) by injecting nitrogen into a flowing stream of continuous liquid phase. The stream is driven by a syringe pump and enters the capillary tube at the

'T' junction. The syringe pump controls the flow rate of the stream. The nitrogen, which is pushed into the stream is supplied from a nitrogen cylinder and is passed through a Gas purifier (Deierite, OH, Cat. No. 27068), before it enters the system. The flow rate of the nitrogen is controlled through the regulator present at the cylinder. As the nitrogen is pushed into the stream, it is broken into gas segments by liquid flow. By manipulating the flow rate of the nitrogen and the liquid, gas segments of different sizes can be obtained. We find that these segments can form bubbles of equivalent spherical diameter, as low as 0.25 mm and as high as 2 mm. Once the train of segments is formed in the capillary tube, both the flow of nitrogen and the liquid are stopped. Then slowly the liquid is pushed in the capillary tube, so as to release the desired segment from the end of the capillary tube into the vertical column and its terminal rise velocity and size is measured. The vertical column consists of a vertical borosilicate tube, 25 mm in diameter (Wilmad Glass, NJ) and 75 cm in length. With the help of a union, this tube is attached to another quartz tube of diameter 25 mm and length 70 cm. The upper part, where the bubble motion is recorded, is of square cross section. This is done to minimize the optical distortions. A set of three cameras are installed to measure the size and the terminal velocity of the bubbles. A parallel beam of light from a collimating lens system provides the back light for each of these

cameras. A pair of CCD cameras (Camera 1 & 2 in Figure 3.2), obtained from Dage MTI, IN and capable of capturing images at 30 frames per second are used to measure the average velocity of the bubbles. These two cameras are located at a distance of 260 mm apart. Camera 1 is located at a distance of approximately120 cm from the tip of the capillary, from where the bubbles are released into the column. Along with a 2X cosmicar multiplier, a cosmicar television lens f/1.4 50 mm is used to observe the bubbles. Both the cameras are connected to the VG-5 Scion Frame Grabber on the Macintosh G3. When the bubble passes through the first camera, the camera sends the signal to the computer which records the time, precise to 1/60 of a second. When the bubble passes through the second camera, it also sends the signal to the computer. The difference in these two times provides the time taken by the bubble to travel between the two cameras. Knowing the distance between the two cameras and the time taken by the bubble to travel this distance, the average velocity is measured. The fast video camera (Camera 3 in Figure 3.2), obtained from Kodak Ektapro, AZ), is utilized to capture the motion of the rising bubbles at 2000 frames per second. An Apollo television lens f/1.4 50 mm along with a cosmicar 2X multiplier is used on this camera. These images are used to measure the instantaneous velocity and the size of the bubbles. The high-speed camera is located at a distance of 210 mm above camera 2. The measured average velocity and the instantaneous velocities are compared to determine if the steady state is reached.

To minimize the surfactant contamination of the column, the glassware is cleaned, first with the mixture of nochromix and concentrated sulfuric acid while the stainless steel and plastic fittings were cleaned with methanol. After cleaning they were rinsed with deionized water, to remove the acid or methanol. After this cleaning procedure was completed, the column was filled with water and sparged with nitrogen gas. This is done to remove any trace amount of surfactant

that may still be present. These bubbles would bring these surfactants to the top of the column, from where they were continuously removed by siphoning out the water.

In our study, the viscosity of the continuous medium is measured in the following manner. The viscosity of glycerol-water mixture at $21^0$C is ~ 36 cp and is a strong function of both the temperature and composition of the mixture, therefore after every set of experiments a sample of the glycerol-water mixture was drained out from the column. Using a stress control rheometer AR-1000, (TA Instruments, DE), viscosity of the sample is measured at the temperature at which the experiments to measure the terminal velocity of the bubbles were conducted. The density of the mixture at room temperature ($21^o$C) was measured to be 1.192 gm/l, and is a weak function of temperature. However viscosity of water as a function of temperature has been studied extensively Coe and Godfrey [Coe & Godfrey (1944)], Korosi and Fabuss [Korosi & Fabuss (1968)] & Korson et al [Korson et al (1969)]. Therefore to determine the viscosity of water at the temperature of experiment, no attempt was made to measure it experimentally but the following correlation given by Korson et al was used.

$$\log_{10}\left(\frac{\eta_T}{\eta_{20}}\right) = \frac{1.1709(20-T) - 0.001827(t-20)^2}{t+89.93} \qquad (3.12)$$

where T is temperature in degrees centigrade, $\eta_T$ is the viscosity at temperature T, $\eta_{20}$= 1.0020 cp, viscosity at 20 $^0$C. Literature values were also used for the density of water.

## 3.3 RESULTS AND DISCUSSION

### 3.3.1 Measurements of the equilibrium surface tension of hexanol at the air/glycerol-water mixture surface as a function of concentration

Figure 3.3 presents the measurements of the equilibrium tension as a function of hexanol concentration ($C_0$), obtained from the longtime behavior of the tension relaxations in the pendant bubble technique. The surface tension keeps decreasing, until it becomes constant at a concentration of around 81 mM, which is the solubility limit of hexanol in 70:30 glycerol-water mixture. Hexanol does not form micelles as its head group (-OH) is small, which prevents the alcohol molecules to form micelles. This solubility limit is higher than in pure water (59 mM), reflecting the fact that glycerol being less polar than water makes the glycerol-water mixture more accommodating for the surfactant chains.

The least square fit of the equilibrium surface tension data by using both the Langmuir and Frumkin equation for kinetic exchange is presented in Figure 3.3. The parameters that yield a best fit of the Langmuir kinetic equation, are $\Gamma_\infty = 6.657 \times 10^{-10}$ mol/cm$^2$. $\alpha/\beta = 9.454 \times 10^{-6}$ mol/cm$^3$. According to Joos & Serrien, for the air/water interface these parameters are $\Gamma_\infty = 6.0 \times 10^{-10}$ mol/cm$^2$. $\alpha/\beta = 3.675 \times 10^{-6}$ mol/cm$^3$. Comparison of $\Gamma_\infty$, shows that the air/glycerol-water interface can accommodate slightly more surfactant molecules than the air/water interface. The comparison of the ratio of $\alpha/\beta$ shows that the activation energy for desorption is less in the case of air/glycerol-water mixture as compared to air/water interface, again pointing out to the fact that the glycerol-water mixture is less polar than water. The parameters that yield a best fit of the Langmuir kinetic equation, with the experimental data are $\Gamma_\infty = 6.62 \times 10^{-10}$ mol/cm$^2$, $\alpha/\beta = 9.564 \times 10^{-6}$ mol/cm$^3$ and the interaction parameter K = -0.0616. The slightly negative value of K

shows the presence of small cohesive interactions between the hydrocarbon chains, which with increase in surface coverage, increases the activation energy for desorption. The parameters $\Gamma_\infty$ and $\alpha/\beta$ are similar to the values obtained for Langmuir kinetic equation, confirming that Langmuir model can predict the sorption kinetics quite accurately and would be used to carry out any further analysis of the experiments.

### 3.3.2 Measurements of the dynamic surface tension of hexanol at the air/glycerol-water mixture surface as a function of concentration

In Figure 3.4, the dynamic surface tension measurements for adsorption of hexanol onto a clean air/glycerol-water interface is presented at hexanol concentrations of 2mM and 4mM. These experiments were done at these high concentrations of hexanol so as to observe an appreciable amount of drop in surface tension (>1.5 dynes/cm) from the clean value (Also refer Fig. 3.3). This is necessary as the error in measurements of surface tension can be as high as 0.5 dynes/cm. For each of these concentrations, equilibrium was reached within 1 second of formation of the clean interface. To interpret these results in terms of values for the kinetic parameters, we note first that surfactant molecules transfer to the interface through two transport mechanisms. They diffuse from bulk to the sublayer and kinetically adsorb from the sublayer to the interface. The characteristic time scale for diffusion is given by $\tau_{diffusion}=(\Gamma_\infty/C_0)^2/D$. The characteristic time scale for kinetic adsorption is given by $\tau_{kinetic}=1/(\beta C_0+\alpha)$. Hence the ratio of the characteristic kinetic time scale to diffusive time scale is given by

$$\tau_{kinetic}/\tau_{diffusion}=(\Gamma_\infty/C_0)^2/(\beta C_0+\alpha))/D. \qquad (3.19)$$

To get a lower bound for the kinetic sorption coefficients, we can assume that the mass transfer process is purely kinetically limited since estimates with this assumption provide the smallest values for the constants. For hexanol in glycerol-water mixture at concentrations of 2 and 4 mM, the equilibrium is reached within 1 second (refer Figure 3.4). Thus $\tau_{kinetic}$ is of order 1 second or shorter. Knowing the ratio of $\alpha/\beta$, a lower bound for $\alpha$ is calculated from $\tau_{kinetic}=1/(\beta C_0+\alpha)$. to be O(1) $sec^{-1}$. For this value of $\alpha$ and at experimental conditions, the ratio $\tau_{kinetic}/\tau_{diffusion}$ were found to be O(1), which shows that the process follows mixed kinetics.

To obtain a tighter bound on the kinetic constants, dynamic tensions are measured for the case in which a pendant bubble with an equilibrium monolayer is rapidly compressed. The rate of contraction to be used is obtained from the following considerations. If the rate of contraction is large, then the hydrodynamic effects would change the shape of the bubble and hence the surface tension cannot be measured accurately. However if the contraction rate is too small, then the kinetic rate constants for hexanol cannot be measured accurately because these surfactants (medium chain alcohols) have large kinetic rate constants and so they exchange rapidly to/from sublayer/interface. Therefore if the rate of change in surface area of the pendant bubble is small, the interface would remain at equilibrium and only bounds for kinetic rate constant would be determined.

To determine the optimum rate of contraction of the pendant bubble, experiments were carried out in a pure 70:30 mixture of glycerol-water. Pendant bubbles of similar size were formed and then contracted at contraction rates of 7.5 $mm^2/s$, 13 $mm^2/s$ and 180 $mm^2/s$. The surface tension was measured continuously during compression at these rates. Fig. 3.5 presents the result of the study. As the system is pure, i.e. no surfactant impurities were present, it is expected that the measured surface tension should remain constant. However it is found that at

the compression rates of 7.5 and 13 $mm^2/s$, the surface tension remained nearly constant for approximately 2.5 and 1.2 seconds after compression was started, respectively. However, surface tension starts to change appreciably after that. It is due to the fact that by then the bubble has been compressed to a very small size and then the bulk flows are causing hydrodynamic effects, strong enough to alter the shape of the bubble. For contraction rate of 180 $mm^2/s$, it was found that the surface tension started to change appreciably with contraction. At this contraction rate the inertial effects becomes significantly large enough to change the shape of the bubble and the surface tension cannot be measured accurately. Therefore for all the dynamic surface tension measurements, the next highest compression rate of 13 $mm^2/s$ was chosen. The compression was carried out for one second, as after that the pendant bubble became too small to measure surface tension accurately.

In Figure 3.6 the dynamic tension measured following equilibrium compressions of a hexanol monolayer is presented. The experiments are carried out at bulk concentrations of 4mM and 8mM and at a temperature of $23^0$C. The bubble was contracted approximately at a rate of 13 $mm^2/s$ and the contraction process was carried out for approximately 1 second. The results can be interpreted in terms of a simple kinetic model to describe the transport. If the surfactant follows the Langmuir kinetic scheme and the transport is kinetically controlled,

$$\frac{1}{A_t}\frac{\partial(A_t\Gamma(t))}{\partial t} = \beta C_0(\Gamma_\infty - \Gamma(t)) - \alpha\Gamma(t)e^{K\Gamma(t)} \qquad (3.13)$$

where $A_t$ is the area of the interface at time t. Figure 3.7 presents a sample area of the pendant bubble, which is changing with time, during compression at a rate of 13 $mm^2/s$. This data can be fit by a quadratic equation

$$A_t = A_0t^2 + A_1t + A_2 \qquad (3.14)$$

An analytical solution to the above equation in terms of the quadratic fit is is:

$$\Gamma(t) = \frac{A_0\Gamma_e}{A_t} e^{-(\beta C_0+\alpha)t} + \frac{\beta C_0 \Gamma_\infty}{A_t} e^{-(\beta C_0+\alpha)t}\left[\frac{A_t}{\beta C_0+\alpha} e^{(\beta C_0+\alpha)t} - \frac{e^{(\beta C_0+\alpha)t}}{(\beta C_0+\alpha)^2}\frac{dA_t}{dt} + \right.$$
$$\left. \frac{2A_2}{(\beta C_0+\alpha)^3}(1+e^{(\beta C_0+\alpha)t}) - \frac{A_0}{\beta C_0+\alpha} - \frac{A_1}{(\beta C_0+\alpha)^2}\right] \quad (3.15)$$

Also presented in Figure 3.6 are the curves predicting the dynamic surface tension for the values of $\alpha$ equal to 0,1,10 and 100 $sec^{-1}$. These curves are generated by coupling equation 3.15 (which describes the kinetically limiting transport of surfactant to the surface of the bubble) and the Langmuir equation of state which provides a relationship between surface concentration and surface tension. In these experiments (refer figure 3.6a & b) a dip in the surface tension can be seen at initial time, when the compression of the bubble starts. The drop in the surface tension is more than for the case when the surfactant is assumed insoluble ($\alpha$=0), which is the lowest surface tension that can be achieved by the compression of the monolayer with equilibrium surface concentration. The dip is caused by the hydrodynamic effects generated when the syringe pump starts to suck the air from these bubbles and the contraction process starts. In particular, the start-up of the fluid motion represents an effective constant acceleration which subtracts from the gravitational acceleration to yield a reduced acceleration which accounts for the reduction in tension.

From the results it can be seen that a minimum value of $\alpha$ of 10 $s^{-1}$ can predict the kinetic exchange observed in our experiments. For this value of $\alpha$ and at experimental conditions, the ratio $\tau_{kinetic}/\tau_{diffusion}$ obtained from equation 3.23 is determined to be 0.4, when the concentration of hexanol in the solution is 4 mM, and 1.1 when the concentration is 8mM. It shows that the

process is not limited by diffusion but follows mixed kinetics and therefore $\alpha$ can actually be larger than the estimate of 10 $s^{-1}$.

We note that for the kinetic exchange of hexanol at the air/water interface, Joos and Serrien found $\alpha$ to be O(100). On comparing the solubility and the ratio $\alpha/\beta$ of hexanol in glycerol-water mixture and in pure water, we noticed that glycerol-water mixture is less polar or more accommodating to hexanol molecules, as compared to pure water. Therefore the ratio of $\alpha/\beta$ for hexanol in glycerol-water mixture should be higher than for hexanol in water. In our study we found the lower bound to $\alpha$ to be O(10) $sec^{-1}$, but $\alpha$ could be as high as O(100) and further set of experiments are required to confirm it.

### 3.3.3 Terminal Velocities of Bubbles Rising in Bulk Liquid Containing Alcohol Surfactants

The terminal velocity of the bubbles for the pure system i.e. without surfactants dissolved in the bulk phase, were measured first. These results were compared with the theoretically predicted values, using the correlations available in Magnaudet et al [Magnaudet, Rivero & Fabre (1995)], Clift et al [Clift, Grace & Weber (1978)] & Beard and Pruppacher [Beard & Pruppacher (1969)]. A successful comparison would indicate that our cleaning procedures are adequate and the calibrations are accurate.

After measuring the average and instantaneous velocity of the bubbles, these velocities are compared to determine if the terminal velocity was reached. The difference in the velocity was within 2% and we assume that the steady state is reached. The average of these two velocities are reported and presented in figure 3.8, where the terminal velocities of the bubbles

are plotted as a function of their size. The Weber number and the Capillary number for these bubbles are small. Therefore the motion of the bubbles does not cause any significant deformation to the shape of the bubbles and the bubbles remain spherical. This is confirmed by the video images of the rising bubbles, which show the bubbles are spherical.

Also presented in figure 3.8, is the predicted terminal velocity of a spherical bubble and a similar solid sphere. To determine the predicted velocity of a bubble of given size and rising in a bulk fluid of known density and viscosity, the following correlations given by Magnaudet et al are used.

$$C_D = \frac{8ag}{3U^2} = \frac{16}{\mathrm{Re}}(1 + 0.15(2\,\mathrm{Re})^{0.5}) \qquad \mathrm{Re} < 25 \tag{3.16a}$$

$$C_D = \frac{8ag}{3U^2} = \frac{48}{\mathrm{Re}}(1 - 2.21(2\,\mathrm{Re})^{-0.5}) \qquad \mathrm{Re} > 25 \tag{3.16b}$$

where Re is the Reynolds number and is given by $\mathrm{Re}=\rho Ua/\mu$, $\rho$ is the density of the continuous medium, U is the velocity of the bubble, a is the radius of the bubble and $\mu$ is the viscosity of the continuous medium. The predicted velocity is obtained by solving for U in the equation.

To determine the predicted velocity of a solid sphere, the following correlations provided in Clift et al are used.

$$C_D = \frac{8ag}{3U^2} = \frac{24}{\mathrm{Re}}\left(1 + 0.1935(2\,\mathrm{Re})^{.6305}\right) \qquad \mathrm{Re} > 20 \tag{3.17a}$$

$$C_D = \frac{8ag}{3U^2} = \frac{24}{\mathrm{Re}}\left(1 + 0.1315(2\,\mathrm{Re})^{(0.82 - 0.015\log_{10}\mathrm{Re})}\right) \qquad \mathrm{Re} < 20 \tag{3.17b}$$

From our measurements of the terminal velocities of bubbles (refer Figure 3.8a & b), we note that smaller bubbles rise with velocities less than the predicted values and near the solid sphere value, while large bubbles behave more like clean bubbles, indicating that even after our rigorous cleaning procedure, there is still some trace amount of surfactant impurity present in our system. This trace amount of surfactant effects small bubbles more than the large bubbles. As compared to a large bubble, small bubbles have a larger Marangoni number, $Ma = RT\Gamma_\infty/\mu U$. As described in chapter 2, a large Marangoni number represents a large retarding or Marangoni forces. Therefore a small bubble has a tendency to become interfacially immobile faster than a large bubble**.**

Medium chain alcohols were used as surface active species in our experiments. Butanol was used as surface active species with water, while hexanol was used with 70:30 mixture of glycerol/water. All these experiments were done at a temperature between 21 – $25^0$C. In our analysis of the experiments with butanol in water, the viscosity of the mixture is assumed to be similar to that of pure water and is obtained from the correlation described by equation (3.23). The viscosity of hexanol in glycerol-water mixture was obtained by measuring it using a stress control rheometerAR-1000, (TA Instruments, DE). After every set of experiments, a sample of the bulk liquid was drained out from the column and the viscosity of the sample is measured at the temperature at which the experiments to measure the terminal velocity of the bubbles were carried out. The key properties of these two systems are presented in Table 3.1.

First experiments to measure the terminal velocities of bubbles of different sizes were done with butanol in water. These experiments were done in the range of butanol concentrations of 0.5 mM to 350mM. The experimental results are presented in figure 3.9. The observed

velocity is normalized by both the clean bubble and the solid velocity. The normalized velocity is defined by the following formula:

$$U_{NR}= (U_o-U_{BUBBLE})/(U_{SOLID}- U_{BUBBLE})*100 \quad (3.18)$$

where $U_{NR}$ is the normalized velocity, $U_o$ is the measured velocity, $U_{BUBBLE}$ is the velocity of a clean bubble and $U_{SOLID}$ is the velocity of a similar solid sphere. Thus a $U_{NR}$ of 0 would represent that the bubble is behaving like a clean bubble or with a completely mobile interface. On the other hand $U_{NR}$ of 100 would represent that the bubble is behaving like a solid sphere or that the interface is completely immobile.

When the concentration of butanol in water is 0.35mM, the bubbles in the diameter range of 0.25-0.3 mm are 90% immobilized, while bubbles with the diameter range of 0.55-0.6 mm are 30% immobilized. For these bubbles (k+1)Bi = O(0.1), (for average sized bubble, (k+1)Bi =0.23**)** which is less than one., and the parameter $\chi(k+1)/pe^{1/2}$ <<1,(for an average sized bubble, $\chi(k+1)/pe^{1/2}$ =0.09). Thus at this concentration of butanol in the bulk solution, surface convection dominates both diffusive and kinetic exchange. Therefore there is a formation of stagnant caps on the surface of these bubbles. As the concentration of butanol is increased, the parameters $\chi(k+1)/pe^{1/2}$ and (k+1)Bi also increases. At the highest concentration (350 mM), in our study and for an average sized bubble, $\chi(k+1)/pe^{1/2}$ is O(100), while (k+1)Bi is O(10).Therefore at these concentrations, the surfactant mass transfer due to diffusion and kinetic exchange is greater than surface convection. Therefore the degree of surfactant concentration gradient on the bubble surface is also decreased. However no remobilization is achieved, as the marangoni stress is not reduced. As described in chapter 1 and section 3.1 of this chapter, the marangoni stress acting on the bubble surface, described by equation (3.8), is eliminated or reduced, when k>>1, kBi>>1, Bi >>1 and $\chi(k+1)/pe^{1/2}$>>1. However this system satisfies all the above mentioned criteria, except

for the biot number Bi, which is 0.4 <1. Therefore no remobilization is achieved and the surface of the bubble remains immobile.

Butanol could not remobilize the interface of the bubbles rising in water. This is due to the small biot number (Bi=αa/U) Therefore to increase the biot number, or reduce terminal velocity (U), glycerol was added to water. This increases the viscosity of the bulk liquid and thus, reduces the terminal velocity of the bubbles and therefore surface convection. Figure 3.10, presents the results of the experiments carried out to measure the normalized terminal velocities of nitrogen bubbles of diameter ranging from 0.95-2.05 mm, rising in a 70:30 mixture of glycerol/water containing hexanol as the surface active species. This study was carried out with hexanol concentration ranging from as low as 0.038 mM to as high as 70.11 mM.

At a concentration of 0.038 mM of hexanol in the solution, for an average sized bubble the parameters, (k+1)Bi is >O($10^{-2}$) and $\chi(k+1)/pe^{1/2}$ is O($10^{-3}$). We are not sure of exactly how the rate of kinetic exchange compares with surface convection as through our pendant bubble experiments, only the lower bound of the coefficient for desorption ($\alpha$) for the exchange of hexanol at air/glycerol-water interface could be measured. However since $\chi(k+1)/pe^{1/2}$ <<1 or surface convection dominates over diffusive flux, therefore regardless of how kinetic exchange compares with surface convection, there is formation of stagnant caps on the surface of these rising bubbles.

At the highest concentration of hexanol in our study of 70.11 mM, we observed an average remobilization of 22%. If we compare our results to the theoretical study carried out by Chen and Stebe [Chen & Stebe (1996)], for the bubbles rising in a surfactant solution, in creeping flow limits, with kinetically limited mass transfer. Under similar experimental conditions (Refer Table 3.1) of Marangoni number of 10, biot number of 0.2 (as determined by

the lower bound for $\alpha$) and k (non dimensional bulk concentration) of 10, their study suggests that no remobilization should be achieved. However according to the same authors, under similar conditions but with a biot number of 2.5, 22% remobilization should be observed, which is same as the one that we observed in our experiments with bubbles rising at Reynolds number of O(1). We believe that one order of magnitude of Reynolds number should not be significant in the observation of remobilization, pointing to the fact that the actual value of Biot number or $\alpha$ maybe one order of magnitude larger than the lower bound for $\alpha$ or Bi, that we measured. This claim can be substantiated from the study carried out by Joos and Serrien where they measured $\alpha$ for hexanol in water to be 98 $s^{-1}$, which is one order of magnitude greater than the lower bound that we measured. Since glycerol-water mixture is less polar than water, therefore it is expected that $\alpha$ for hexanol in glycerol-water mixture to be greater than for hexanol in water. Similar observations were made by Palaparthi et al [Palaparthi et al (2005 & 2006)] in their study. They observed that both $C_{12}E_6$ and $C_{10}E_8$ have higher value of $\alpha$ in glycerol-water mixture as compared to water. Using Frumkin model, these authors found the lower bound of $\alpha$ for $C_{12}E_6$ and $C_{10}E_8$ in 70:30 glycerol-water to be $9X10^{-3}$ and $3.5X10^{-1}$ $s^{-1}$ respectively. These values are greater than $\alpha$ for $C_{12}E_6$ and $C_{10}E_8$ in water, which are $1.4X10^{-4}$(measured by Pan et al [Pan, Green & Maldarelli (1998)] and $9.7X10^{-1}$ $s^{-1}$, measured by Chang et al [Chang et al (1998)] respectively.

## 3.4 CONCLUSIONS

In this chapter, we described our experimental investigation on the effect of soluble surfactants which remain in monomeric form at high concentrations on the mobility of the

gas/liquid interface of a bubble rising in a continuous liquid phase in the high concentration limit. The change in the interfacial mobility affects the drag experienced by a translating bubble and hence its terminal velocity. The lower the mobility, the higher is the drag and when the mobility reduces to zero, the drag is maximum and is equal to that of a similar solid sphere.

The surfactants used in our study were medium chain alcohols and the continuous liquid phases were water and a 70:30 mixture of glycerol-water. In this study, we measured the terminal velocities of buoyantly rising bubbles as a function of bulk concentration of the surfactant dissolved in the continuous phase. The size of the bubbles rising in water were limited to 0.25-0.8 mm in diameter, while those rising in more viscous glycerol-water mixture were 0.95-2.05 mm in diameter. These bubble sizes were chosen so that the Weber and capillary numbers are less than one and therefore the bubble experiences negligible distortion and remains spherical in shape. The Reynolds number was O(1) for bubbles rising in glycerol-water mixture and O(10) for those rising in water. Our results show that at low concentrations of surfactants in the continuous phase, the interface is partially immobile, due to the formation of stagnant caps on the bubble surface. As the concentration of the surfactant in the bulk liquid phase is increased, the bubbles loose their interfacial mobility and become completely immobile. According to our study even at the highest concentration of 350 mM of butanol, dissolved in water the interface of the bubble remains immobile. However at this concentration, the interface of the bubble is uniformly retarded, instead of having a stagnant cap covering the whole or part of surface. At the highest concentration of 70.1 mM of hexanol dissolved in glycerol-water mixture, an average remobilization of 22% is achieved. To use these results to experimentally verify the criteria for remobilization (described in chapter 2 and section 3.1 of this chapter), the kinetic parameters for adsorption and the diffusion coefficient of the surfactant in the continuous liquid phase were

determined. Kinetic coefficients for butanol in water were obtained from literature, while for hexanol in glycerol-water mixture, lower bound for the kinetic coefficient of desorption ($\alpha$) was obtained from dynamic surface tension measurements obtained. We compared our results to the study carried by Chen and Stebe [Chen & Stebe (1996)] and found that $\alpha$ is at least one order of magnitude greater than minimum value that we measured through our experiments using pendant bubble tensiometry.

| | *Hexanol in glycerol -water mixture* | *Butanol in water* |
|---|---|---|
| Solubility ,*mM* | 81.1 | 983.5 |
| D, $cm^2/s$ | $1.6X10^{-7}$ | $8.8X10^{-6}$ |
| k* | 7.4 | 7.4 |
| $\alpha$, $s^{-1}$ | >10 | 86.7 |
| $\alpha/\beta$,$mole/cm^3$ | $9.45X10^{-6}$ | $4.7X10^{-5}$ |
| $\Gamma_\infty$ , $moles/cm^2$ | $6.6X10^{-10}$ | $6.0X10^{-10}$ |
| Re | O(1) | O(10) |
| Ma | 12.4 | 295.2 |
| Bi* | >0.2 | 0.4 |
| Bi(1+ k)* | >21.8 | 10.7 |
| Pe | $O(10^6)$ | $O(10^4)$ |
| $\chi(k+1)/pe^{1/2}$ * | O(10) | O(100) |
| Remobilization* | 22% | 0% |

* at the highest concentration of our study.

**Table 3.1 Properties of hexanol in glycerol-water mixture and butanol in water and characteristic values of non-dimensional groups.**

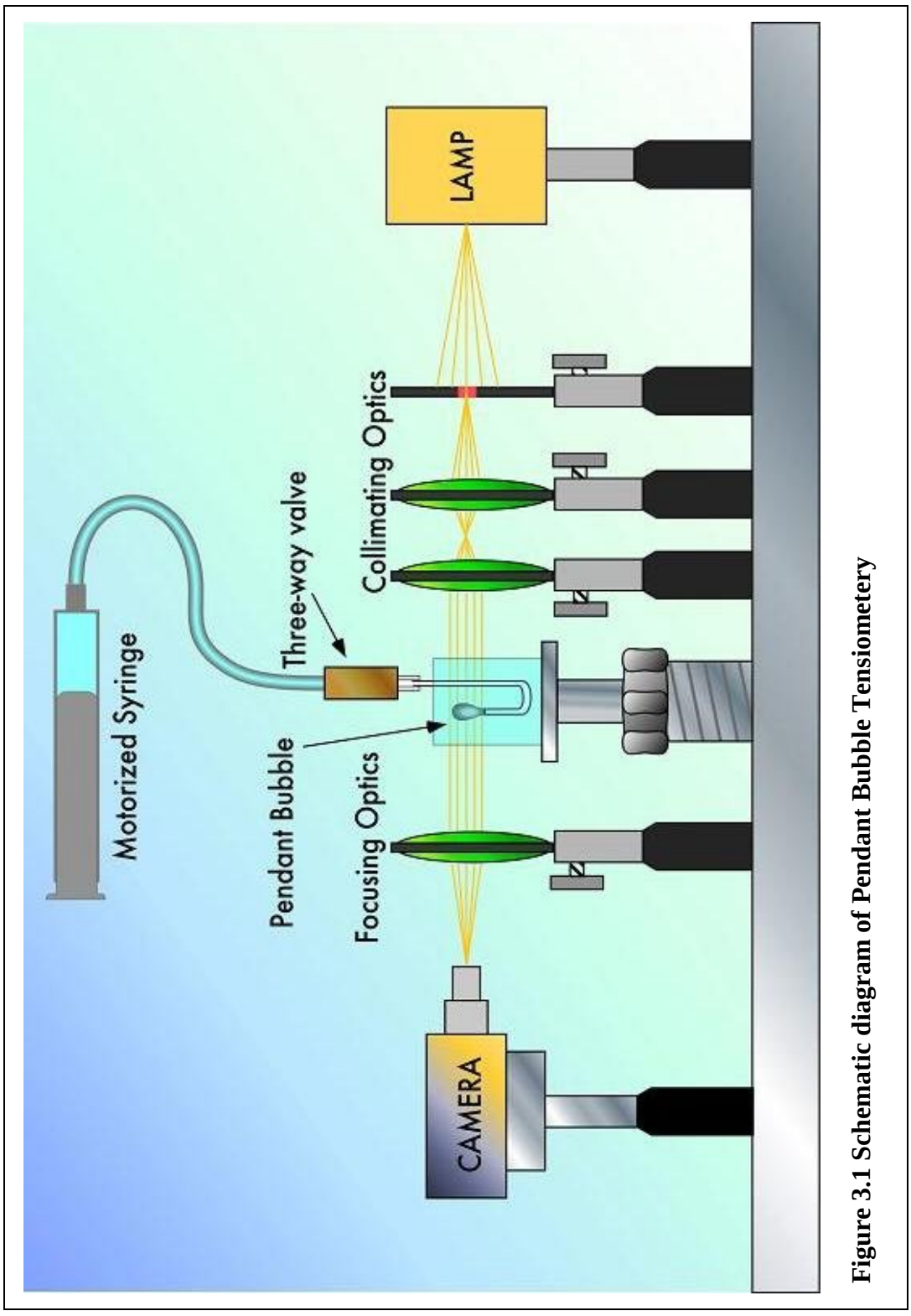


**Figure 3.1 Schematic diagram of Pendant Bubble Tensiometery**

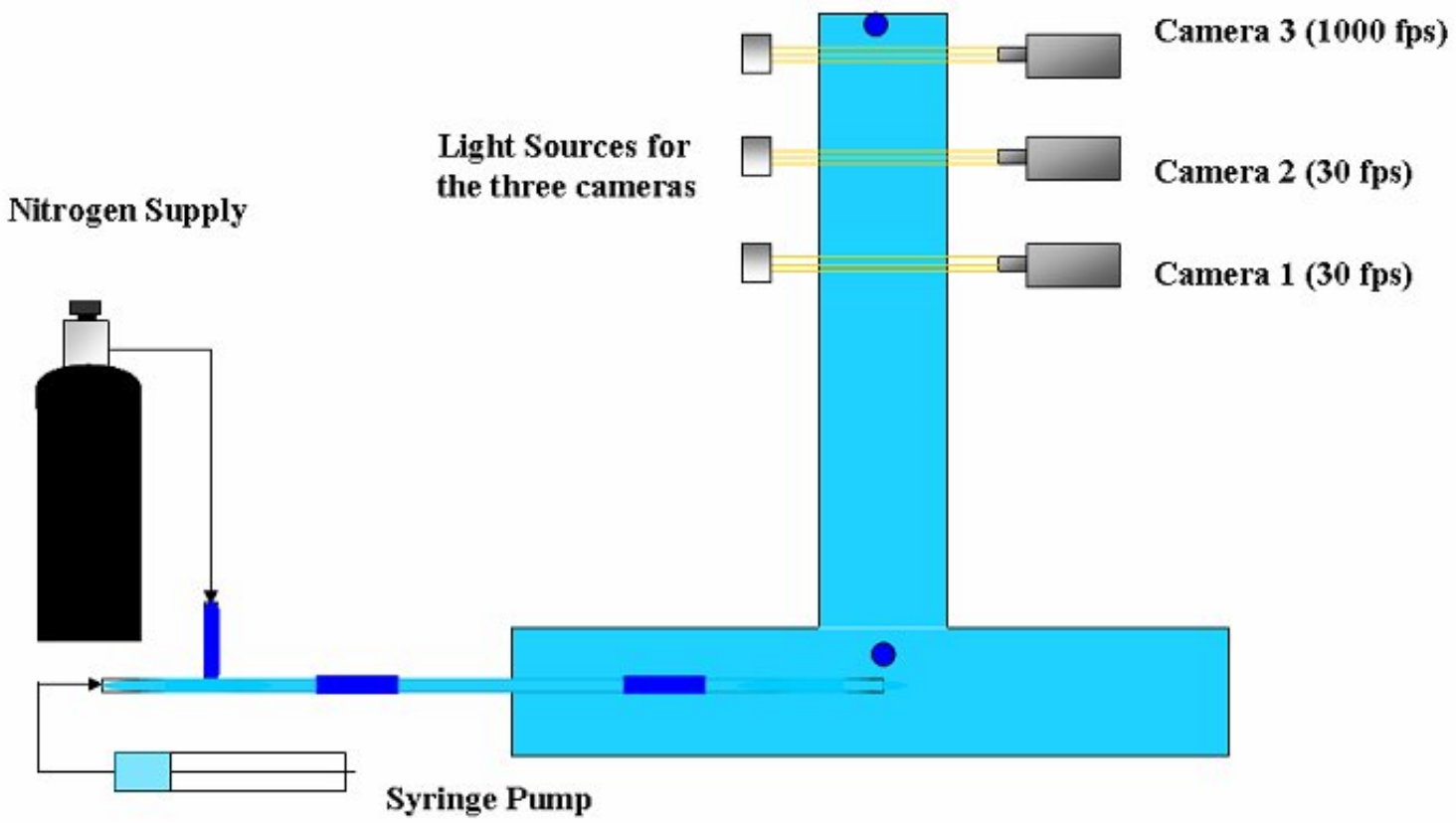


**Figure 3.2 A Schematic diagram of experimental setup to measure terminal velocity of rising bubbles**

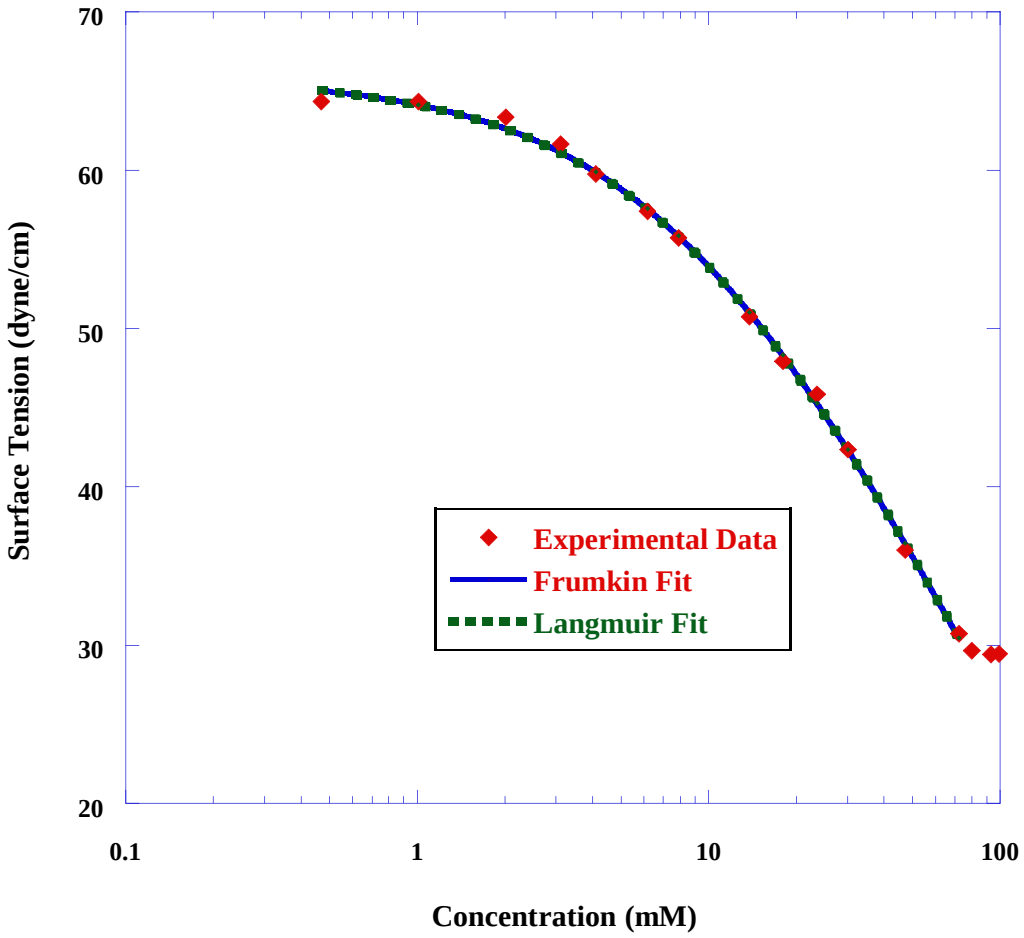


**Figure 3.3 Equilibrium surface tension measurements for solutions of Hexanol in glycerol/water mixture at air/glycerol-water mixture and Langmuir and Frumkin fit of this data**

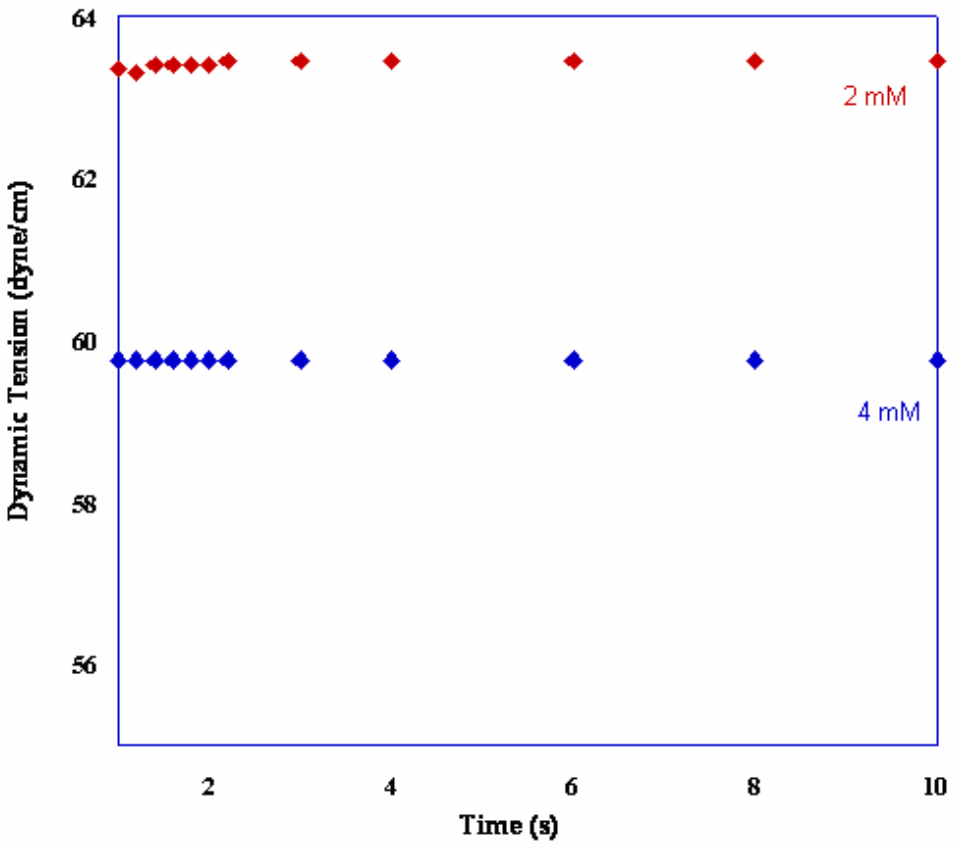


**Figure 3.4 Dynamic surface tension relaxation for adsorption of hexanol at initially clean air/70:30 glycerol-water interface as measured by pendant bubble technique**

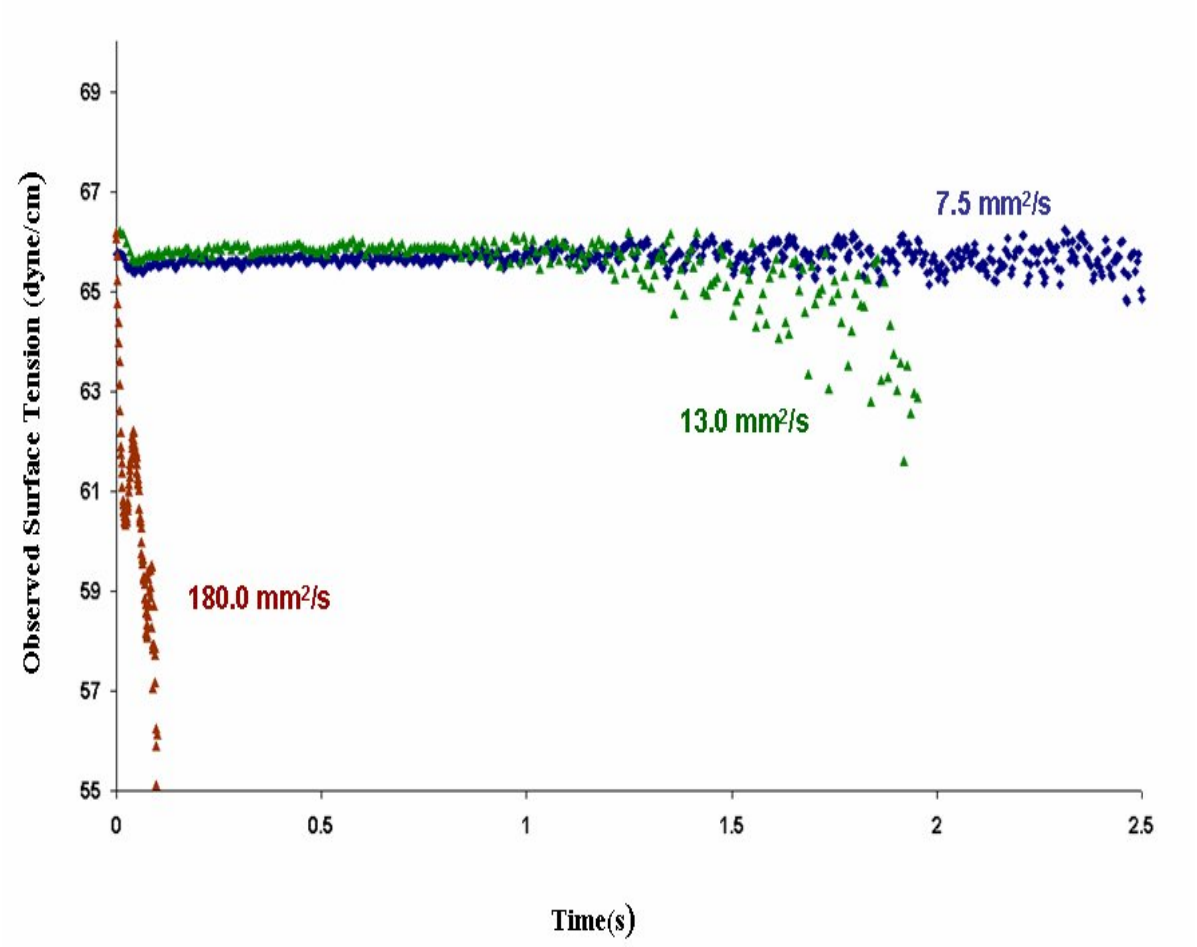


**Figure 3.5 Surface Tension measurements for pure Glycerol/Water Mixture at compression rates of 7.5, 13, 180 $mm^2/s$**

.

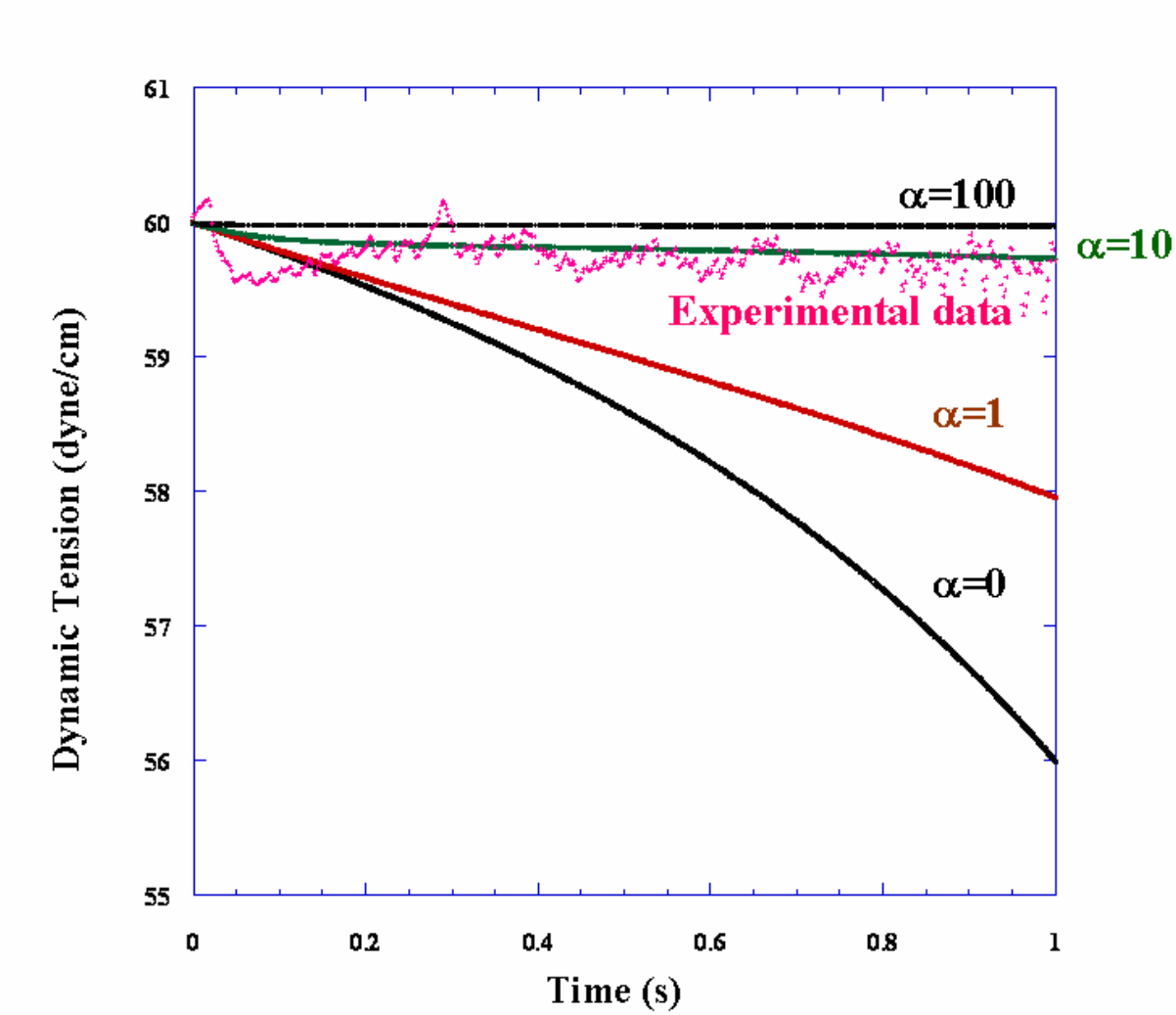


**Figure 3.6a Dynamic surface Tension measurements at a Hexanol concentration of 4mM and comparison with theoretical predictions for value of α = 0,1,10,100 and the bubble contraction rate of 13 $mm^2/s$**

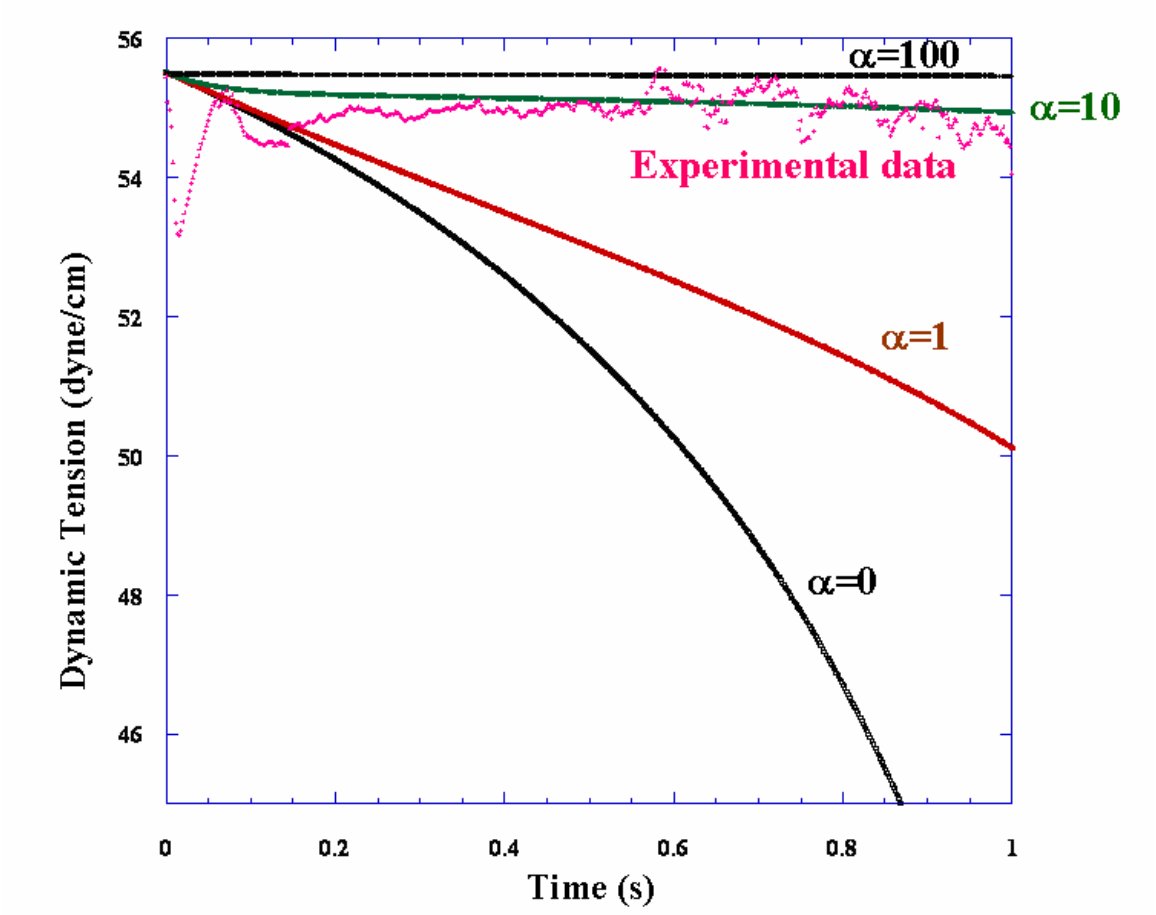


**Figure 3.6b Dynamic surface Tension measurements at a Hexanol concentration of 8mM and comparison with theoretical predictions for value of α = 0,1,10,100 and the bubble contraction rate of 13 mm$^2$/s**

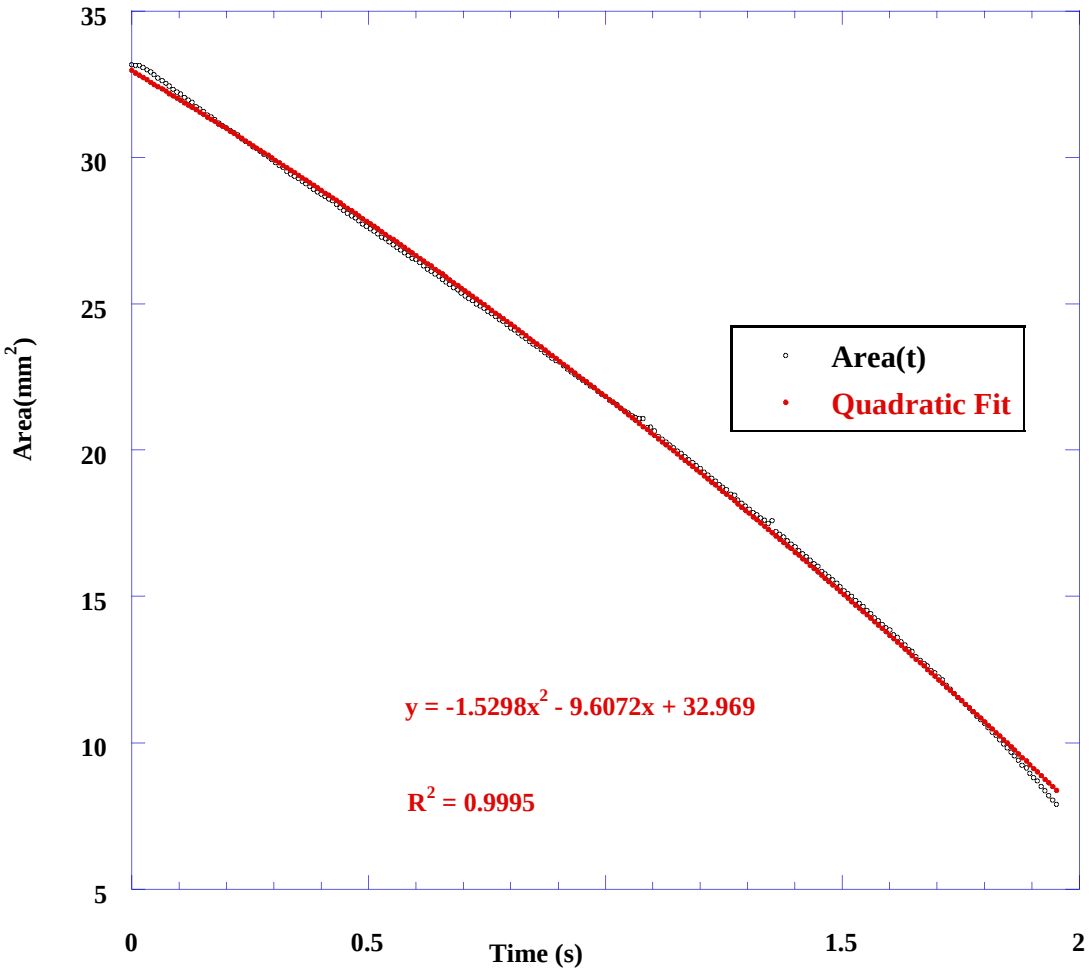


**Figure 3.7 Area change of the compressing pendant bubble during compression at the rate of 13 mm$^2$/s and a quadratic fit to the data**

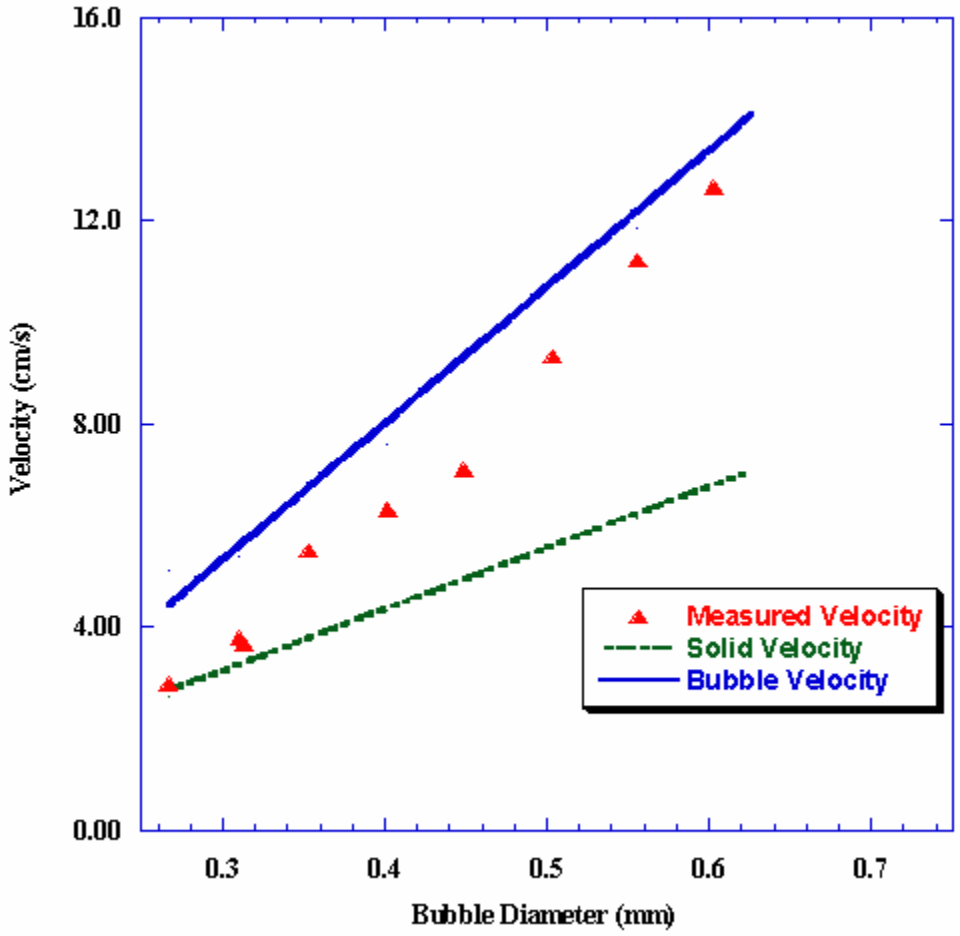


**Figure 3.8a Measured bubble terminal velocities in pure water -Comparison with theoretical prediction by equation 3.25 and 3.26**

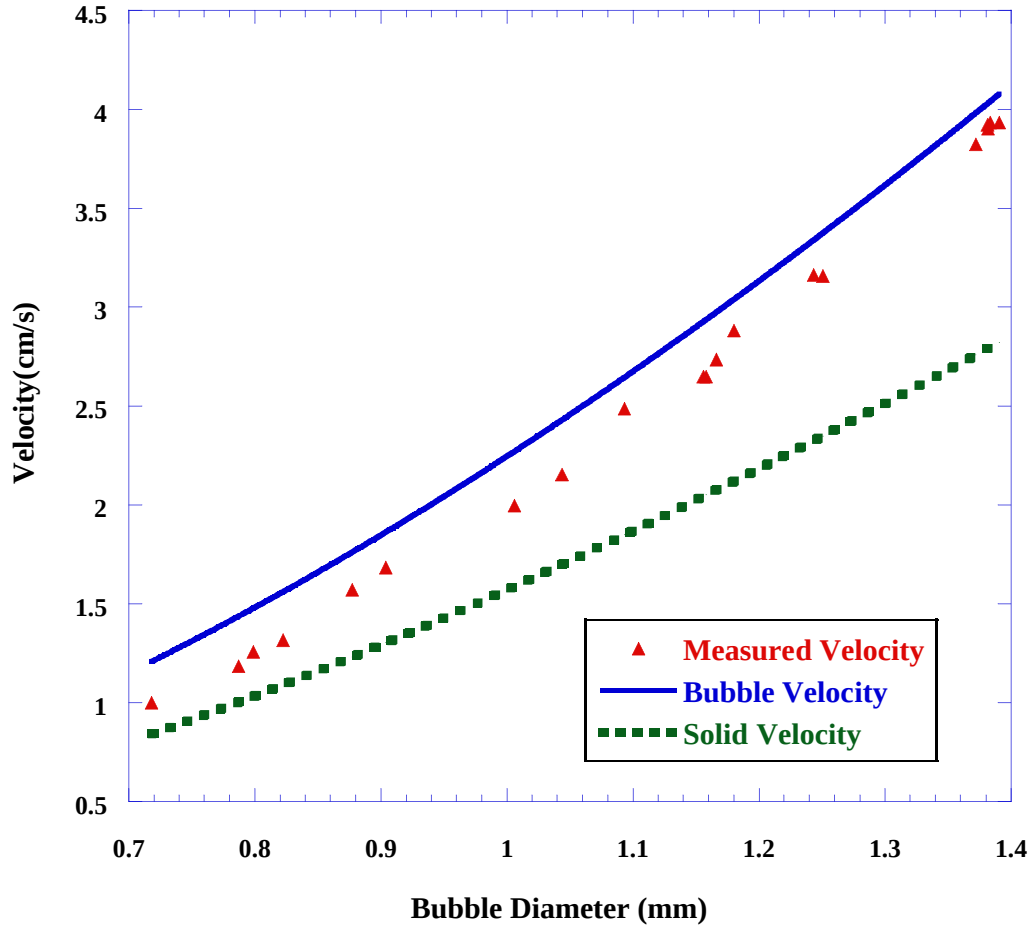


**Figure 3.8b Measured bubble terminal velocities in 70:30 glycerol-water mixture- Comparison with theoretical predictions by equation 3.25 and 3.26**

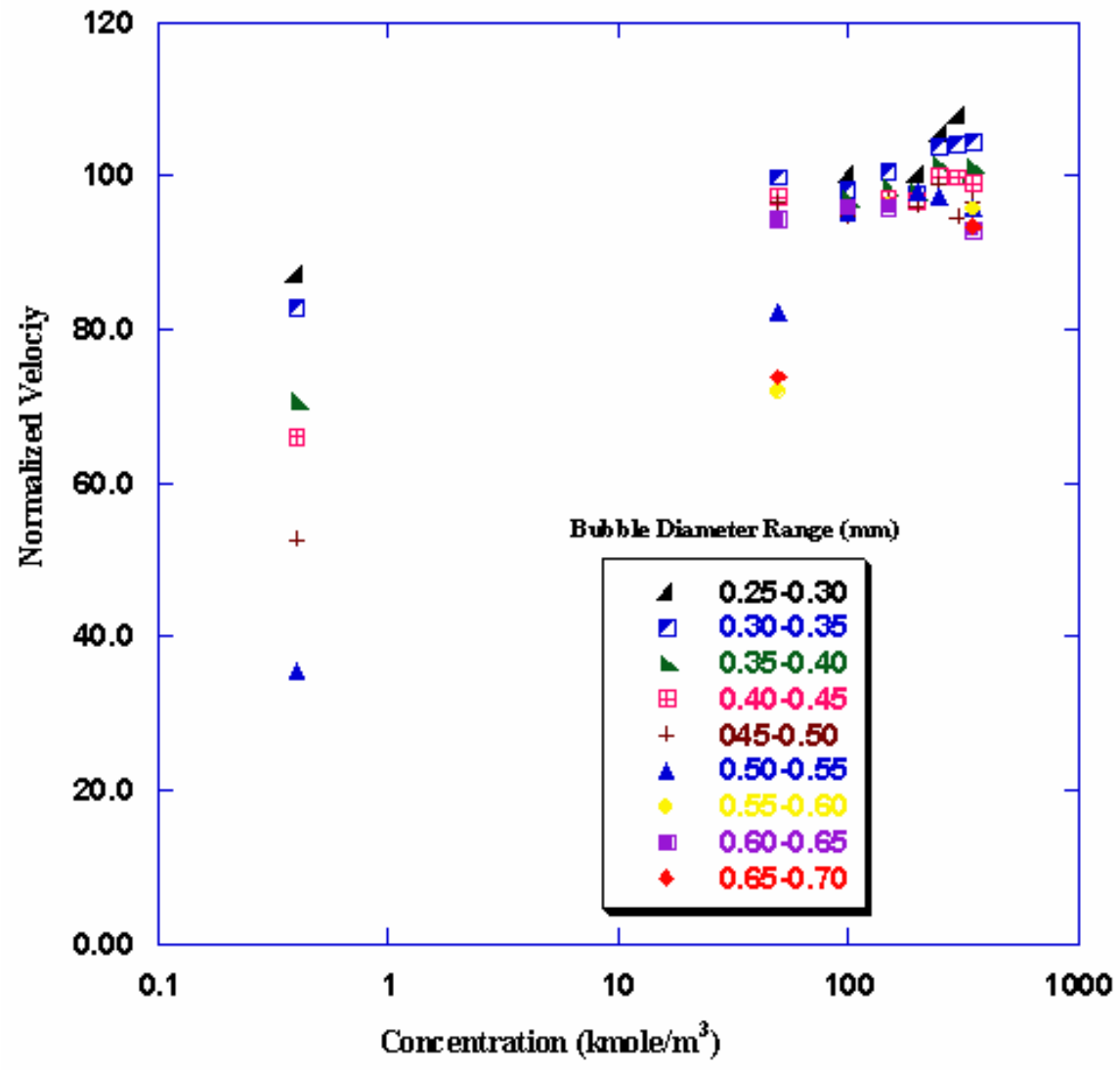


**Figure 3.9 Effect of butanol concentration on the normalized velocity of nitrogen bubbles rising in water**

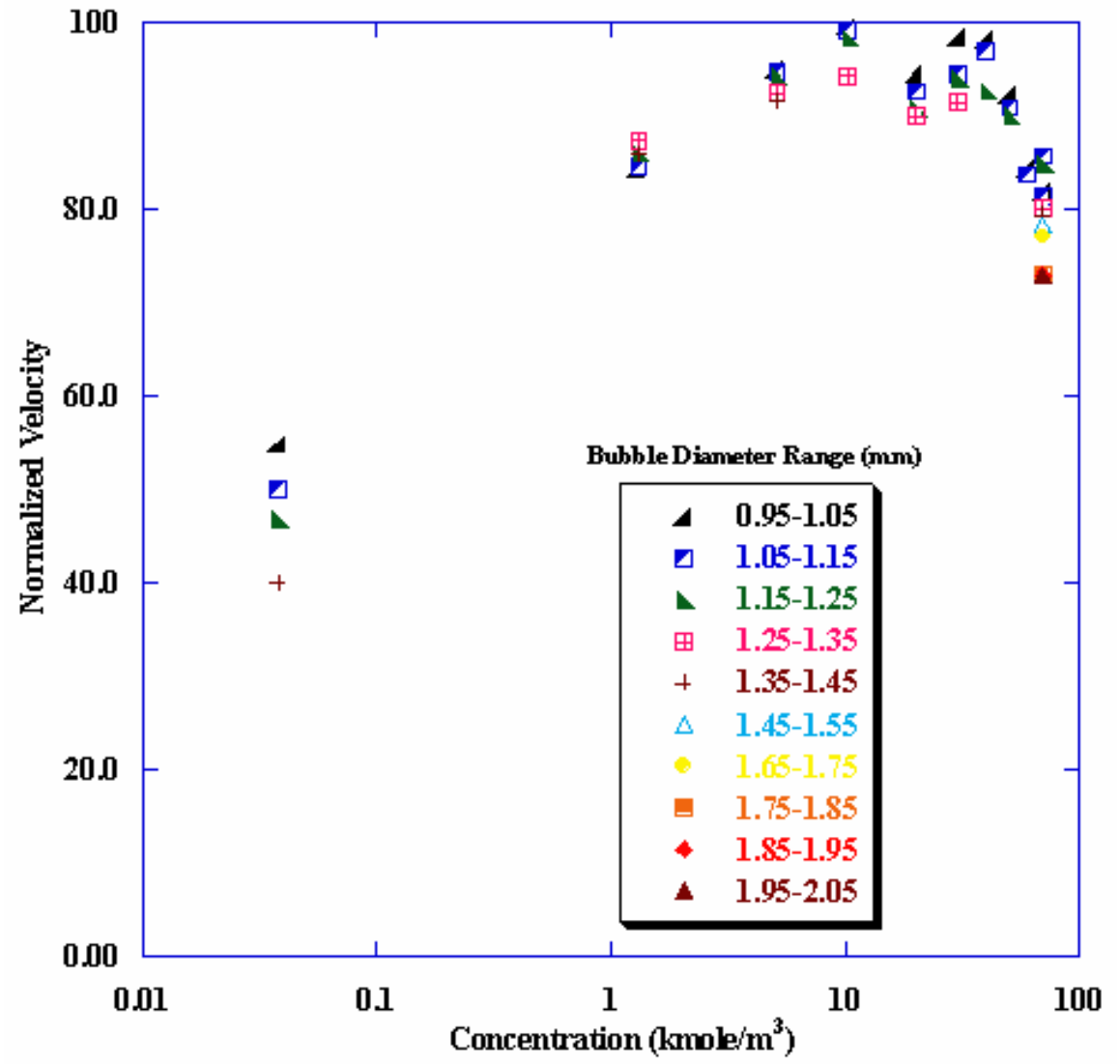


**Figure 3.10 Effect of concentration of hexanol on the normalized velocity of nitrogen bubbles rising in 70:30 mixture of glycerol-water**

# CHAPTER 4

# Theoretical Study of Micelle-Facilitated Remobilization of the Interface of Moving Bubbles Retarded by Surfactant Adsorption

## 4.1 INTRODUCTION

In the introduction, Chapter 1, and later in the literature review, Chapter 2, we developed criteria for which the surface of a bubble translating in a continuous liquid phase can remain mobile even when surfactant adsorbs from the continuous phase onto the bubble interface. The two criteria are: (i) the desorption rate of the surfactant relative to the surface convection has to be large, and (ii) the concentration of surfactant far from the bubble has to be large enough that the adsorption of surfactant at the interface saturates. Under these conditions, the surface concentration becomes uniform and the retarding Marangoni stresses become zero. Consider the simple case of Langmuir adsorption, $\frac{\partial \Gamma}{\partial t} = \beta \Gamma_\infty C_s - (\beta \Gamma_\infty C_s + \alpha)\Gamma$, where $C_s$ is the sublayer concentration, $\Gamma$ is the surface concentration, $\alpha$ is the coefficient of desorption, $\beta$ is the coefficient of adsorption and $\Gamma_\infty$ is the maximum packing density of surfactant at the interface. As we showed in Chapters 1 and 2, the two criteria for remobilization for Langmuir adsorption can be expressed as: (i) $Bi = \frac{\alpha a}{U} >> 1$ and $\frac{\chi k}{Pe^{1/2}} >> 1$ where the bubble of radius a translates with velocity U, the diffusion coefficient of the surfactant is D, $Pe = \frac{Ua}{D}$ and k is the nondimensional bulk concentration, $k = \frac{\beta C_o}{\alpha}$ where $C_o$ is the far field bulk concentration of

surfactant. In these nondimensional criteria, the large concentration limit is denoted as k>>1. The above criteria assume that the Peclet number is large; if it is of order one or smaller, the $Pe^{1/2}$ should be replaced by Pe to reflect a change in the diffusion length scales. In Chapter 3 we demonstrated that when these criteria are met for the rise velocity of bubbles in a glycerol/water continuous phase containing a medium chain length alcohol (which are characterized by fast desorption rates), remobilization can be achieved at high concentrations. As described in the Introduction, Palaparthi *et al* also attempted to verify remobilization under these criteria for bubbles translating in a glycerol/water solution, using the polyethoxylated surfactant $C_{10}E_8$ instead of the medium chain length alcohols. The polyethoxylated surfactant also satisfies the kinetic constrain that Bi is larger than one. As the concentration of $C_{10}E_8$ was raised to the point at which $\frac{\chi k}{Pe^{1/2}} = O(1)$, micelle aggregates began forming in the bulk since the critical micelle concentration was reached ($C_{CMC}$, or nondimensionally $k_{CMC} = \frac{\beta}{\alpha} C_{CMC}$). In the case of the alcohols, micelles do not form, and because of their high solubility, high remobilizing concentrations for which $\frac{\chi k}{Pe^{1/2}} >> 1$ could be achieved. What Palaparthi *et al* found for concentrations higher than the CMC is that significant remobilization did occur, despite the fact that in terms of the monomer transport $\frac{\chi k_{CMC}}{Pe^{1/2}} = O(1)$. Their experiments provided direct evidence that micelles facilitate the remobilization process at the interface of the bubble.

The aim of this chapter is to construct a hydrodynamic model for micelle-facilitated remobilization of the surfactant retarded interface of a translating bubble. For simplicity, we will examine the case of a Newtonian continuous phase in which inertia is negligible in the bubble motion. The bubble motion will be assumed to be axisymmetric and buoyancy-driven. Langmuir

adsorption kinetics will be adopted, and the kinetic exchange will be assumed to be infinitely fast relative to surface convection so that the sublayer and surface are in equilibrium. In this way we focus our study on the micelle removal of the diffusion barrier to remobilization. We will assume that at a critical bulk concentration, micelles form and we choose a nondimensional value for $k_{CMC}$ equal to 270, which is the measured value for the surfactant $C_{10}E_8$. The kinetics of micellization will be treated in the limit in which the kinetics is assumed to be fast with respect to diffusion and convection of monomer in the continuous phase so that monomer and micelle are in local equilibrium. We reviewed micelle kinetics in Chapter 1, where we noted that the nature of this local equilibrium is that the monomer concentration is maintained at the CMC. Thus in the model we will detail, when micelles are present in a region, the monomer concentration is regarded as uniform and equal to the CMC. This numerical study will examine the case of small Peclet numbers. The extension of the results to higher values of the Peclet number characteristic of Palaparthi *et al*'s experiments requires further numerical discretization, but the mechanism illustrated at low Peclet number remains the same.

## 4.2 MECHANISM FOR MICELLE-FACILITATED REMOBILIZATION AND MODEL FORMULATION

The presence of micelles in the continuous phase can remobilize the interface of a translating bubble by the following mechanism. First consider the case of the far-field surfactant bulk concentration to be just below the CMC. At this concentration, the surfactant is present in the bulk in the form of monomers. However due to surface convection on the surface of the bubble, the accumulation of surfactants at the trailing end of the bubble leads to an increase of the local sublayer concentration to exceed the CMC. Therefore a region is formed around the

trailing end of the bubble where micelles are present. This zone is called the micelle zone. Therefore in this case the surfactant monomers adsorbed on the front end of the bubble surface are swept to the trailing end of the bubble, where they desorb into the sublayer and form micelles. These micelles diffuse away from the bubble and towards the micelles zone boundary, where they breakup and release monomers. Now consider the case of far field concentration of surfactant to be greater than the CMC. In this case, at the leading end of the bubble, monomer is adsorbed and swept to the back end by surface convection. This depletes the leading sublayer of monomer and lowers the local monomer concentration below the CMC, causing a micelle-free zone to form. At the outer edge of the zone, micelles breakup, forming monomers, which diffuse towards, and adsorb on to the interface. Surface concentration gradients are developed in this zone, as surface convection sweeps the surfactant out of the region and the monomer can diffuse towards the surface of the bubble to replenish it. The surfactant is swept towards the rear end of the bubble, into regions where the surrounding sublayer contains micelles.

If the micellization kinetics is fast enough relative to the rates of surface convection of surfactant and the bulk diffusion of monomer and micelles, then in the zones where micelles are present, the concentration of monomers is uniform. Also if the surfactant monomers can exchange rapidly, between the sublayer and the bubble surface, then the sublayer concentration would be in equilibrium with the bubble surface concentration. Consequently, the portion of the surface of the bubble adjoining the micelle zone would have uniform concentration and relieved of Marangoni stress. Therefore the surface flow is only retarded at the front end of the bubble. As the far field concentration is increased, the micelle free zone shrinks and after a particular value of concentration it vanishes and the interface becomes completely mobile.

To model the micelle-facilitated remobilization we consider the two circumstances which are described above. In the first, the bulk concentration far from the interface, $C_0$, is assumed to be just below the CMC, while in the second case $C_0$ is assumed to be greater than or equal to the CMC. We have restricted our attention to axisymmetric, buoyancy driven, inertialess motion, and the flow is described in a spherical coordinate system fixed to the bubble, with the origin of the coordinate system coincident with the center of the bubble. The bubble is of radius a and velocity U. Hence in this reference frame, the fluid is approaching the bubble at a velocity U, refer to Figure 4.1. Kinetic exchange is described by the Langmuir adsorption with parameters $\alpha$, $\beta$, and $\Gamma_\infty$ as defined above. Sorption and micellar kinetics are assumed to be fast relative to convection and diffusion of monomer and micelles in the bulk. We will examine only small and order one Peclet numbers for both monomers and micelles. Although Peclet numbers are at most only of order one, we will assume that the surfactant is relatively surface active (surface activity parameter $\chi = \frac{\alpha a}{\beta \Gamma_\infty} << 1$) so that $\chi / Pe << 1$ which is the usual circumstance (see the discussion in the Introduction). As the bulk concentration of surfactant, nondimensionally k, is increased from zero the mobility of the surface can be described by three landmark concentrations. At dilute concentrations (k<<1, below CMC) diffusion is much smaller than surface convection ($\chi(1+k)/Pe \approx \chi / Pe << 1$) and a stagnant cap forms. The size of the cap grows with k until at a value of $k_c$ the surface is completely stagnant. With further increase in concentration, the sublayer concentration at the back end exceeds the CMC and micelles form in the back sublayer at a concentration $k^*$. Finally at high enough concentrations $k^\#$ above the CMC ($k>k_{CMC}$) micelles completely surround the bubble and the interface is completely remobilized. In summary,

1. $k_C$: Complete stagnation of the interface
2. $k^*$: Incipience of the Micelle Zone at the back end of the bubble
3. $k^{\#}$: Complete Remobilization

### 4.2.1 Calculation of the Concentration Necessary for Complete Stagnation, $k_c$

At a surfactant bulk concentrations (which we denote as $k_c$) for which a stagnant cap has just extended over the entire surface, the surface concentration at the leading pole ($\Gamma(0)$) is zero. However as the bulk concentration is increased, the surface concentration at the leading pole also increases. The integration of the nondimensional stress condition yields:

$$\tau_{r\theta}^{solid}(r=1,\theta) = Ma\left\{\frac{1}{1-\Gamma}\right\}\frac{\partial\Gamma}{\partial\theta} \qquad 0<\theta<\pi \qquad (4.1)$$

$$\frac{1}{Ma}\int_0^{\theta}\tau_{r\theta}(r=1,\theta;\Psi=0) = -\ln\left\{\frac{1-\Gamma(\theta)}{1-\Gamma(0)}\right\} \qquad 0<\theta<\pi \qquad (4.2)$$

where Ma is the Marangoni number, Ma= $RT\Gamma_\infty/\mu U$ and $\tau_{r\theta}^{solid}(r=1,\theta)$ is the nondimensionalized tangential stress on the surface of the rigid spherical particle (nondimensionalized by $\mu U/a$) in Stokes flow. For a far-field bulk concentration $C_0$, the surface concentration at the front stagnation pole is obtained by requiring the net flux of surfactant to the bubble surface to be equal to zero:

$$Nu = \int_0^{\pi}\left.\frac{\partial C(r,\theta)}{\partial r}\right|_{r=1}\sin\theta\, d\theta = 0 \qquad (4.3)$$

where $C(r,\theta)$ is the non dimensional bulk concentration distribution of the unaggregated monomer and Nu defines the Nusselt number which represents the net diffusive flux of the

surfactant to the bubble interface. Once the surface concentration is known, the quasi-equilibrium condition can be used to obtain the sublayer concentration $C_s(\theta)$:

$$kC_S(\theta) = \frac{\Gamma(\theta)e^{K\Gamma(\theta)}}{1-\Gamma(\theta)} \tag{4.4}$$

The concentration of surfactant in the bulk can be obtained by solving the convective diffusion equation:

$$v_r^{solid}(r,\theta)\frac{\partial C}{\partial r} + \frac{v_\theta^{solid}(r,\theta)}{r}\frac{\partial C}{\partial \theta} = \frac{1}{Pe}\left\{\frac{1}{r^2}\frac{\partial}{\partial r}\left\{r^2\frac{\partial C}{\partial r}\right\} + \frac{1}{r^2\sin\theta}\frac{\partial}{\partial \theta}\left\{\sin\theta\frac{\partial C}{\partial \theta}\right\}\right\} \tag{4.5}$$

This equation can be solved by guessing a value for the surface concentration at the front pole, and using equations 4.2 and 4.4 to obtain the sublayer concentration. Using the boundary condition on the sublayer concentration and the far-field concentration as $C_0$, equation 4.5 can be solved. The Nussselt number is then calculated from equation 4.3, and the surface concentration at the leading pole of the bubble is changed until Nu is sufficiently close to zero.

The concentration $k_c$ determined in this way is a function of Ma and Pe, but not of $\chi$ since we have assumed that $k_c$ is small enough such that $\chi(1+k_c)/Pe << 1$, i.e. that diffusion is much slower than convection and stagnant caps form. After calculation of $k_c$ this criteria has to be checked; if it is not true, the interface has become partially mobile at this value of k, and cannot be described as completely stagnant.

### 4.2.2 Calculation of the Concentration Necessary for a Micelle Zone to Form, $k^*$, Calculations of Micelle Zones and the Concentration Necessary for Complete Remobilizaton $k^{\#}$

At a critical value of k larger than $k_c$ but smaller than $k_{CMC}$, a micelle zone emerges at the back end of the bubble due to the larger sublayer concentration at the back end. This concentration is denoted as $k^*$. For $k_{CMC}>k>k^*$, this zone intersects the surface at an angle φ measured from the front stagnation pole (Figure 4.2). Outside this zone, only un-aggregated monomer exists. Monomer diffuses at the front end of the bubble, where it is swept by surface convection to the back end. If we assume that the rate of micelle formation and break-up are much faster than the rates of convection and bulk diffusion of monomer and aggregate, then in this micelle region, the bulk concentration of surfactant monomer is uniform and equal to the CMC. Micelles form in the sublayer region and diffuse to the end of the zone where they break-up, releasing monomer which then diffuses out into the bulk solution. The surface adjoining the micelle zone has a uniform surface concentration equal to the value of the surface coverage at the equilibrium for the bulk concentrations equal to and larger than the CMC, i.e. in terms of the adsorption isotherm $\lambda = \frac{\Gamma_{e,CMC}}{\Gamma_\infty} = \frac{1}{1+\frac{\alpha}{\beta C_{CMC}} e^{K\frac{\Gamma_{e,CMC}}{\Gamma_\infty}}} = \frac{k_{CMC}}{k_{CMC}+e^{K\frac{\Gamma_{e,CMC}}{\Gamma_\infty}}}$, where λ is the nondimensional surface concentration obtained for bulk concentrations larger than the CMC. Because the surface concentration is uniform, the Marangoni stress is zero and in this region, the interface is stress free. At the front end, the surface concentration is nonuniform, increasing with θ and the surface velocity greater than zero, but less than that for a completely mobile interface.

This is due to the assumption that $\frac{\chi k_{CMC}}{Pe} = O(1)$. As the bulk concentration is increased to greater than $C_{CMC}$ (Figure 4.3), a micelle free zone develops at the front end of the bubble. This micelle free zone intersects the surface at an angle φ measured from the front stagnation pole. When the bulk concentration is further increased, this zone decreases and so does the angle φ. At a concentration (which we denote as k#) the micelle free zone completely diminishes or φ becomes equal to 0. For $k^{\#}>k>k_{CMC}$, the micelle free zone exists and in this zone only un-aggregated monomer exists. Micelles diffuse towards the boundary of this zone, where they breakup into monomers. These monomers diffuse to the front pole of the bubble, get adsorbed and are swept to the back end of the bubble, from where they desorb and form micelles. If we assume that the rate of micelle formation and break-up are much faster than the rates of convection and bulk diffusion of monomer and aggregate, then in this micelle region, the bulk concentration of surfactant monomer is uniform and equal to the CMC. The surface adjoining the micelle zone has a uniform surface concentration equal to λ. Because the surface concentration is uniform, the Marangoni stress is zero and in this region, the interface is stress free. At the front end or micelle free zone, the surface concentration is nonuniform, increasing with θ. It is uniformly retarded, owing to the assumption that $\frac{\chi k_{CMC}}{Pe} = O(1)$. However at the back-end the surface has uniform concentration and is stress free due to the presence of micelle zone. The hydrodynamic condition on the bubble surface for bulk concentrations $k^{*}<k<k^{\#}$ is presented in figure 4.4.

The above discussion makes it clear that the hydrodynamics of the bubble motion can be described in terms of a stress free interface in the downstream region contacting the micelle zone

($\varphi < \theta < \pi$), and a retarded region in the upstream region contacting the micelle-free zone ($0 < \theta < \varphi$).

In the absence of inertia (Re=0), an analytical solution exists for the flow field in terms of the surfactant surface concentration distribution. For this axisymmetric flow, the velocity field is written in terms of the nondimensional stream function $\psi^{cap}(r,\theta;\varphi)$ (nondimensionalized by $Ua^2$):

$$v_r(r,\theta) = -\frac{1}{r^2 \sin\theta}\frac{\partial \psi}{\partial \theta} \tag{4.6}$$

$$v_\theta(r,\theta) = \frac{1}{r \sin\theta}\frac{\partial \psi}{\partial r} \tag{4.7}$$

and the equation of continuity and the Stokes equation can be reduced to the following single equation for the stream function:

$$E^2\left\{E^2\psi\right\} = 0; E^2\psi = \frac{1}{\sin\theta}\frac{\partial^2\psi}{\partial r^2} + \frac{1}{r^2}\frac{\partial}{\partial\theta}\left\{\frac{1}{\sin\theta}\frac{\partial\psi}{\partial\theta}\right\} \tag{4.8}$$

A general solution to the above equation which satisfies the conditions of matching to the free stream velocity at infinity, and of zero radial velocity on the bubble surface can be written as an infinite series expansion of Gegenbauer polynomials $C_n^{-1/2}(\cos\theta)$:

$$\psi(r,\theta) = \frac{1}{2}\left\{r^2 - r\right\}\sin^2\theta + \sum_{n=2}^{\infty} B_n^*\left\{r^{-n+1} - r^{-n+3}\right\}C_n^{-1/2}(\cos\theta) \tag{4.9}$$

If the surfactant surface concentration is known, the coefficients $B_n$ are also known and given by:

$$B_n = \left(\frac{Ma\cdot(n+1)}{2}\right)\int_0^{\pi} \ln(1-\Gamma(\theta))P_{n-1}(\cos\theta)\sin\theta\, d\theta \qquad n>2 \tag{4.10}$$

Where $\Gamma(\theta)$ is the surface concentration distribution, $P_n$ is the Legendre Polynomial and Ma is the Marangoni number. Refer to Appendix A, for derivation of equation (4.10).The net drag exerted by the continuous phase on an axisymmetric bubble in creeping flow limit, is given by [Payne & Pell (1960)].

$$Drag = -8\pi\mu Ua \lim_{r\to\infty} \frac{\psi - \frac{1}{2} r^2 \sin^2\theta}{r \sin^2\theta} \tag{4.11}$$

The drag can be expressed in terms of a single coefficient ($B_2$) in the series, and hence the drag is known once the surfactant surface concentration is known.

The surfactant concentration gradient on the surface of the bubble, which follows from the above transport picture, may be determined as follows. The surface adjoining the micelle zone has a uniform surface concentration equal to $\lambda$. As depicted in Fig. 4.2 and 4.3, the surfactant transport is a two region problem which consists of a micelle zone and a micelle-free zone. In the micelle free zone surfactant monomer with nondimensional concentration C satisfies the convective diffusion equation:

$$v_r(r,\theta;Re,\varphi)\frac{\partial C}{\partial r} + \frac{v_\theta(r,\theta;Re,\varphi)}{r}\frac{\partial C}{\partial \theta} = \frac{1}{Pe}\left\{\frac{1}{r^2}\frac{\partial}{\partial r}\left\{r^2\frac{\partial C}{\partial r}\right\} + \frac{1}{r^2\sin\theta}\frac{\partial}{\partial \theta}\left\{\sin\theta\frac{\partial C}{\partial \theta}\right\}\right\} \tag{4.12}$$

where $v_r(r,\theta;Re,\varphi)$ and $v_\theta(r,\theta;Re,\varphi)$ denote the r and $\theta$ components of the velocity field (nondimensionalized by U) for the case with the un-remobilized region subtended by particular angle $\varphi$. In the micelle zone, the concentration of monomer is uniform, and the concentration of the aggregate (denoted nondimensionally as $C_M$, also nondimensionalized by $C_o$), satisfies a convective diffusion equation:

$$v_r(r,\theta;\mathrm{Re},\varphi)\frac{\partial C_M}{\partial r}+\frac{v_\theta(r,\theta;\mathrm{Re},\varphi)}{r}\frac{\partial C_M}{\partial \theta}=\frac{B}{Pe}\left\{\frac{1}{r^2}\frac{\partial}{\partial r}\left\{r^2\frac{\partial C_M}{\partial r}\right\}+\frac{1}{r^2\sin\theta}\frac{\partial}{\partial\theta}\left\{\sin\theta\frac{\partial C_M}{\partial\theta}\right\}\right\} \tag{4.13}$$

where B is the ratio of the diffusion coefficient of the micelle to that of the monomer. At the boundary surface Ω the micelle and monomer concentrations match; since the micelle concentration is equal to zero on the micelle-free side of the surface, the micelle concentration in the micelle zone as the surface is approached is equal to zero.

$$C_M(r,\theta)=0 \qquad r,\theta \ni \Omega^- \tag{4.14}$$

Finally since the concentration of monomer is equal to the CMC on the micelle zone side of the boundary, the monomer concentration is equal to the CMC on the micelle-free zone side of the boundary:

$$C(r,\theta)=1/X \qquad r,\theta \ni \Omega^+ \tag{4.15}$$

where X is the ratio of the $C_o$ to CMC (i.e. $X=\frac{C_o}{C_{CMC}}$). On the boundary Ω between the micelle and micelle-free zones, the surfactant fluxes from either side match; since concentrations match on either side of the interface, the convective contributions cancel and we obtain:

$$\mathbf{n}\bullet\left\lfloor\sigma B\{\nabla C_M\}-\{\nabla C\}\right\rfloor=0 \tag{4.16}$$

where **n** is the vector normal to the surface Ω (in the direction of the micelle zone) and σ is the mean aggregation number.

If we denote by g(θ) the tangential velocity on the surface of the bubble, (i.e. $g(\theta)=v_\theta(r=1,\theta;\mathrm{Re},\alpha)$), then the mass balance of surfactant on the surface yields:

$$\frac{\partial C}{\partial r}_{r=1}=\frac{Pe}{k\chi\bullet\sin\theta}\left[\frac{\partial(\sin\theta\bullet g(\theta)\Gamma)}{\partial\theta}\right] \qquad (0<\theta<\alpha) \tag{4.17a}$$

$$\sigma B \frac{\partial C_M}{\partial r}_{r=1} = \frac{Pe\lambda}{k\chi \bullet \sin\theta}\left[\frac{\partial(\sin\theta \bullet g(\theta))}{\partial\theta}\right] \qquad (\alpha < \theta < \pi) \quad (4.17b)$$

The formulation of the mass transfer is then completed by specifying that the far field concentration to be equal to one as the radial coordinate becomes infinite:

$$C(r,\theta) = 1 \quad r \to \infty \qquad (4.18)$$

To solve this set of equations we use a "front-trapping" method in which we first define a composite function Ξ(r,θ) continuously throughout the solution field r >1 which represents the local total concentration of surfactant molecules.

$$\Xi(r,\theta) = C(r,\theta) + \sigma C_M(r,\theta) \qquad (4.19)$$

The composite function is continuous throughout the solution field: In the micelle free zone Ξ < 1/X; in the micelle zone Ξ >1/X and on the boundary Ξ =1/X. To cast a convective-diffusion conservation equation for the composite function, we define a continuous, differentiable, non-dimensional diffusion coefficient function B*(Ξ) as given by the relations:

$$B^*(\Xi) = 1 \qquad (\Xi < 1/X) \qquad (4.20a)$$

$$B^*(\Xi) = B \qquad (\Xi > 1/X) \qquad (4.20b)$$

It is assumed that B*(Ξ) in the immediate vicinity of 1/X monotonically decreases from 1 to B; the interval over which this decrease takes place does not have to be specified when the equations are solved numerically since it is assumed to be smaller than the mesh size of the grid on which the equations are solved. From the convective diffusion equations in each zone it is clear that the composite function satisfies separately in each region a conservation equation which can be written in the form:

$$v_r(r,\theta;Re,\varphi)\frac{\partial \Xi}{\partial r}+\frac{v_\theta(r,\theta;Re,\varphi)}{r}\frac{\partial \Xi}{\partial \theta}=\frac{1}{Pe}\left\{\frac{1}{r^2}\frac{\partial}{\partial r}\left\{r^2B^*\bullet\frac{\partial \Xi}{\partial r}\right\}+\frac{1}{r^2\sin\theta}\frac{\partial}{\partial \theta}\left\{\sin\theta\bullet B^*\frac{\partial \Xi}{\partial \theta}\right\}\right\} \tag{4.21}$$

In addition we note that: (i) the composite function is equal to 1/X on the boundary Ω from either side of the boundary, and (ii) by integration of the above equation over a "pill-box" straddling the boundary Ω, using the divergence theorem, and then taking the limit as the thickness of the box in the direction across the interface tends to zero, the composite function satisfies the mass balance equation for surfactant on the boundary. Thus if we solve the conservation equation uniformly on the domain, the solution will represent the solution for our two region problem with the boundary Ω demarcated as the position in which the composite function is equal to 1/X. To complete the solution of the composite function, we recast the boundary conditions in terms of Ξ(r,θ):

$$B^*\left.\frac{\partial \Xi}{\partial r}\right|_{r=1}=\frac{Pe}{k\chi\sin\theta}\frac{\partial}{\partial\theta}\left(\Gamma(\theta)\sin\theta\, g(\theta)\right) \qquad 0<\theta<\varphi \tag{4.22a}$$

$$B^*\left.\frac{\partial \Xi}{\partial r}\right|_{r=1}=\frac{Pe\lambda}{k\chi\sin\theta}\frac{\partial}{\partial\theta}\left(\sin\theta\, g(\theta)\right) \qquad \varphi<\theta<\pi \tag{4.22b}$$

$$\Xi(r\to\infty;\theta)=1 \tag{4.23}$$

# 4.3 NUMERICAL SOLUTION

## 4.3.1 Implementation of Finite Volume Method

The finite volume method employed to discretize the unsteady bulk surfactant transport is a 'volume of fluid method'. A staggered mesh as shown in Figure (4.5) is employed. The location of the nodes for the different variables is chosen as follows. The nodes for the

concentration field C in the radial direction, start at the bubble surface (r=1) and end at the outer edge of the numerical domain ($r=r_\infty$), while the nodes in the θ direction start at θ =0 and end at θ= π. The nodes for the surface concentration Γ coincide with those of C on the bubble surface. The nodes for the radial velocity component u, follow the nodes for C but are staggered in the θ direction so that a u node is placed midway between neighboring C nodes at a given radial position. It follows, then, that there are no *u*-nodes on the symmetry axes θ = 0 and θ = π. The radial location for the v nodes are staggered relative to the C nodes so that they are located midway between two C-nodes. Hence, the first v-node is located just above the surface of the bubble and the last *v*-node is positioned at $r < r_\infty$ midway between the last and second to last *C*-nodes. In the θ-direction the v-nodes are positioned at the same azimuthal locations as the *C*-nodes. Hence, they start from θ = 0 and end at θ = π. The control volume for concentration node is identified such that the node for that variable is placed at the center of the control volume. This is shown in the inset to Figure (4.4), the west side could represent the bubble surface.

The discretization of the concentration equation is achieved as follows. The concentration equation is written in a form which facilitate a finite volume implementation, and which treat the convective terms explicitly in order to obtain linear equations, as shown below:

$$\frac{\partial C}{\partial t} + \nabla \cdot \left( C\mathbf{v}^{\infty} - \frac{1}{Pe} \nabla C \right) = 0 \qquad (4.24)$$

where ($\mathbf{v}^{\infty} = u^{\infty}\mathbf{e}_r + v^{\infty}\mathbf{e}_\theta$) is the velocity field for a bubble. Keeping this in mind on integrating the concentration field equation (4.37) over its control volume and discretized in time over a time-step $\Delta t$. The result is

$$\frac{C-C^n}{\Delta t}\Delta V + \left(\mathrm{Cu}^{\infty} - \frac{1}{P_e}\frac{\partial C}{\partial r}\right)_e dA_e - \left(\mathrm{Cu}^{\infty} - \frac{1}{P_e}\frac{\partial C}{\partial r}\right)_w dA_w$$
$$- \left(\mathrm{Cv}^{\infty} - \frac{1}{rP_e}\frac{\partial C}{\partial \theta}\right)_n dA_n + \left(\mathrm{Cv}^{\infty} - \frac{1}{rP_e}\frac{\partial C}{\partial \theta}\right)_s dA_s = 0 \qquad (4.25)$$

In the first term *C* denotes the value at the center of the cell. Here $dA_i$ is the area of face *i*, where *i= east, west, north, south* of the control element of volume *dV*. In discretizing the area terms which contain *C* and either $\frac{\partial C}{\partial r}$ or $\frac{\partial C}{\partial \theta}$ values of *C* from immediately adjacent cells are used. Central differencing scheme was used to evaluate derivatives of cell faces.

Numerical solutions for *C* are updated over a time step by employing the ADI scheme (Alternating Directions Implicit Method). For example, C are calculated from time level n to level n+1 by using the ADI method and so resulting in tridiagonal solvers (details can be found in [Peyret & Taylor(1983)]). The steady state is assumed to be reached once the variation in *C*, is less than 1.0 % when measured 100 time steps apart.

The Boundary conditions at inlet and outlet (refer Figure 4.5) are

$$C = 1 \qquad 0 < \theta < \pi/2 \text{ (inlet)}, \qquad (4.26a)$$

$$\frac{\partial C}{\partial z} = 0 \qquad \pi/2 < \theta < \pi \text{ (outlet)}, \qquad (4.26b)$$

$$\frac{\partial C}{\partial \theta} = 0 \qquad \theta = 0, \pi \text{ (symmetry)}. \qquad (4.27c)$$

The outflow conditions on *C* are used in order to accurately model the solute wake that is present in the vicinity of the downstream axis of symmetry, at high Peclet numbers. Such boundary conditions have been used successfully in the related thermocapillary migration problem, at high Marangoni numbers, by [Balasubramaniam, R. & Lavery (1989)].

### 4.3.2 Grid Construction

Directly creating a grid on the physical domain ($r,\theta$), requires an expanding mesh. We therefore use a grid based on a ($x$,$y$) coordinate system which transforms the physical domain into a rectangular domain through the logarithmic transformation $x = \ln(r)$ and the linear transformation $y = \theta/\pi$. Grid spacing is then set-up with even divisions in $\Delta x$ and $\Delta y$. In the simulation studies carried the Reynolds number, Re is of order zero, and the Peclet number, Pe is of order 0.1 and $10^3$. At high values of the Peclet number there are significant boundary layer effects that would require more points near the surface. Considering the transport of the surfactant from the bulk to the interface, the convective terms are dominant since the Peclet numbers are large (of order $10^3$). For a fluid-fluid interface, at large Peclet numbers, there are steep gradients in the surfactant concentration field inside a boundary layer near the bubble surface. The thickness of this concentration boundary layer scales as $Pe^{-1/2}$, and so a finer mesh is required near the bubble surface. To account for these large concentration gradients, we construct a hybrid grid to discretize the surfactant convection-diffusion equation. This grid is linear in $r$, extending from the surface of the bubble to a distance of $aPe^{-1/2}$ and contains 10 grid points. The edge of this inner mesh is made to coincide with the first radial grid line of the exponential coarse grid. The number of points in the outer grid was determined by keeping the ratio of grid spacing in r direction for inner mesh to that of the spacing in $r$ between the first two radial grid lines in the outer grid, to be between 0.5 & 1.0. So for a Pe of $10^3$ and with 10 points in the inner mesh, 500 points were taken in outer grid. However, when the Peclet number is small, then there is no boundary layer formation and diffusive fluxes scales as $DC_0Pe/a$. So in such cases we defined the inner mesh from bubble surface to 2a, with 110 points in the r

direction, in the inner mesh and 400 points in the outer mesh. We found from numerical experiments designed to validate the code (see Section 4.2.4), for a Pe of $10^3$ and $r_\infty / r_0$ of 5 with a coarser exponential grid of 500 X 300 and a fine inner mesh of 10 X 300 are sufficient and for a Pe of 0.1 and $r_\infty / r_0$ of 50 with a coarser exponential grid of 400 X 300 and a fine inner mesh of 110 X 300 are sufficient. Figure (4.6) shows an example of an exponential grid with a finer mesh near the surface of the bubble used for the surfactant bulk concentration.

### 4.3.3 Algorithm for Numerical Solution

The algorithm used to obtain the dimensionless critical bulk concentration $k_c$ is described below.

a) For a spherical bubble completely covered with a solid cap, the hydrodynamic flow around the bubble was obtained analytically using stroke's equation for flow past a solid sphere**.**

b) Once the shear stress distribution $\tau_{r\theta}(\theta)$ on the bubble surface is obtained, for a fixed value of Marangoni number (Ma), the surfactant concentration $\Gamma(0)$ at the front pole of the bubble surface is fixed. Using tangential stress balance surfactant concentration distribution on the bubble surface is calculated. This can be done with the following equations.

$$[\tau_{r\theta}]_{r=1} = \left[ r \frac{\partial}{\partial r}\left(\frac{v}{r}\right)\right]_{r=1} = Ma \left[\frac{1}{1-\Gamma}\right] \frac{\partial \Gamma}{\partial \theta} \qquad (4.28)$$

but shear stress experienced by a solid sphere is given by

$$\tau_{r\theta}\big|_{r=1} = -\frac{3}{2}\sin\theta \qquad (4.29)$$

Substituting (4.28) in (4.29) and on integrating the equation we get

$$\Gamma(\theta) = 1 - \exp\left(-\frac{3}{2}\frac{(1-\cos\theta)}{Ma}\right)(1-\Gamma(0)) \tag{4.30}$$

c) Using the calculated surfactant concentration on the bubble surface, surfactant distribution in the continuous phase is calculated. This needs a value of the surfactant bulk concentration k. To start, a value of k is guessed. When the kinetic exchange is fast (Bi >> 1) the sublayer and surface are in a quasi-equilibrium. For a surfactant following Langmuir kinetics the dimensionless sublayer concentration can be calculated directly from the surface distribution as

$$C(1,\theta) = \frac{1}{k}\left[\frac{\Gamma(\theta)}{1-\Gamma(\theta)}\right] \qquad 0 < \theta < \pi \tag{4.31}$$

d) With the sublayer concentration known and given a Peclet number, the distribution of surfactant in the continuous phase is obtained by solving the convection-diffusion equation with the velocity given by the stokes equation**.** The flux to the bubble surface, given by the Nusselt number Nu (see equation 4.32), is then computed from the surfactant distribution in the continuous phase. The first derivatives on the bubble surface required in estimating the net flux of the surfactant to the bubble surface, and which is needed to solve for the surfactant transport equation, are calculated using three-point formulas.

$$Nu = \int_0^{\pi}\left[\frac{\partial C}{\partial r}\right]_{r=} \sin\theta d\theta = 0 \tag{4.32}$$

e) At steady state, the amount of the surfactant adsorbing at the front end of the bubble, should balance the amount desorbing at the back end, hence implying the Nu is zero. In the results presented here, we assume convergence in k, if the absolute value of Nu is less

than 0.1. This convergence criterion is due to the fact that at high Peclet numbers, Nu is of the order $Pe^{1/3}$ to $Pe^{1/2}$(the former estimate for a solid and the latter for a clean fluid interface). For the Peclet number of $10^3$, Nu is of order 10-$10^2$, unless k has the value satisfying the steady state zero flux condition. If the steady state flux is not converged to this value, the value of k is changed and steps (c) through (d) are repeated, in an iterative manner, until Nu converges to its null steady value. Once convergence is reached , the value of k, Pe, Ma and $\Gamma(0)$, C(1,θ) are noted.

f) Steps (a) through (d) are repeated for different $\Gamma(0)$ values. $\Gamma(0)$=0 defines kc

The algorithm used to obtain the angle subtended by the un-remobilized region (φ) for a given bulk concentration k and for determining k* and $k^{\#}$.

a) First for a fixed value of Marangoni number (Ma), Critical Micelle Concentration ($k_{CMC}$) and Peclet number (Pe), a value of bulk concentration (k) is guessed.

b) Initially the bulk concentration is assumed to be equal to the far-field concentration (k). The surface concentration is assumed to be equal to either k/(k+1), when k is less than $k_{CMC}$ and λ, when k is greater than $k_{CMC.}$ For this assumed surface concentration, the velocity field around the bubble is determined by the following equation for the stream function.

$$\psi(r,\theta) = \frac{1}{2}\left\{r^2 - r\right\}\sin^2\theta + \sum_{n=2}^{\infty} B_n^* \left\{r^{-n+1} - r^{-n+3}\right\} C_n^{-1/2}(\cos\theta) \tag{4.33}$$

where $C_n^{-1/2}(\cos\theta)$ are Gegenbauer polynomials and

$$B_n = \left(\frac{Ma\cdot(n+1)}{2}\right)\int_0^{\pi} \ln(1-\Gamma(\theta))P_{n-1}(\cos\theta)\sin\theta\, d\theta \tag{4.34}$$

c) With the surface concentration and velocity field know, the convective diffusion equation given by :

$$\frac{\partial \Xi}{\partial t} + \nabla \cdot \left( \Xi \mathbf{v}^{\infty} - \frac{1}{Pe} \nabla \Xi \right) = 0 \qquad (4.35)$$

is solved using the following boundary conditions

$$B^{*} \left. \frac{\partial \Xi}{\partial r} \right|_{r=1} = \frac{Pe}{\mathrm{k}\chi \sin\theta} \frac{\partial}{\partial \theta} \left( \Gamma(\theta) \sin\theta \, \mathrm{g}(\theta) \right) \qquad \Gamma(\theta)<\lambda \qquad (4.36a)$$

$$B^{*} \left. \frac{\partial \Xi}{\partial r} \right|_{r=1} = \frac{Pe\lambda}{\mathrm{k}\chi \sin\theta} \frac{\partial}{\partial \theta} \left( \sin\theta \, \mathrm{g}(\theta) \right) \qquad \Gamma(\theta)\geq\lambda \qquad (4.36b)$$

$$\Xi(r \to \infty; \theta) = 1 \qquad 0<\theta<\pi/2 \qquad (4.36c)$$

$$\left. \frac{\partial \Xi}{\partial z} \right|_{r=\infty} = 0 \qquad \pi/2<\theta<\pi \qquad (4.36d)$$

$$\left. \frac{\partial \Xi}{\partial \theta} \right|_{\mathrm{r}=1} = 0 \qquad \theta= 0,\pi \qquad (4.36e)$$

where $\Xi(r,\theta) = C(r,\theta) + \sigma C_{M}(r,\theta)$ and $B^{*}$ is the nondimensional diffusion coefficient, which is equal to 1 when $\Xi<1/X$ and is equal to B when $\Xi > 1/X$, where $X=C_0/C_{CMC}$ and B is the ratio of diffusion coefficient of micelle to monomer After each time step, using the sublayer concentration, the corresponding surface concentration is calculated. In the manner described in step (b), this surface concentration is used to calculate the flow field for the next time step.

d) Once steady state is reached, the value of k, Pe, Ma, φ and C(r,θ) are noted.

e) To obtain $k^{*}$, steps (a) through (d) are repeated, for various values of k, until $C_S(\theta = \pi) = k_{CMC}$.

f) To obtain $k^{\#}$, steps (a) through (d) are repeated, for various values of k and for Hadamard-Rybczynski velocity profile (which is obtained by putting $B_n$=0 in step 2). k is varied, until $C_S(\theta = 0) = k_{CMC}$.

### 4.3.4 Validation of Numerical Code

Solving the problem of the transport of a passive scalar in creeping flow conditions towards a translating solid sphere or a bubble in which the particle acts as a sink (surface concentration equals zero, far-field concentration is nondimensionally one), checks the code for the surfactant mass transfer. The Nusselt number defined by the equation (4.32) gives the net scalar flux to the particle surface. A good agreement, for the Nusselt number, between the results obtained in various literature studies and the ones obtained through the present studies was obtained as outlined below.

i. *Solid sphere with no slip on the surface*- Results obtained through the present study were compared with results obtained using Friedlander's approach for low to medium values of Peclet numbers and asymptotic results of [Acrivos & Goddard (1965)] for large Pe - see Figure 4.8**.**

ii. *Bubble with stress free interface*- Good agreement was found between the results obtained through the present study with the asymptotic results for large Pe (Leal, 1994) - see Figure 4.9**.** For the calculation done at zero and low Peclet numbers, a numerical domain extending to 50 bubble radii was used. For Peclet number of the order of $10^3$ or higher a domain extending to 5 bubble radii is found sufficiently accurate with grid of size 515 X 300. Also, a 500 X 300 exponential grid coupled with a 15 X 300 linear grid spread within the solute boundary layer close to the

surface of the bubble (extending from the surface of the bubble to a distance of order $Pe^{-1/2}$) is used.

## 4.4 RESULTS AND DISCUSSION

### 4.4.1 Dependence of critical bulk concentration ($k_c$) for immobilization on Marangoni number (Ma) and Peclet number (Pe)

Figure 4.10 shows the dependence of critical bulk concentration ($k_c$) on the Marangoni number (Ma) for Pe=1000. $k_c$ is the minimum concentration of surfactant in the continuous phase, at which the stagnant cap completely covers the surface of the bubble, making the interface completely immobile. At this critical concentration, the surface concentration at the front pole of the bubble ($\Gamma(0)$) is equal to zero. Through our study we observed that $k_c$ decreases when the Marangoni number (Ma) is increased. This decrease is very sharp when Ma is increased from 1 to 3, and is gradual after that and nearly no change after Ma greater than 20. Physically, from the definition of the Marangoni number $Ma = RT\Gamma_\infty/\mu U$ , smaller sized bubbles have higher Marangoni numbers since they have lower velocities. It can be concluded, therefore, that smaller bubbles are more likely to be completely covered and behave like solid spheres at low bulk concentrations than large sized bubbles. We observed similar behavior in our experiments, which are described in chapter 3. This observation can also be realized if we examine equation 4.1. Marangoni stress which retards the interfacial mobility of the interface is directly proportional to the Marangoni number. Therefore for the same surfactant surface concentration gradient ($\frac{\partial \Gamma}{\partial \theta}$), it is easier to completely retard the interfacial mobility of a small

bubble or one having a large Marangoni number as compared to a large bubble, which has a small Marangoni number.

Consider the case of a bubble rising with the Marangoni number of 12. The critical bulk concentration required to completely immobilize its interface is 0.16. Typical value of Critical Micelle Concentration ($k_{CMC}$) ranges between 100-1000. Therefore the amount of surfactant required to completely immobilize the interface is as low as CMC/1000-CMC/10000.

Figure 4.11 shows the results of the case study, when the bulk concentration is increased above $k_c$, while keeping the Marangoni number (Ma) and Peclet number (Pe) fixed at 12 and 1000 respectively. As the bulk concentration is increased over $k_c$, the surface concentration at the front pole of the bubble also increases from zero. As k increases, the surface concentration gradient becomes more uniform $(\Delta\Gamma \approx 0)$, but because of the higher surface concentrations, larger Marangoni stresses arise from smaller gradients in the surface concentration. In this way the smaller gradients at the higher concentrations still maintain the surface of the bubble to be immobile. This can be seen clearly from the following equation

$$\tau_M^{solid}(r=1,\theta) = Ma\left\{\frac{1}{1-\Gamma}\right\}\frac{\partial\Gamma}{\partial\theta} \tag{4.37}$$

where $\tau_m$ is the Marangoni stress, $\mu$ is viscosity of the continuous phase, U is the velocity of bubble, $\Gamma$ is the surface concentration and $\gamma$ is the surface tension. Thus in the above expression as the surface gradients are reduced, $\Delta\Gamma$ is reduced, but the term $\frac{1}{1-\Gamma}$ increases (as $\Gamma \to 1$) to keep the Marangoni stress large enough to keep the surface of the bubble immobile.

Figure 4.12 shows the dependence of critical bulk concentration ($k_c$) on Peclet number for a Marangoni number of 12. It is observed that $k_c$ is weakly dependent on Peclet number. An increase in the Peclet number from 1 to $10^5$ required an increase in critical bulk concentration of about 15 % only. This weak dependence of $k_c$ on the Peclet number can be explained by the results presented in figure 4.13 and 4.14, where the concentration profile in the bulk are presented for the Peclet numbers of 100 and 1000 respectively. The far field concentration in this study is equal to the critical bulk concentration ($k_c$)

On comparing the figures 4.13 and 4.14 it can be observed that as the Peclet number is increased there are higher concentration gradients at the rear end of the bubble than they are at the front end. Thus as the Peclet number is increased there is a more tendency of the surfactant to diffuse out from the bubble surface than to diffuse in. Thus to achieve a steady state when the influx is equal to the outflux, higher surfactant concentrations of the bulk medium is required. Higher bulk concentration will balance the two fluxes as it will decrease the outflow of surfactants from the bubble surface and increase the inflow of the surfactant to the bubble surface. As the size of the bubble is increased the rise velocity also increases. Thus for a constant diffusion coefficient the Peclet number given by $\frac{Ua}{D}$ increases with bubble diameter.

### 4.4.2 Formation of Micelle and Micelle-Free Zones Around a Translating bubble

Let us consider the case of a bubble translating in creeping flow limits in a bulk fluid containing surfactants. For all the cases discussed in this section, nondimensional critical micelle concentration ($k_{CMC}$) is 270, Peclet number (Pe=0.1), Non dimensional diffusion coefficient of

micelles and monomers (B*) =1, $\chi k_{CMC}/Pe$ is 1.458 and Bi>>1. We studied two cases, with Ma=0.1 and 1.0. We observed that for Ma=1.0, $k_c$= 5.75. i.e. this is the minimum far-field bulk concentration at which the surface of the bubble becomes completely stagnant. For the present case of Ma=0.1 and $\chi$, the surface of the bubble doesn't become completely stagnant. This is due to the fact that Ma is small and $\chi$ larger enough, that the far-field concentration at which surface would have become stagnant, $\chi k_C/Pe$ =O(1) and not $\chi k_C/Pe$ << O(1). As the far-field concentration is further increased the surface of the bubble starts to remobilize, due to the formation of a micelle-zone at the back-end. The minimum far-field concentration at which remobilization starts is denoted by k*. For Ma =0.1, k*= 180 and for Ma=1.0, k* = 195. Figure 4.15a presents the surfactant concentration profile around the bubble, when the Marangoni number (Ma) is 0.1 and non-dimensional far-field bulk concentration (k) is 265, which is less than the critical micelle concentration ($k_{CMC}$), but is greater than k*. It can be clearly seen that there is a presence of a micelle zone at the back-end of the bubble, while the front end of the bubble is only surrounded by monomers. The micelle zone intersects the surface of the bubble at an angle of $94.5^0$ measured from front stagnation point.

Further cases with the same value Ma and Pe were studied but with bulk concentrations of 275, 300, 325 and 345, which are above the critical micelle concentration but less than k# which is 364. For these cases, the concentration profile around the bubble is provided in Figure 4.15 b, c, d & e. In all the cases a micelle free zone is observed in the front-end of the bubble. The area of the bubble covered by these micelle-free zone decreases or amount of remobilization of the bubble surface increases with the increase in bulk concentrations.

Figure 4.16a to e presents the concentration profile for the cases where Ma = 1, Pe=0.1 and k varies as 265, 275,300, 325 and 345. For this case k*=195, while k# = 364. In all these

cases a micelle free zone is seen at the front end of the bubble, while a micelle zone is observed at the back-end. On comparison of plots 4.15a and 4.16a, we observe that the concentration gradients at the front end are smaller when Ma=1, as compared to when Ma =0.1. On the other hand the micelle zone formed at the back-end of the bubble is small when Ma is large. This is due to the fact that for k=265, the surface of the bubble is more retarded for Ma=1 as compared to when Ma=0.1. Therefore for Ma=1, the convection of surfactants to the back-end of the bubble is lower. From equation 4.36 it can be seen that in the front end, this leads to a smaller concentration gradient in the r direction. However at the back-end the surface of the bubble is remobilized (refer Figure 4.20) and therefore here the surface convection is comparable with Ma=0.1 and so is the diffusive fluxes away from the surface. Therefore for Ma=1, less amount of surfactant is convected to the back-end but it gets diffused away from the bubble at a high rate and thus at the back-end the size of the micelle zone is smaller than for Ma=0.1. Similar observations are made, with the micelle free zone at the front end of the bubble to be larger for Ma=1, as compared to Ma=0.1, when the far-field bulk concentration is greater than critical micelle concentration. This can be seen in Figure 4.15 b,c&d and 4.16 b,c&d, where the far-field bulk concentration is 275, 300 and 325 respectively. However when the far-field concentration is further increased to 345 the size of the micelle-free zone is of same size both for Ma=0.1 and 1. This is due to the fact at these concentrations the mobility of the surface (refer figure 4.20 & 4.21) is similar and so is the size of the micelle free zone.

Figure 4.17 and 4.18 respectively, shows the sublayer and surface concentration as a function of far field bulk concentration and Marangoni number. Figure 4.19 shows the variation of angle φ (which is the angle measured from the front stagnation point, where the micelle zone intersects the surface of the bubble) with the far field bulk concentration for Pe = 0.1 and Ma=

0.1 and 1.0. It can be seen that for concentrations of less than the CMC, φis larger for Ma=1 as compared to Ma=0.1. However for k larger than CMC, φ is slightly smaller for Ma=1 as compared to Ma=0.1. One thing to note is that at least for k greater than or equal 265, φ is a very weak function of Marangoni number.

Figures 4.20 and 4.21 respectively show the surface velocity and drag as a function of far field bulk concentration and Marangoni number. In figure 4.20 the surface velocity is non-dimensionlized by the far-field velocity. In figure 4.21, drag is non-dimensionalzed by both the drag experienced by a clean bubble ($D_{BUBBLE}$) and that experienced by a similar solid sphere ($D_{SPHERE}$) and is calculated by the following formula

$$D_{ND} = 100\frac{D - D_{BUBBLE}}{D_{SOLID} - D_{BUBBLE}} \tag{4.38}$$

where $D_{ND}$ is the non-dimensional drag and D is the calculated drag on the surface of a bubble containing surfactants. Figures 4.20 and 4.21 show that the surface of the bubble starts to remobilized with increase in bulk concentration.

### 4.4.3 Dependence of $k^{\#}$ on $k_{CMC}$

Figure 4.22 shows the variation of $k^{\#}$ with critical micelle concentration, $k_{CMC}$. $k^{\#}$ represents the concentration, when the micelle free zone formed at the front end of the bubble diminishes or the surface of the bubble becomes completely mobile. $k^{\#}$ shows a linear relationship with critical micelle concentration $k_{CMC}$.

## 4.5 CONCLUSIONS

We studied the effect of surfactants on the interfacial mobility of the bubbles rising due to buoyancy. In our study, we considered the case of a surfactant following a Langmuir kinetic scheme, the mass transfer of the surfactant is purely diffusion limited and the flow around the bubble is creeping flow. We identified three critical concentrations. $k_c$ is the bulk surfactant concentration for which the surface of the translating bubble becomes completely immobile, k* is the critical concentration less than critical micelle concentration ($k_{CMC}$) for which the surface of the bubble starts to remobilize due to the formation of micelle free zone at the back-end of the bubble and $k^{\#}$ is the critical bulk concentration greater than $k_{CMC}$, for which the surface of the bubble becomes completely mobile or stress free.

Our numerical results show that on addition of trace amount of surfactants, the behavior of the bubble changes from completely mobile or stress free interface to completely immobile or stagnant interface. We found that for a bubble translating in creeping flow limits and having a Marangoni number, Ma = 12, the critical concentration required to completely immobilize the interface of the bubble may be as low as CMC/1000-CMC/10000. We observed that small amount of surfactant concentration is required for a small bubble to loose its interfacial mobility as compared to a large bubble. Also a larger amount of surfactant concentration is required to remobilize the interface of a small bubble as compared to a large bubble. We found that if the marangoni number is kept constant, the critical bulk concentration, $k_{c,}$ required to completely immobilize the surface of the bubble is a weak function of peclet number.

We also studied the remobilization of the interface of a bubble translating in creeping flow limits in a continuous phase containing surfactant with low value of Peclet number (Pe=0.1) and Marangoni numbers (Ma) of 0.1 and 1.0. We observed that at far-field bulk concentrations

less than the CMC, a micelle zone appears at the back-end of the bubble and at concentrations greater than the CMC, a micelle-free appears at the front end of the bubble. As the bulk concentrations are increased the region of the bubble covered with monomers decreases and thus the amount of remobilization of the bubble surface also increases. Our results for Pe=0.1 and Ma=0.1 & 1, show that the amount of the surface of the bubble covered with monomers is a strong function of far-field bulk concentration but a weak function of Marangoni number. It was also observed that the drag experienced by the partially remobilized bubbles depended on the marangoni number and the bubbles with larger marangoni number experienced larger drag, as compared to the ones with smaller marangoni number.

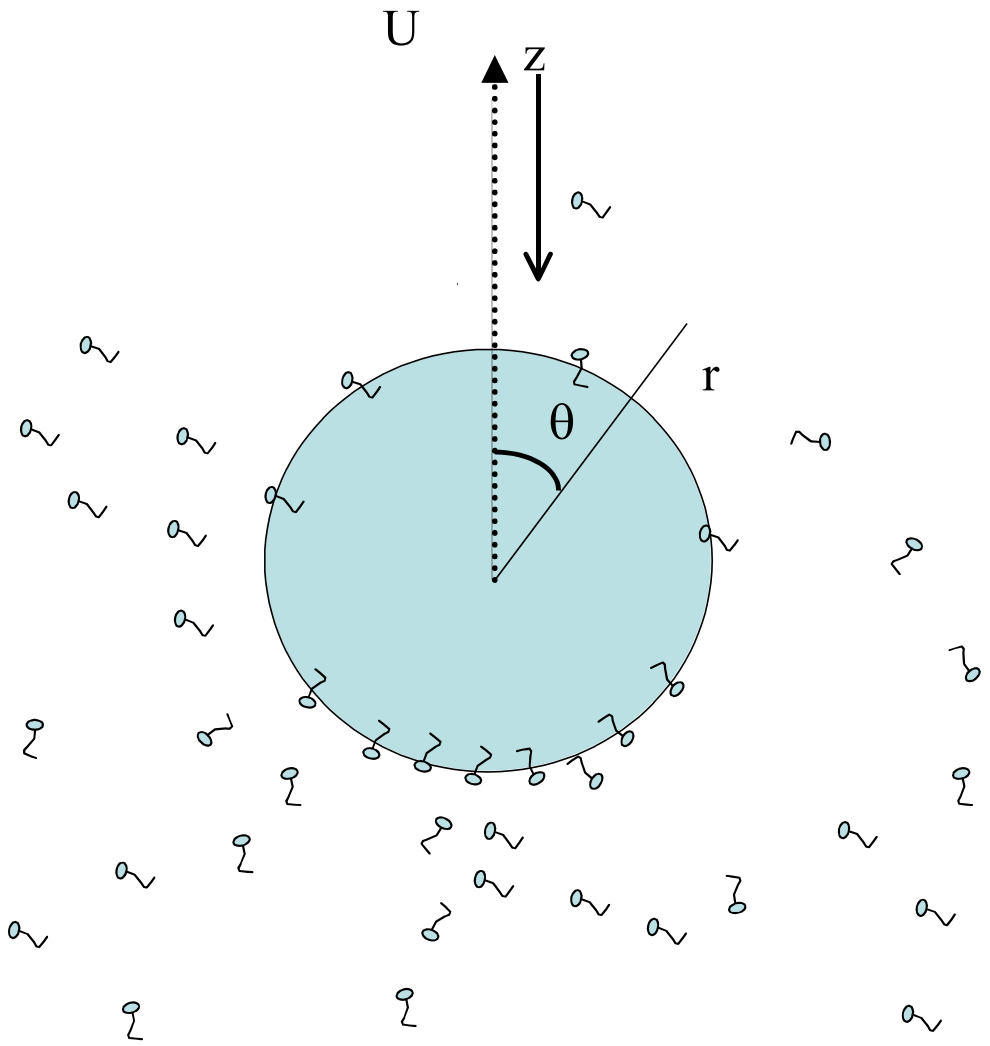


**Figure 4.1 Definition sketch of the flow in a coordinate system moving with the bubble**

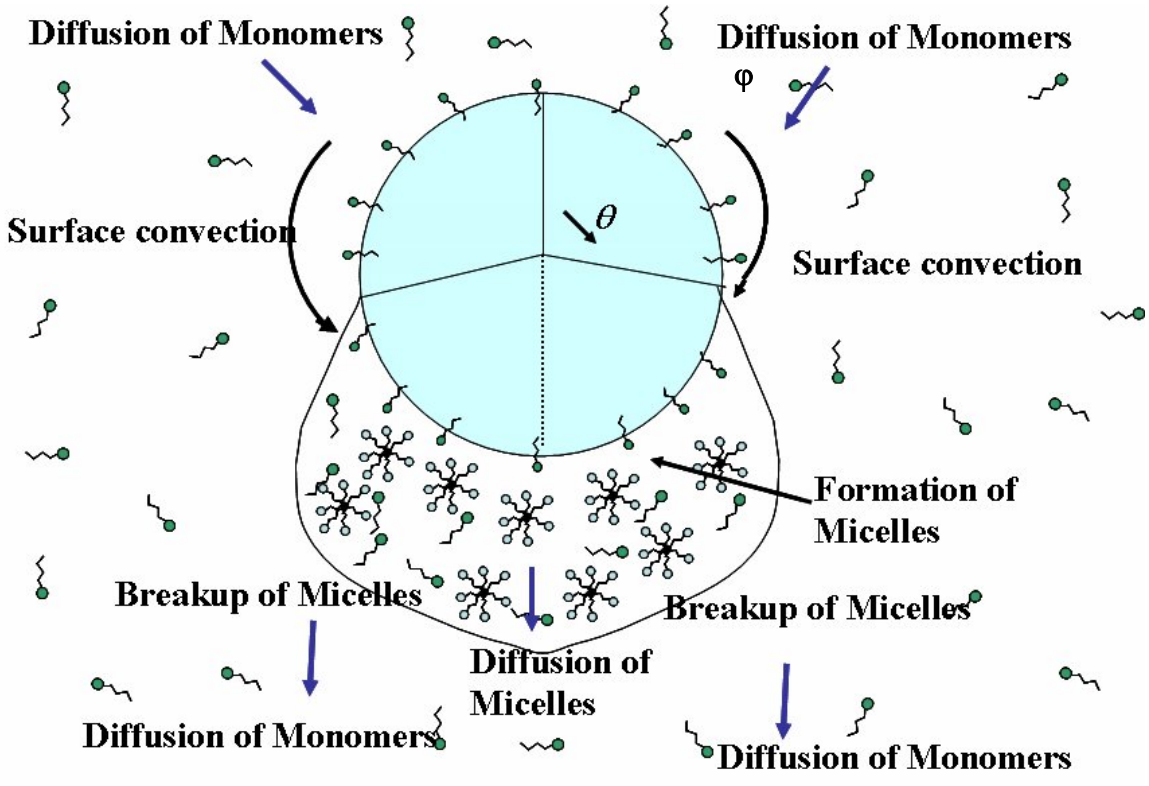


**Figure 4.2 Surfactant transport at bulk concentrations near but less than CMC**

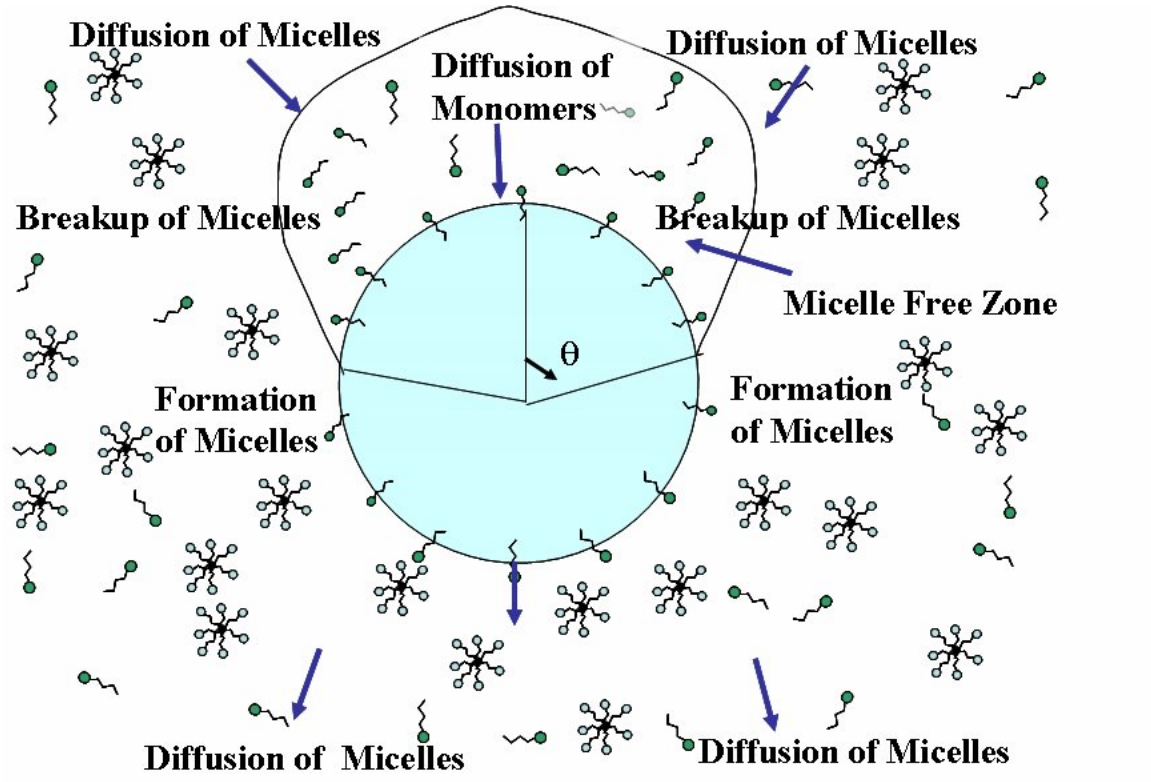


**Figure 4.3 Surfactant transport at bulk concentrations above the CMC**

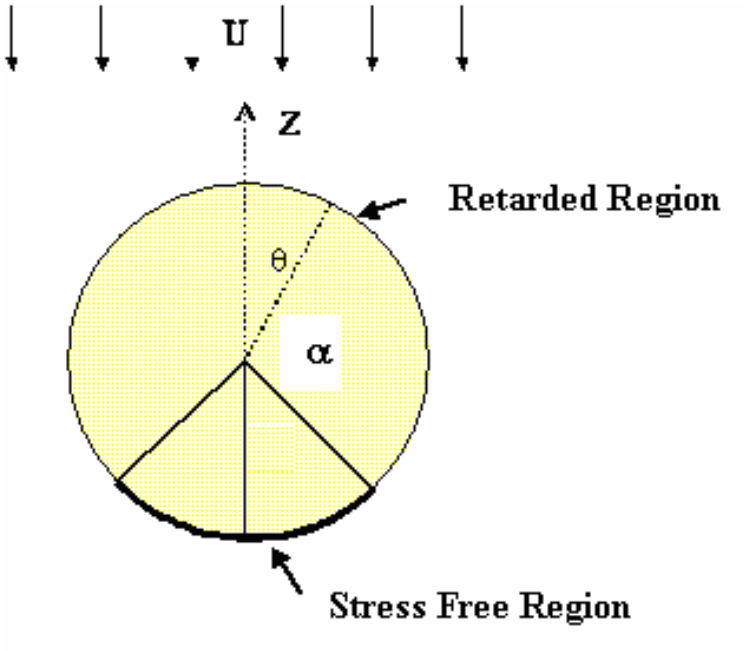


**Figure 4.4 Hydrodynamic conditions on the bubble for concentration k, $k^* < k < k^{\#}$.**

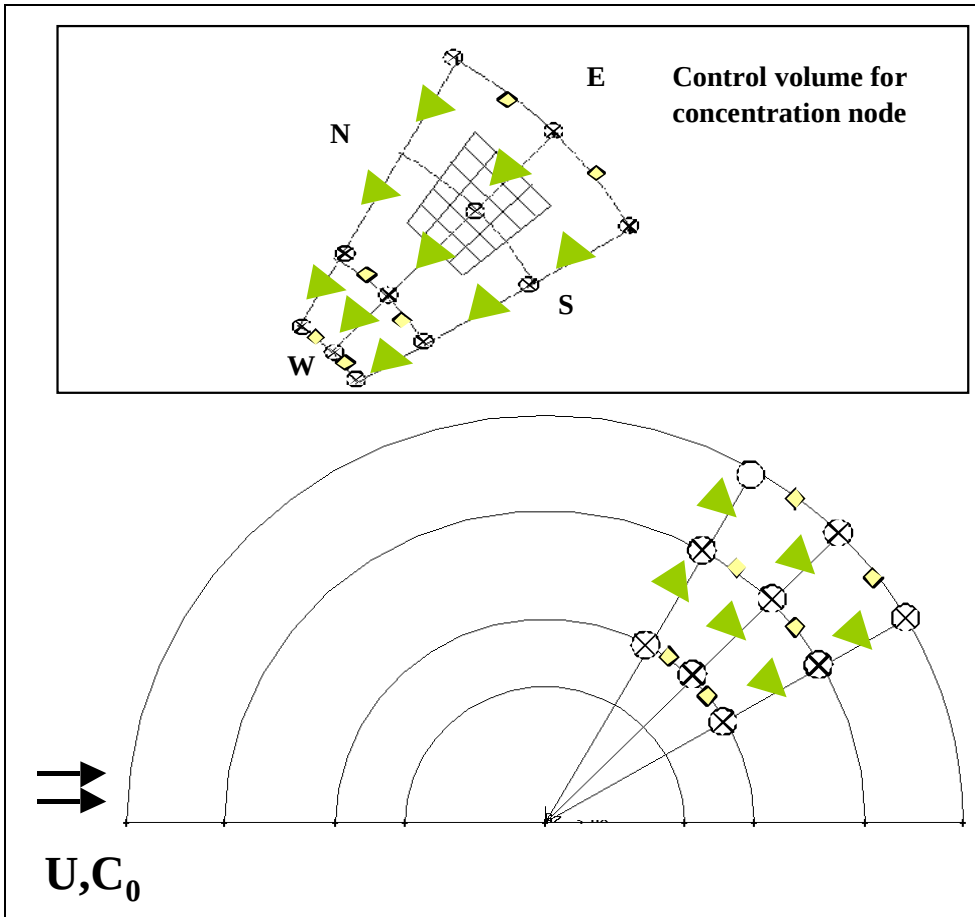


**Figure 4.5 Staggered mesh and control Volume for concentration node**

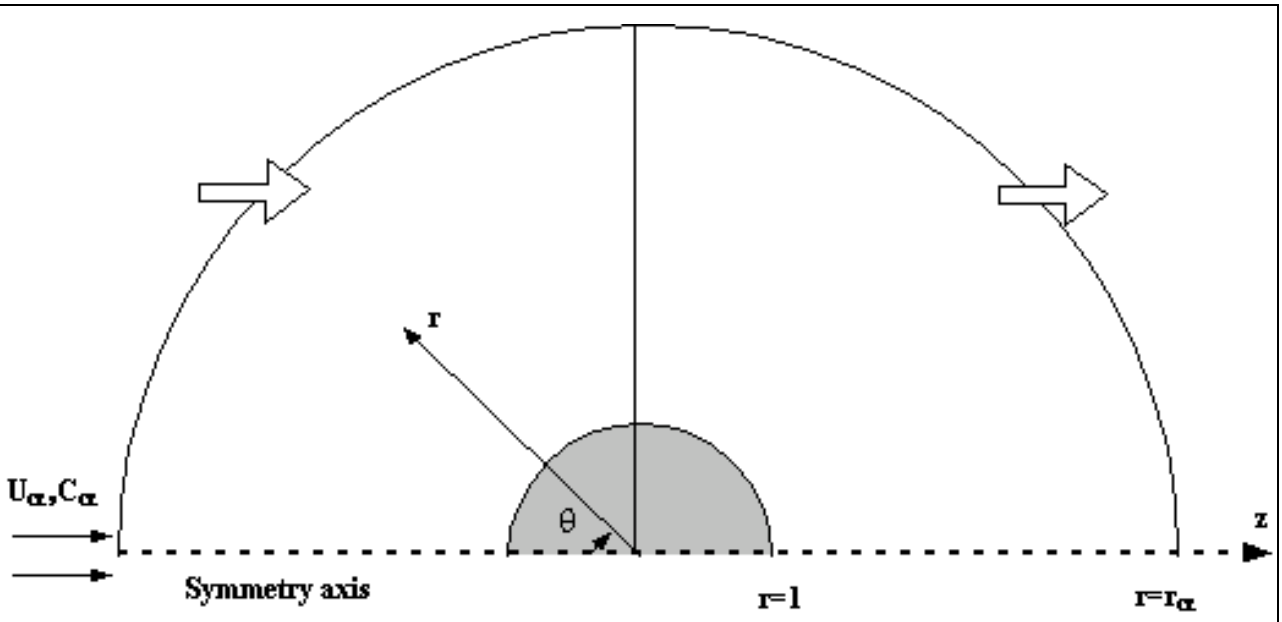


**Figure 4.6 Sketch of the problem. Outer boundary is divided into two Inflow and outflow regions arbitrarily at $\theta=\pi/2$**

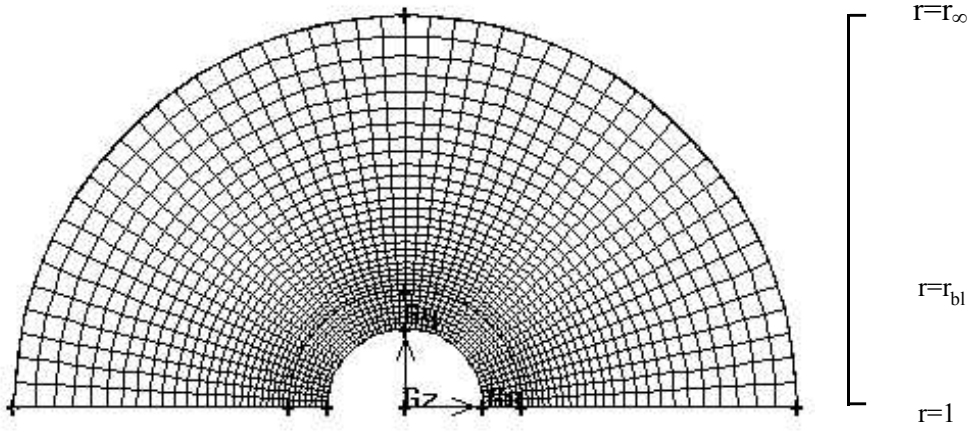


**Figure 4.7 Numerical Grid: a) Finer inner grid from r=1 to r=$r_{bl}$ b) Exponential grid from r=$r_{bl}$ to $r_\infty$**

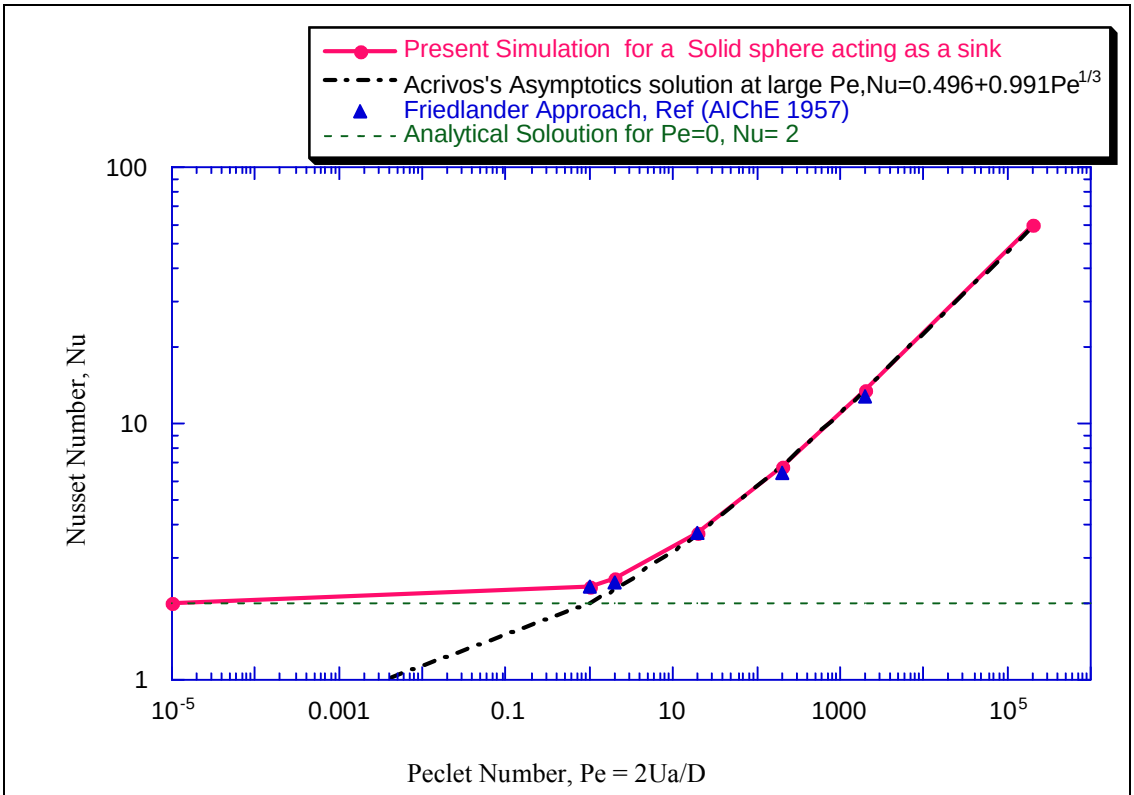


**Figure 4.8 Model Validation: Comparison of Nusset Number (as a function of Peclet number) obtained by the present simulations with those obtained by various other techniques for the case when the surface of the solid sphere is acting as a sink in creeping flow limits**

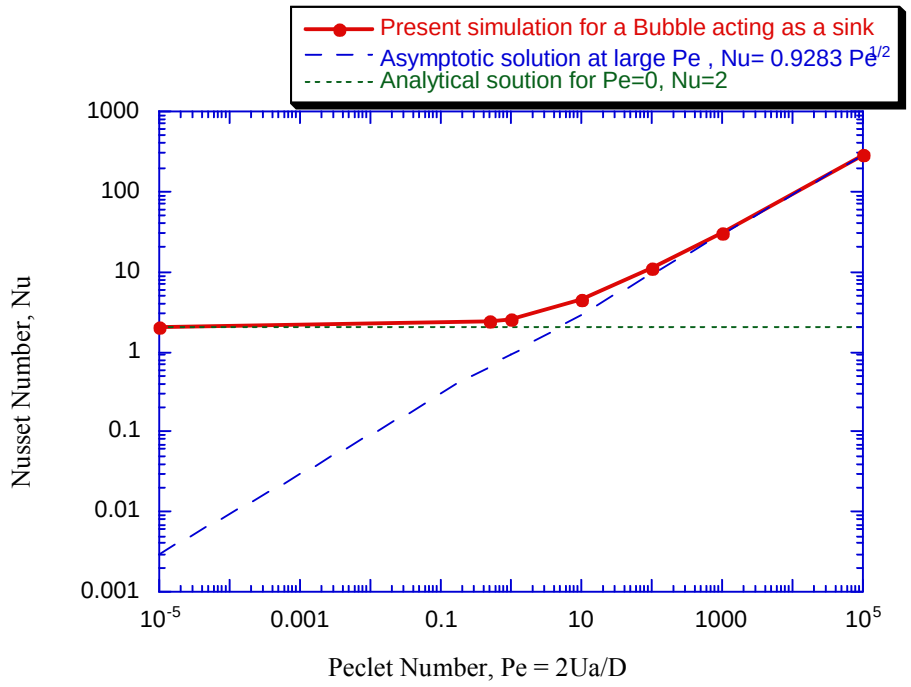


**Figure 4.9 Model Validation: Comparison of Nusset Number (as a function of Peclet number) obtained by the present simulations with those obtained by various other techniques for the case when the surface of the bubble is acting as a sink in creeping flow limits**

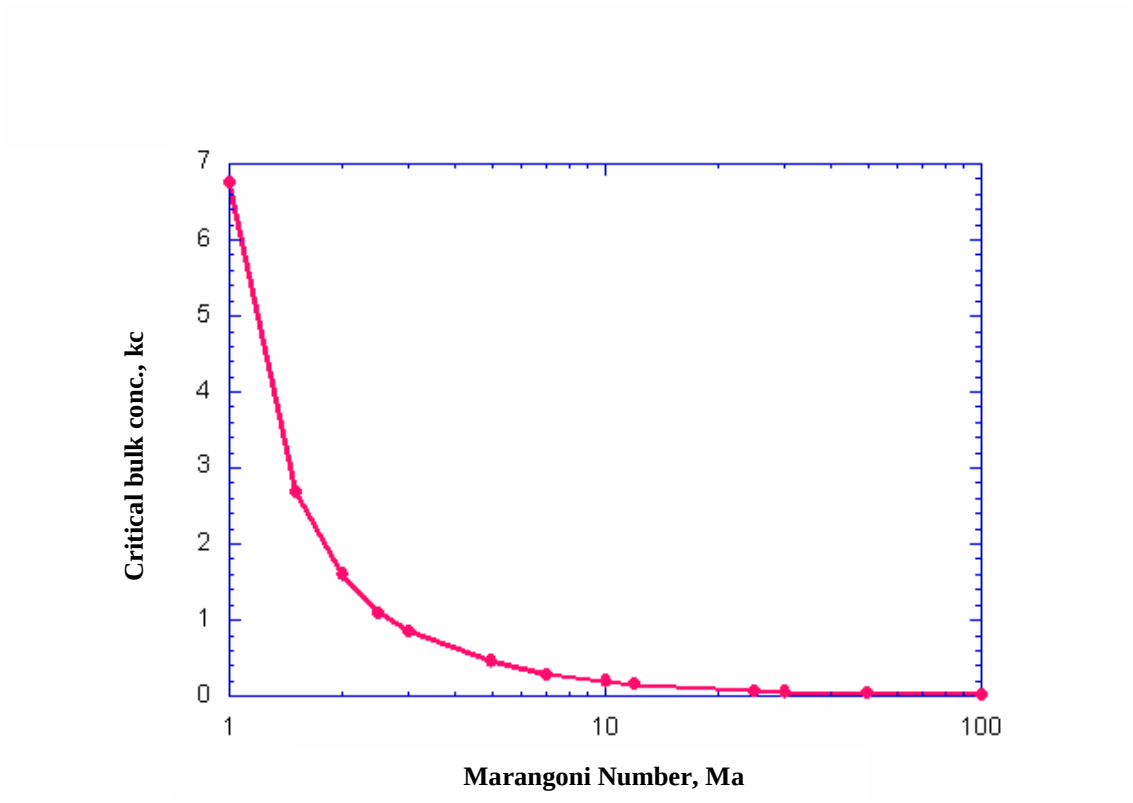


**Figure 4.10 Critical concentration necessary to completely immobilize the surface as a function of Marangoni number**

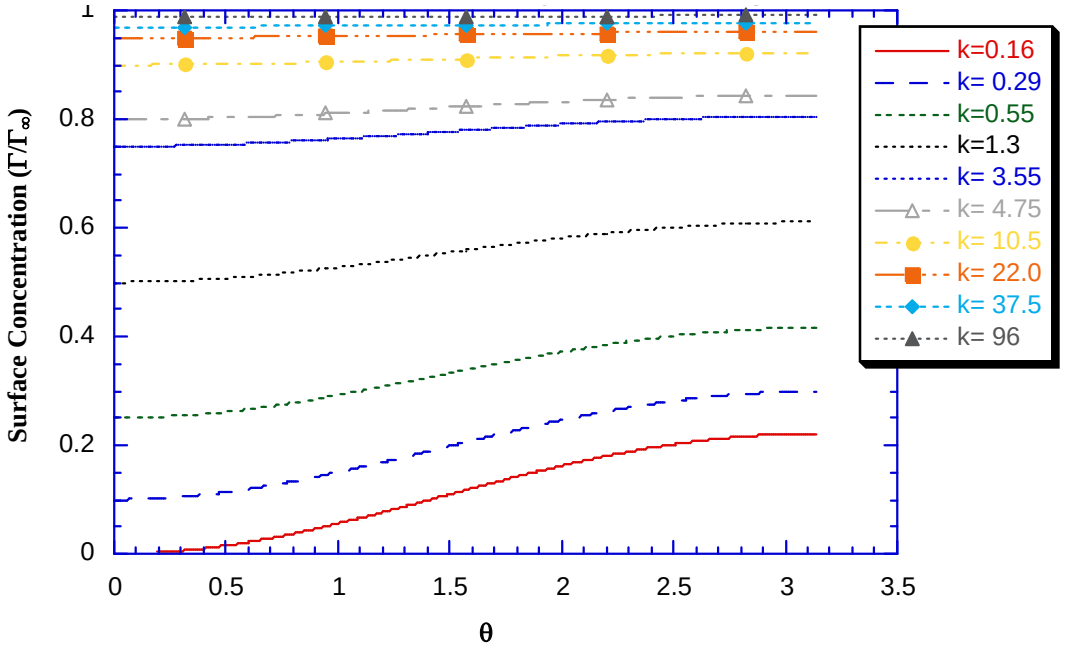


**Figure 4.11 Surface Concentration Distribution. Pe=1000 and Ma=12**

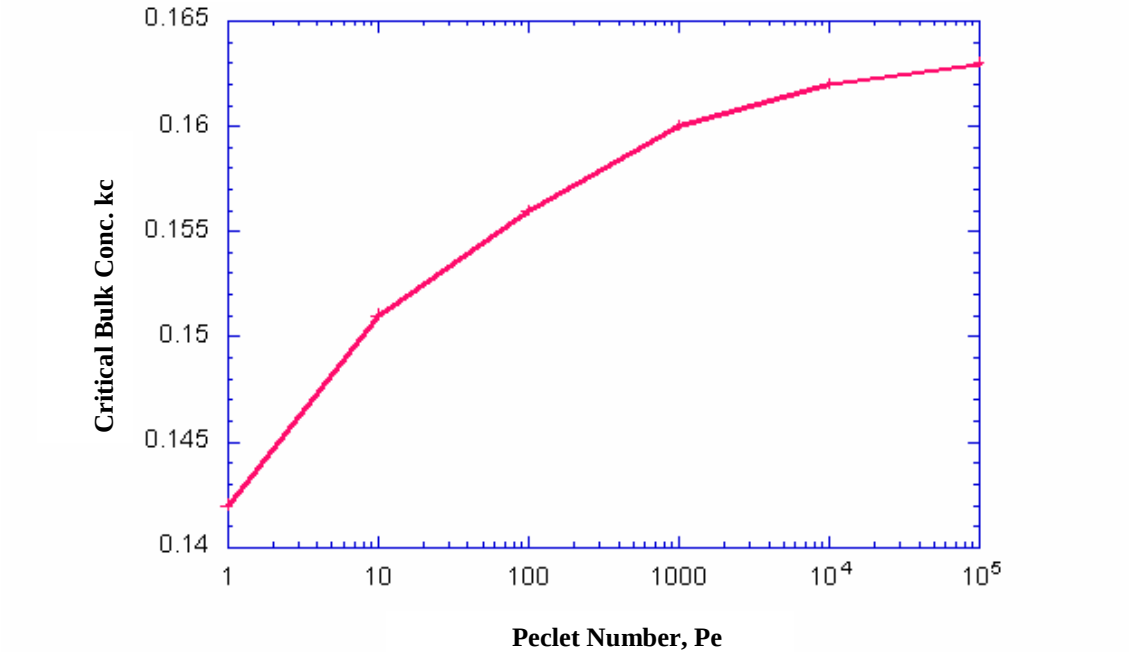


**Figure 4.12 Dependence of Critical Bulk Concentration on Peclet Number, Ma=12**

.

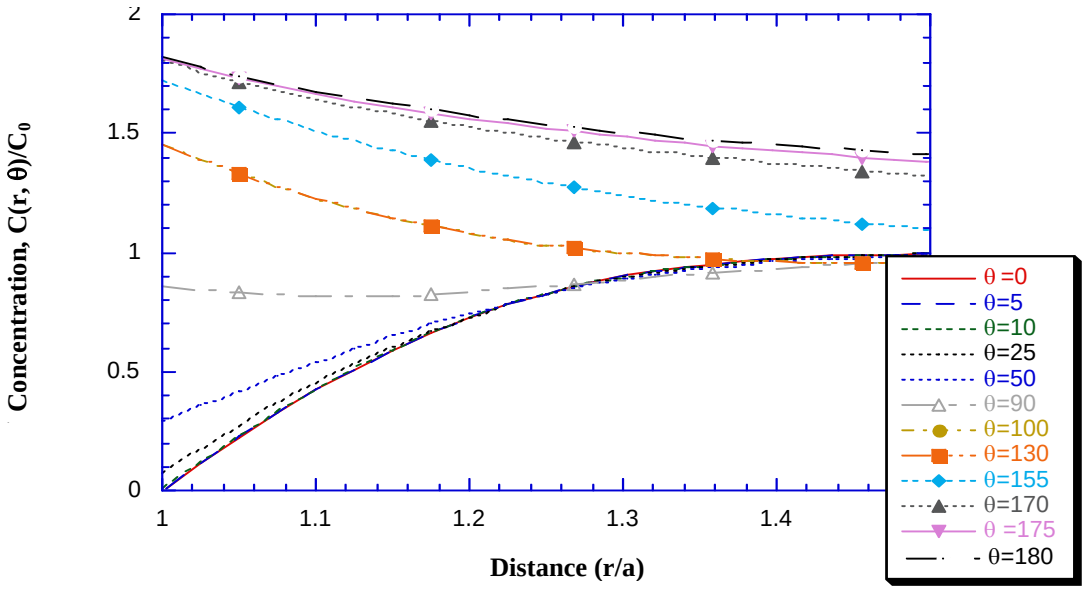


**Figure 4.13 Surfactant concentration profile near a bubble surface at critical bulk concentration (kc). Pe=100, Ma=12, kc=0.156**

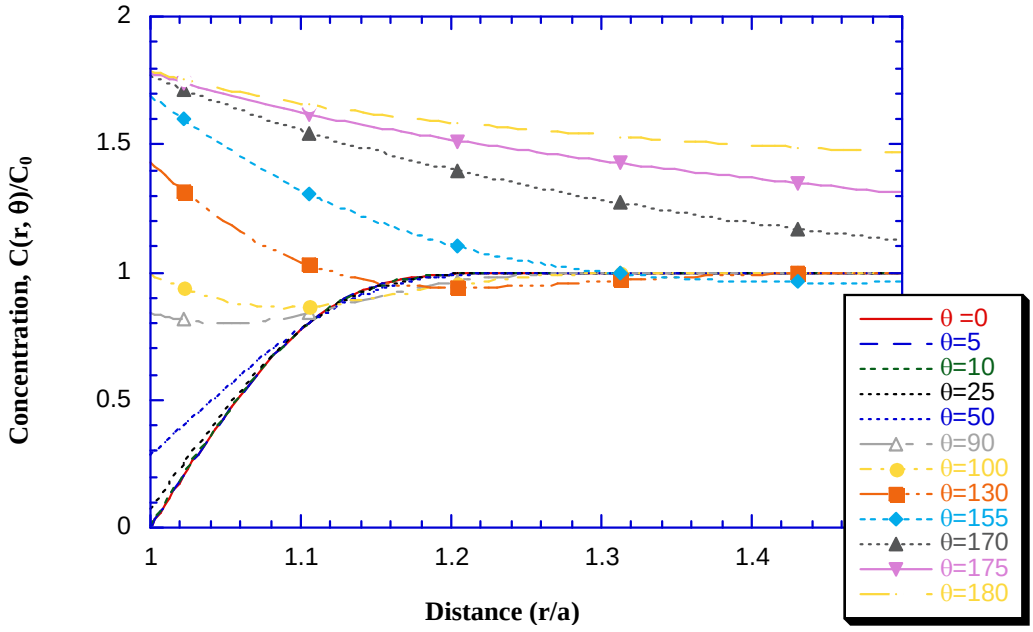


**Figure 4.14 Concentration profile near a bubble surface at critical bulk concentration (kc). Pe=1000, Ma=12, kc=0.159**

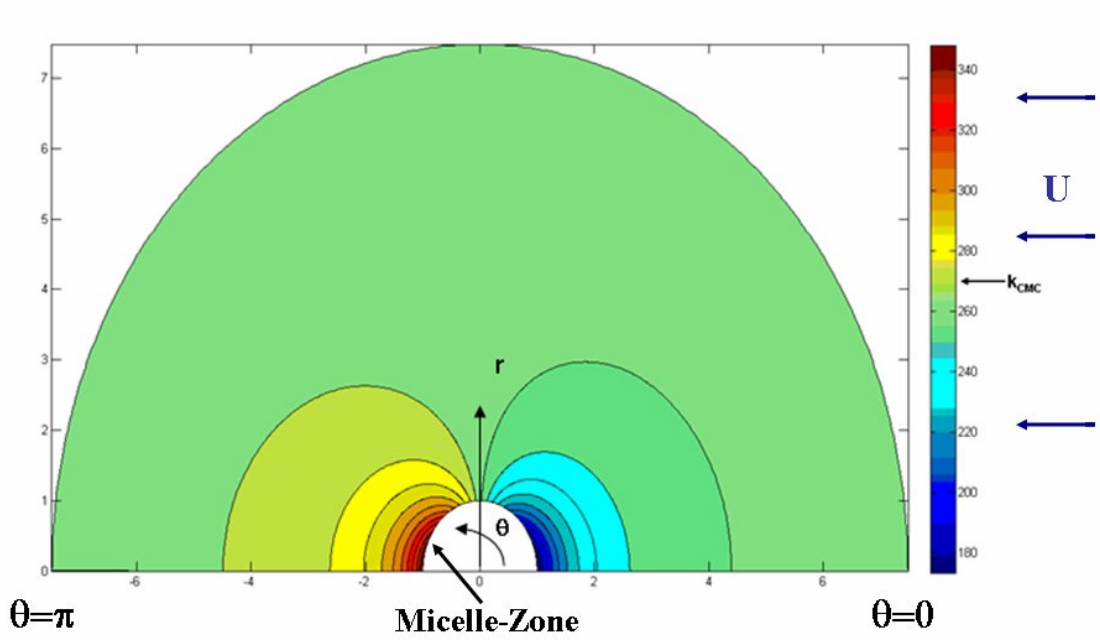


**Figure 4.15a Surfactant concentration profile around a bubble surface. Pe=0.1, Ma=0.1, k=265, $\chi k_{CMC}/Pe$= 1.458, B*=1, $k_{CMC}$= 270 and $\varphi = 94.5^0$**

.

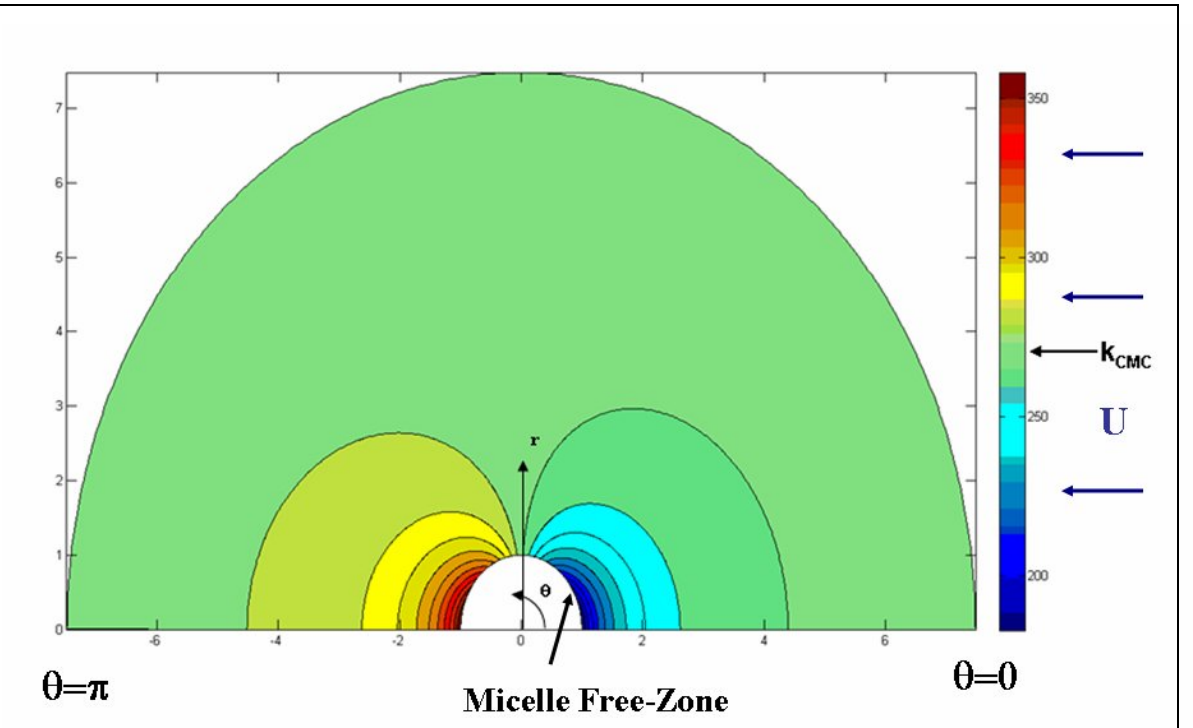


**Figure 4.15b Surfactant concentration profile around a bubble surface. Pe=0.1, Ma=0.1, k=275, $\chi k_{CMC}/Pe$= 1.458, B*=1, $k_{CMC}$= 270 and $\varphi$= 88.2$^0$**

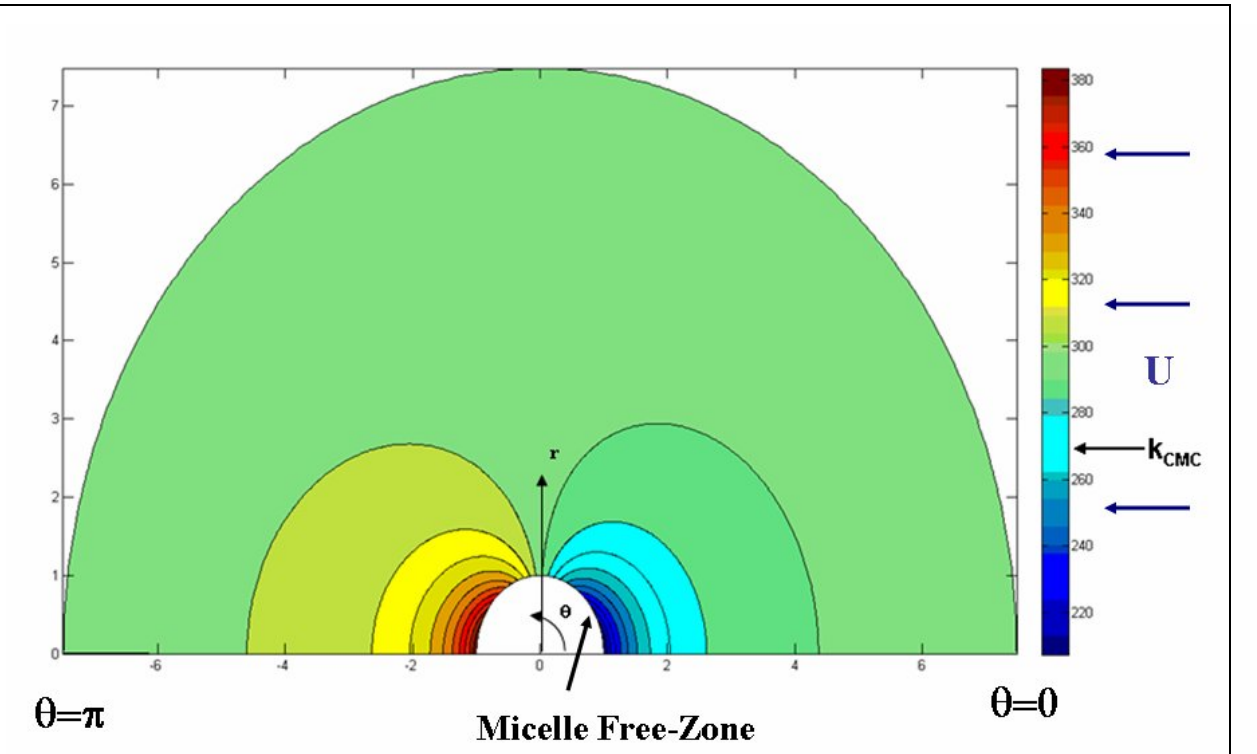


**Figure 4.15c Surfactant concentration profile around a bubble surface. Pe=0.1, Ma=0.1, k=300, $\chi k_{CMC}/Pe$= 1.458, B*=1, $k_{CMC}$= 300 and $\varphi$= 72.6$^0$**

`

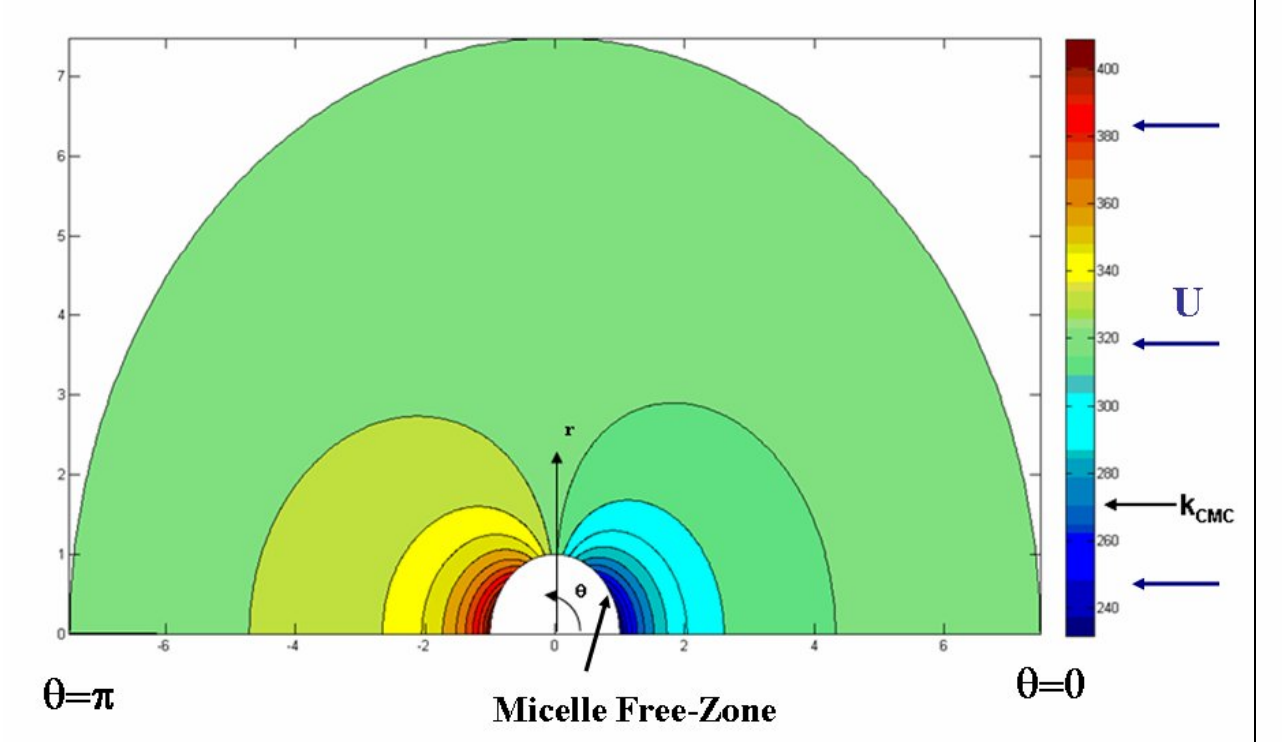


**Figure 4.15d Surfactant concentration profile around a bubble surface. Pe=0.1, Ma=0.1, k=325, $\chi k_{CMC}/Pe$= 1.458, B*=1, $k_{CMC}$= 270 and $\varphi$= $55.2^0$**

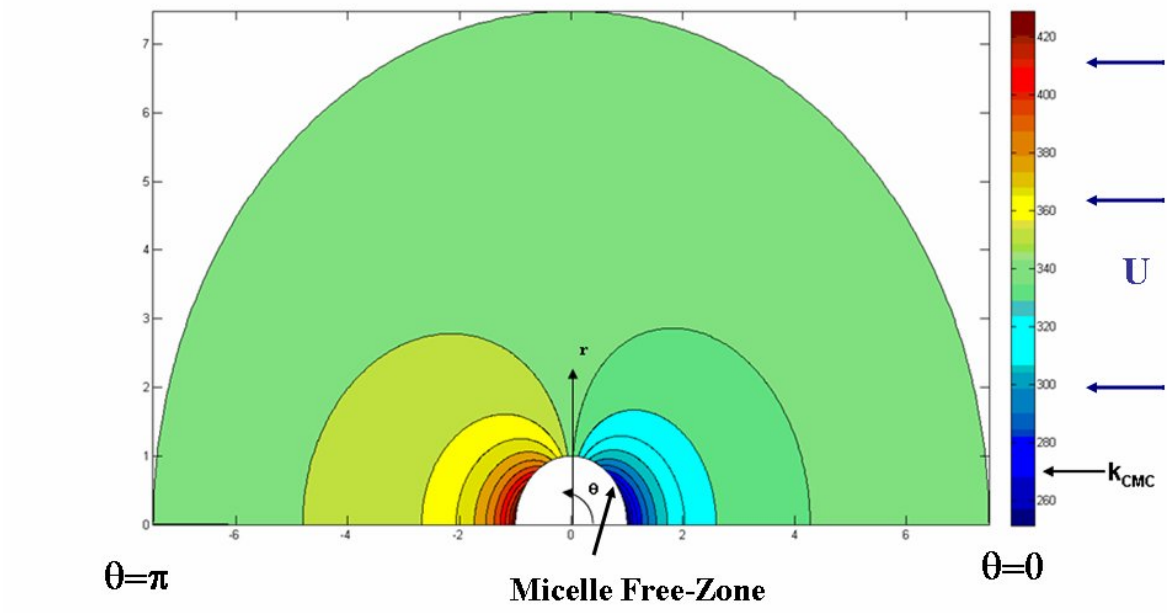


**Figure 4.15e Surfactant concentration profile around a bubble surface. Pe=0.1, Ma=0.1, k=345, $\chi k_{CMC}/Pe$= 1.458, B*=1, $k_{CMC}$= 270 and $\varphi$= $37.8^0$**

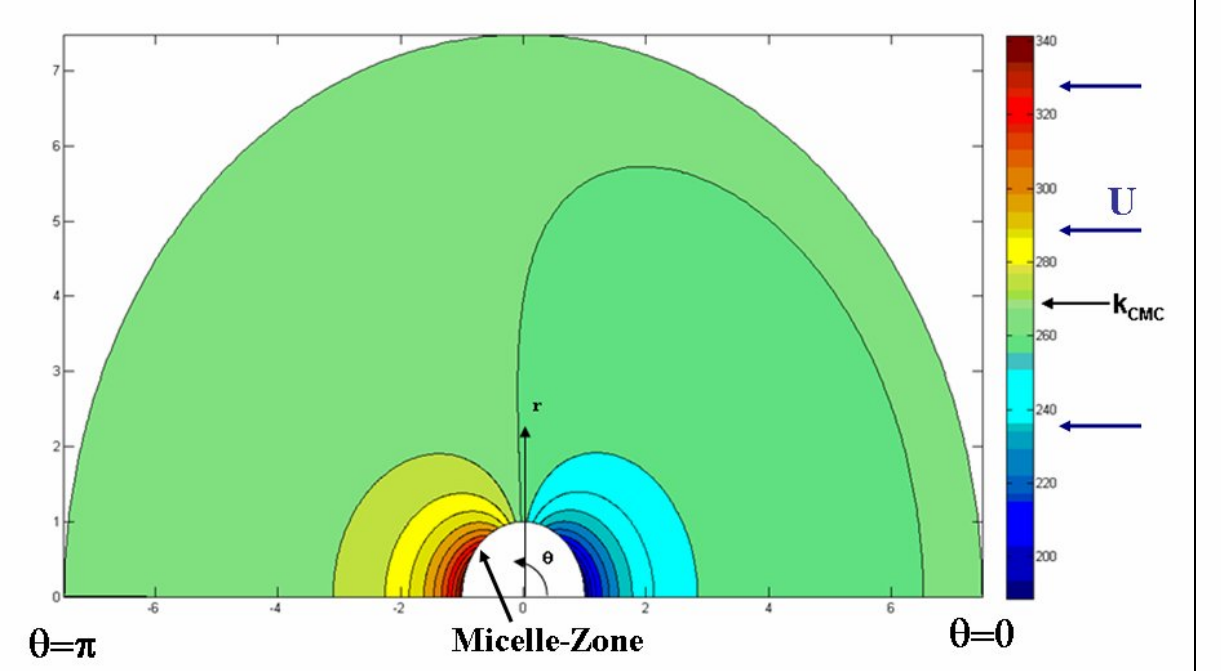


**Figure 4.16a Surfactant concentration profile around a bubble surface. Pe=0.1, Ma=1.0, k=265, $\chi k_{CMC}/Pe$= 1.458, B*=1, $k_{CMC}$= 270 and $\varphi = 96^0$**

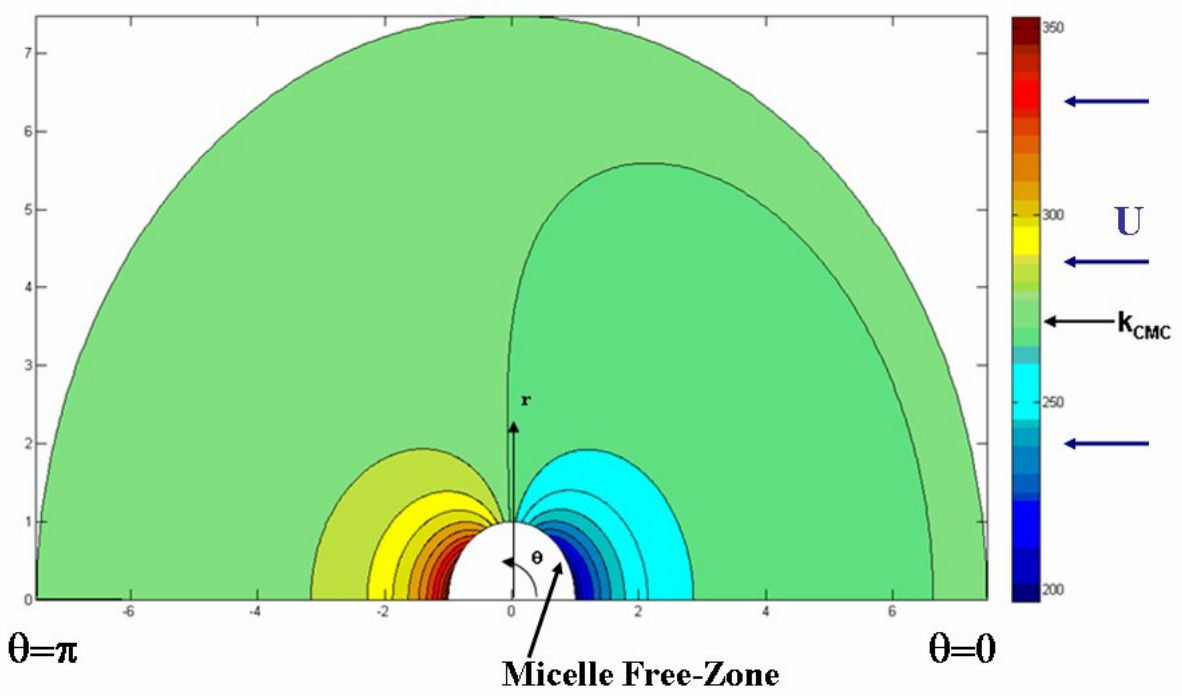


**Figure 4.16b Surfactant concentration profile around a bubble surface. Pe=0.1, Ma=1.0, k=275, $\chi k_{CMC}/Pe$= 1.458, B*=1, $k_{CMC}$= 270 and φ= $88.8^0$**

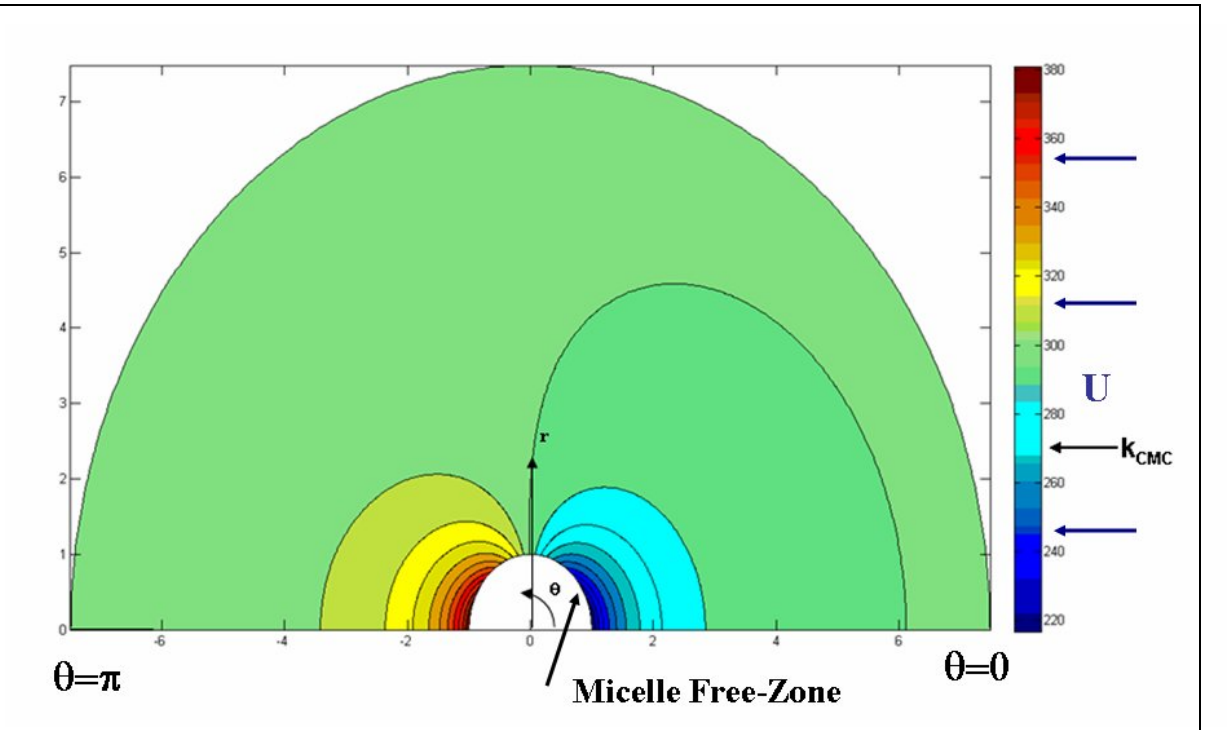


**Figure 4.16c Surfactant concentration profile around a bubble surface. Pe=0.1, Ma=1.0, k=300, $\chi k_{CMC}/Pe$= 1.458, B*=1, $k_{CMC}$= 270 and $\varphi = 72^0$**

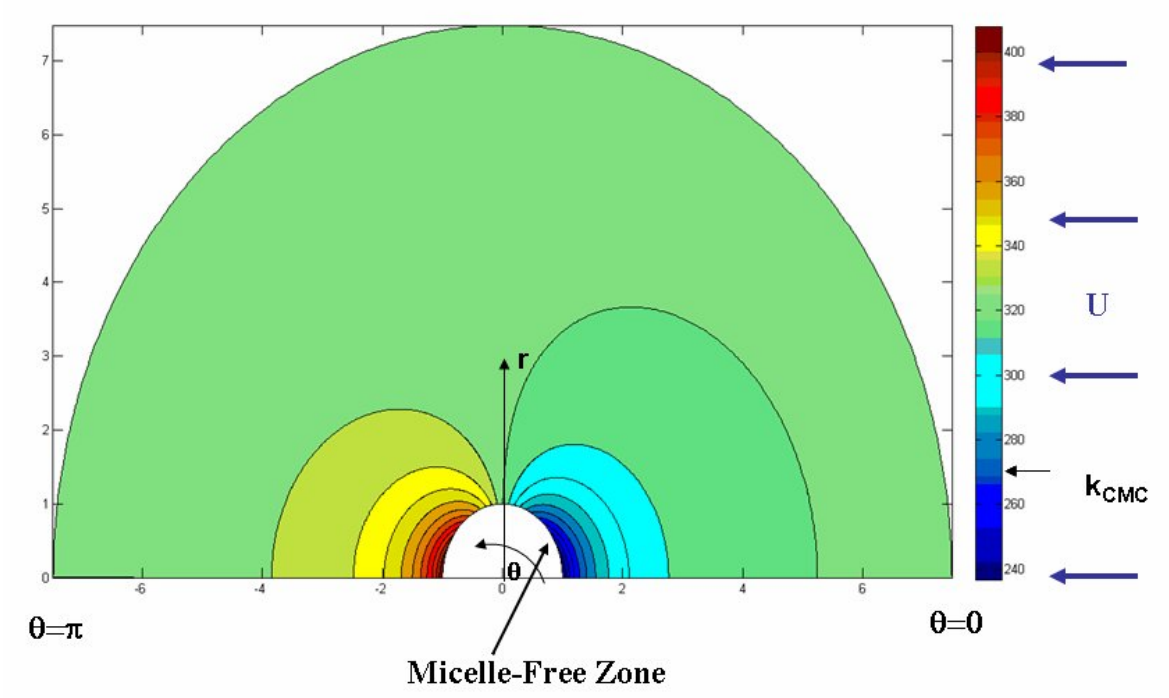


**Figure 4.16d Surfactant concentration profile around a bubble surface. Pe=0.1, Ma=1.0, k=325, $\chi k_{CMC}/Pe$= 1.458, B*=1, $k_{CMC}$= 270 and $\varphi$= $54.6^0$**

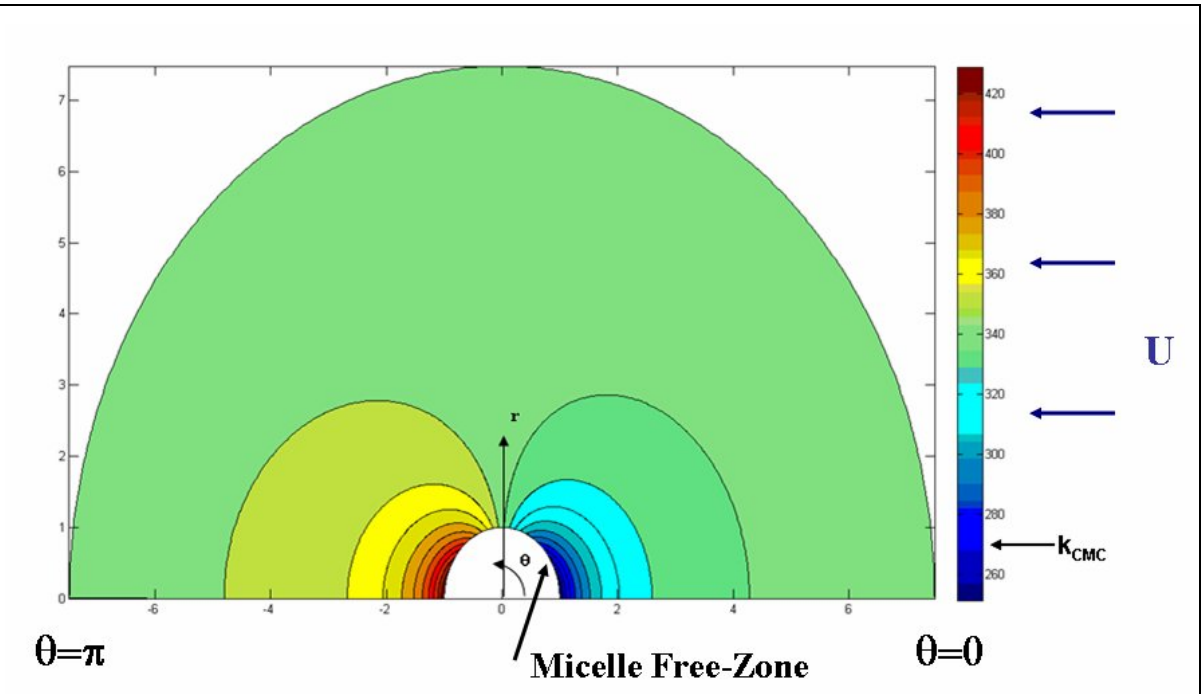


**Figure 4.16e Surfactant concentration profile around a bubble surface. Pe=0.1, Ma=1.0, k=345, $\chi k_{CMC}/Pe$= 1.458, B*=1, $k_{CMC}$= 270 and $\varphi$= $37.2^0$**

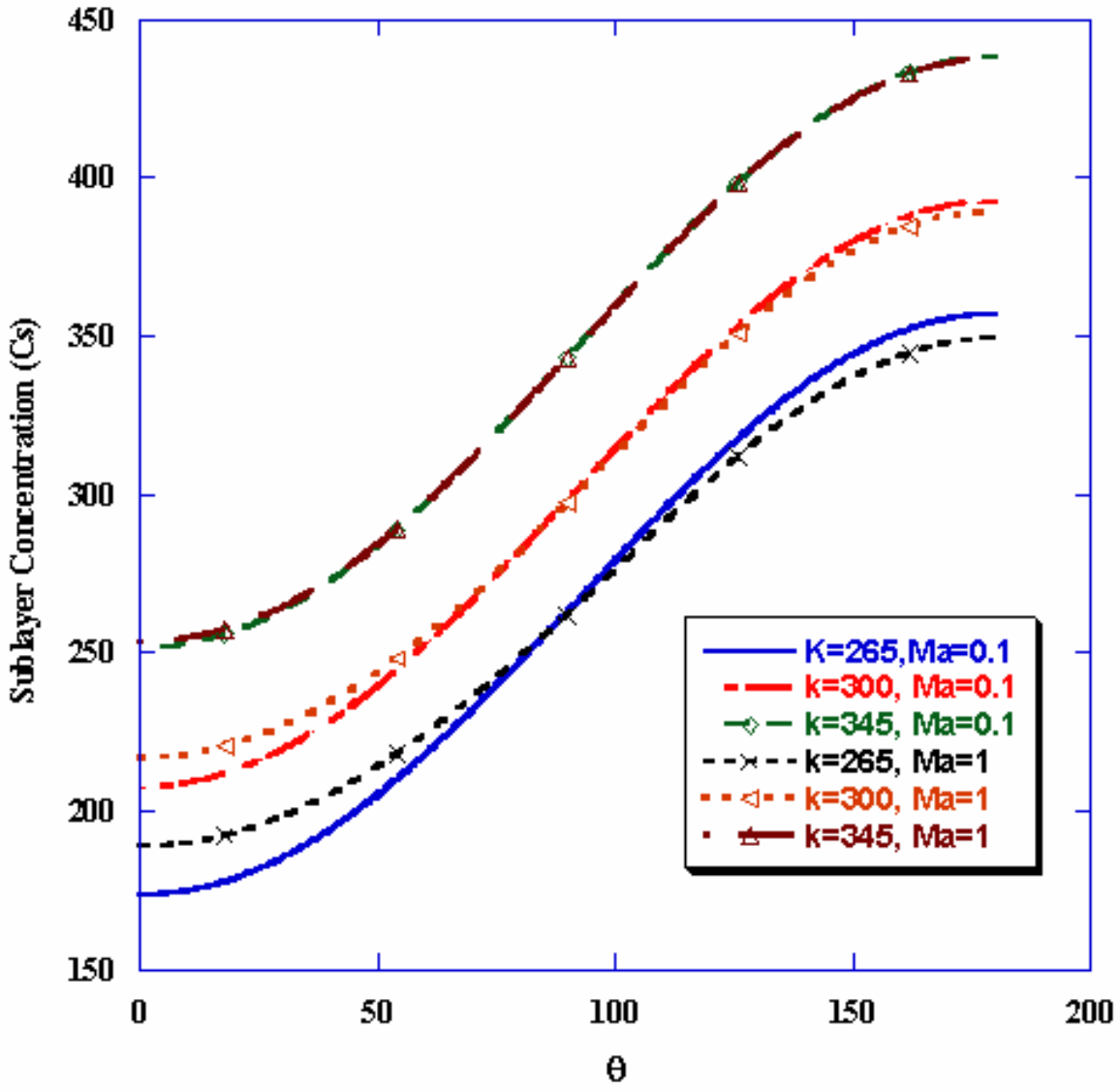


**Figure 4.17 Sublayer concentration as a function of non-dimensional far-field concentration (k). $k_{CMC}$=270, Pe=0.1, , $\chi k_{CMC}$/Pe= 1.458 and B*=1.**

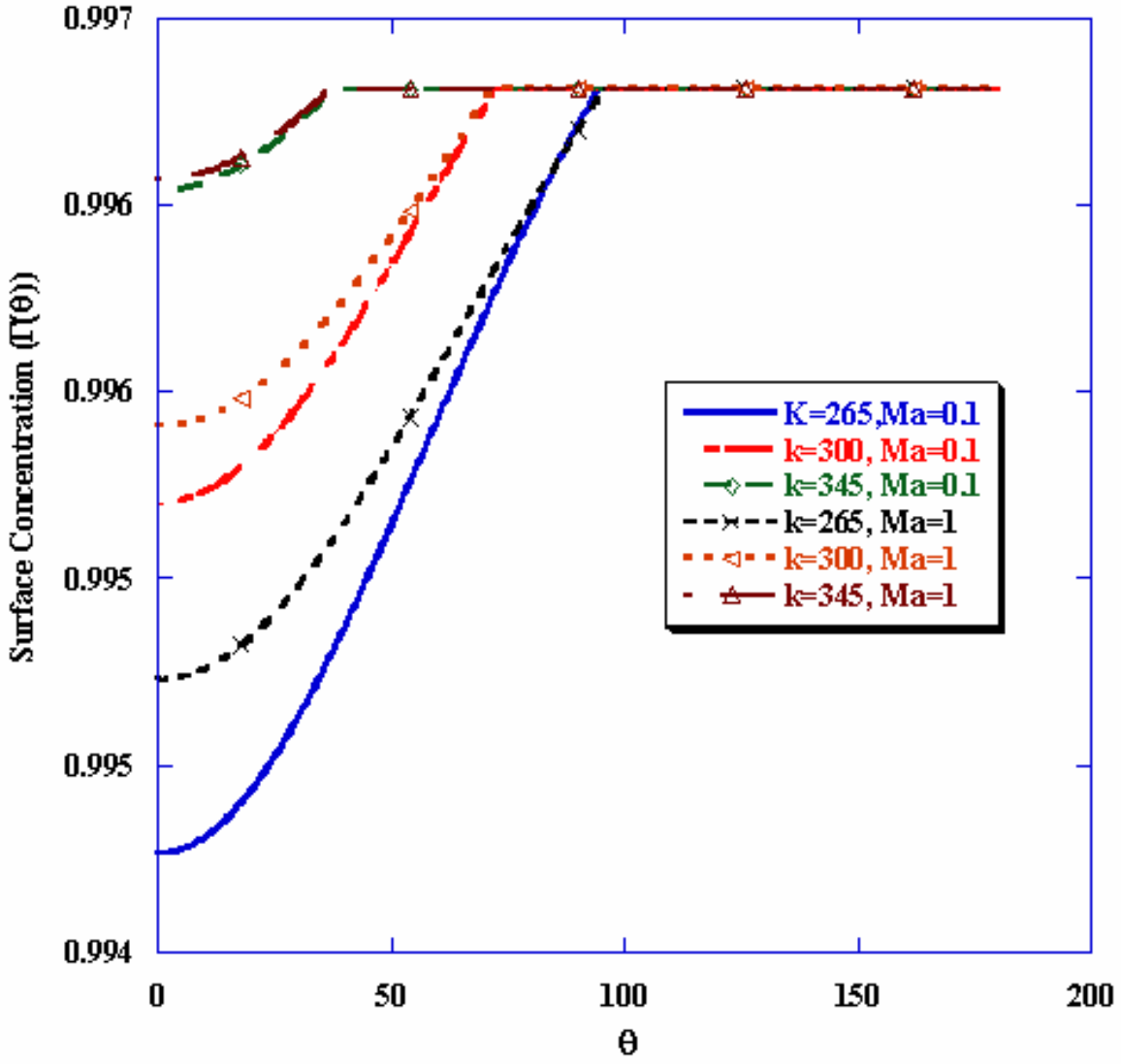


**Figure 4.18 Surface concentration as a function of non-dimensional far field concentration (k). $k_{CMC}$=270, Pe=0.1, $\chi k_{CMC}$/Pe= 1.458 and B*=1.**

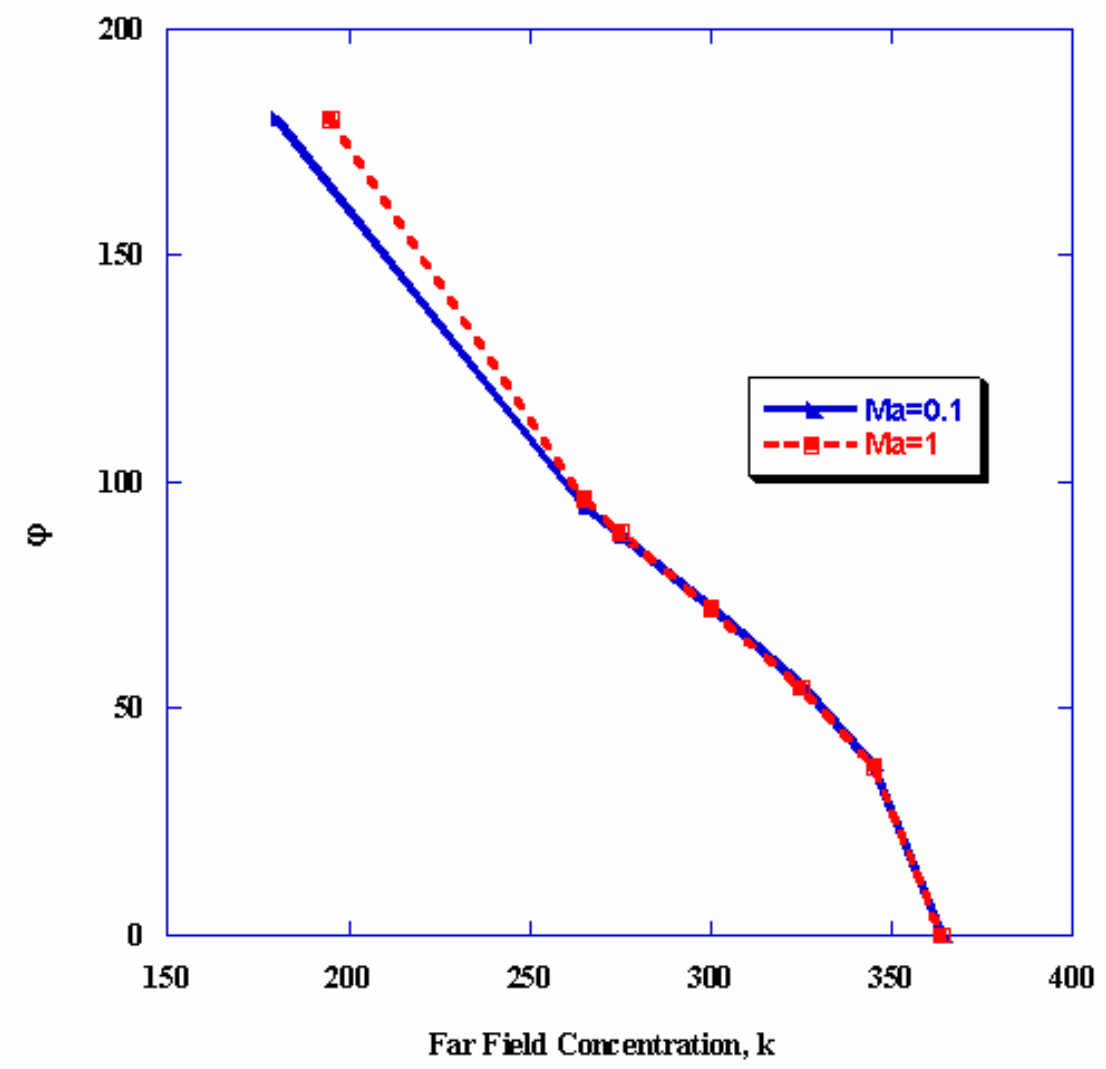


**Figure 4.19 Variation of φ as function of non-dimensional far-field concentration (k) and Marangoni number (Ma) for Pe=0.1, $\chi k_{CMC}/Pe$= 1.458 and B*=1.**

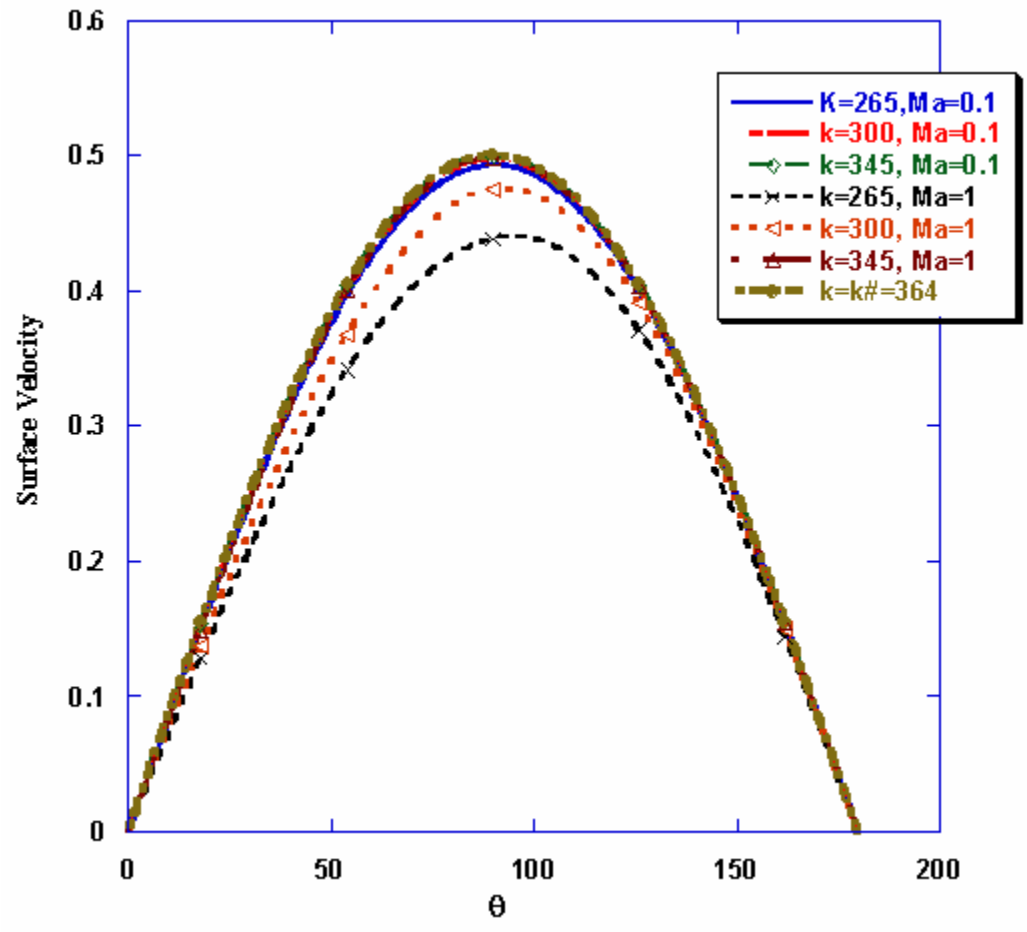


**Figure 4.20 Surface Velocity as a function of far-field concentration (k) and Marangoni number (Ma) for Pe=0.1, $\chi k_{CMC}/Pe$= 1.458 and B*=1.**

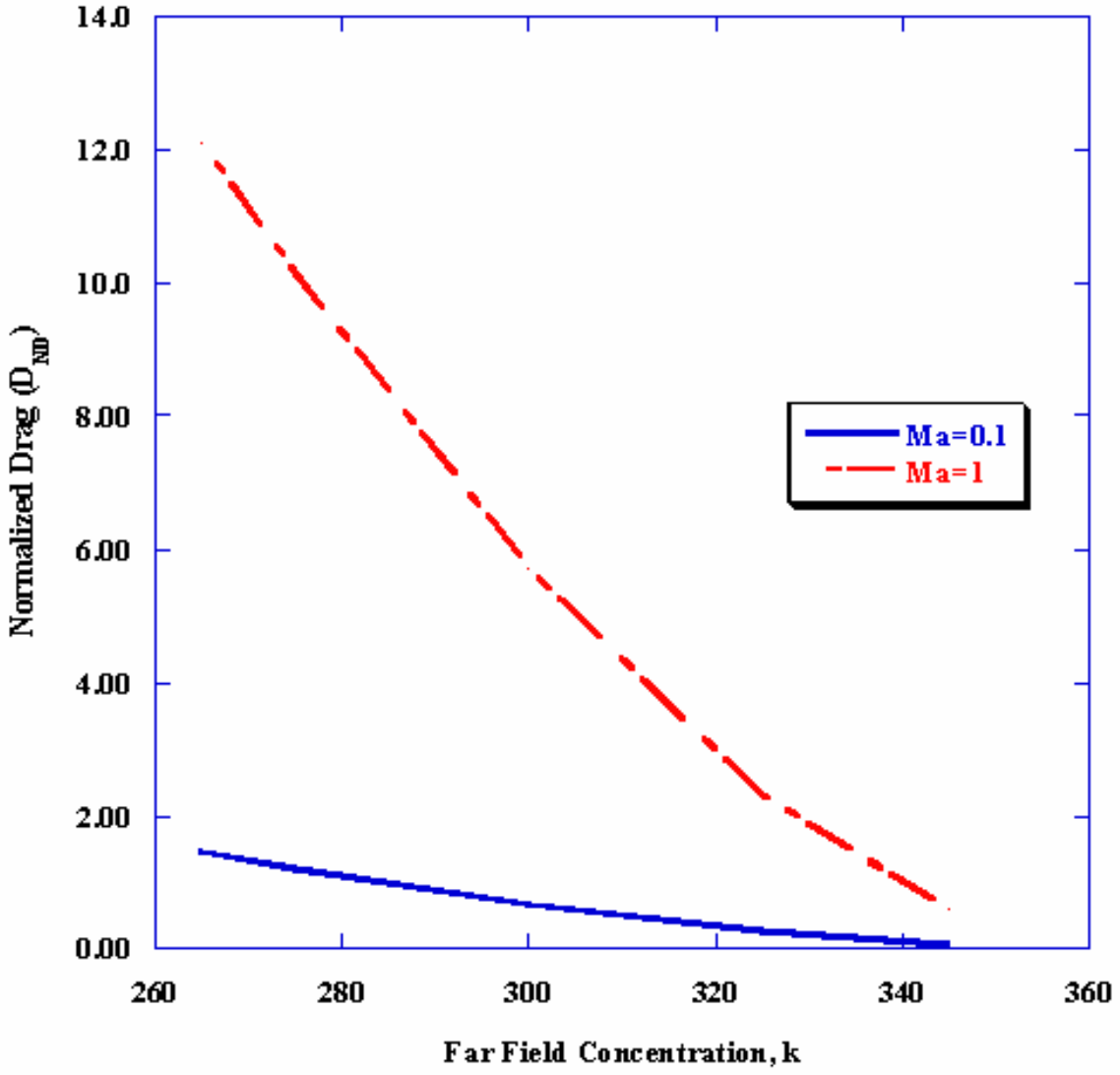


**Figure 4.21 Non-dimensional drag as a function of far-field concentration (k) and Marangoni number (Ma) for Pe=0.1, $\chi k_{CMC}/Pe$= 1.458 and B*=1.**

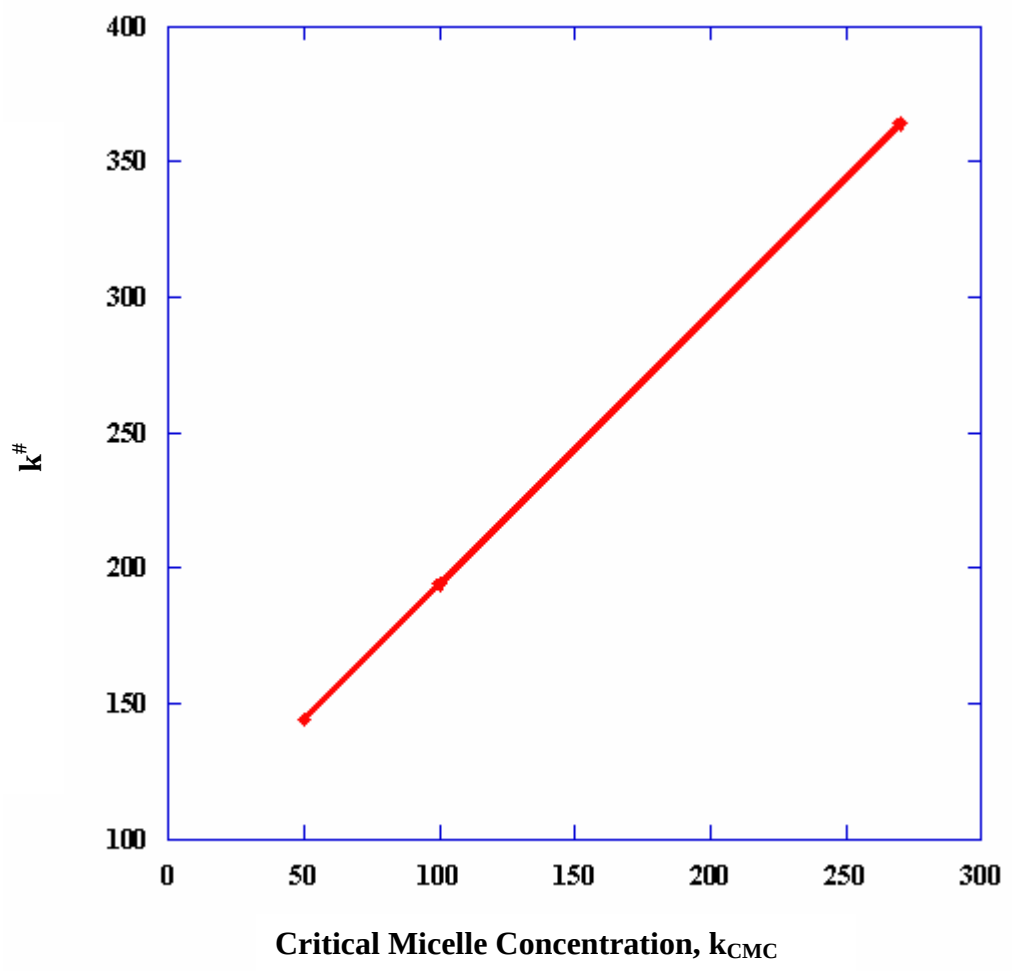


**Figure 4.22 Dependence of $k^{\#}$ on $k_{CMC}$ for Pe =0.1, $\chi k_{CMC}/Pe$= 1.458 and B*=1**

# CHAPTER 5

## Possible Future Work

We studied the effect of surfactants present in the continuous phase on the motion of a bubble. In chapter 3, we have presented our experimental study on the effect of medium chain alcohols on the terminal velocity of nitrogen bubbles rising either in water or in a 70:30 mixture of glycerol-water. We observed that hexanol dissolved in the bulk phase can remobilize the interface of bubbles rising in the glycerol-water mixture. We used pendant bubble tensiometry to measure the dynamic surface tension of hexanol in glycerol-water mixture and obtain mass transfer parameters. As described in chapter 3, the concentrations at which these experiments were carried out, the transport of surfactants from the bulk to the gas/liquid interface was rapid. Therefore to obtain the mass transfer parameters, the dynamic surface tension was measured using contracting bubbles, which initially had equilibrium surfactant monolayer. The faster the kinetic exchange of the surfactant molecules, the faster the bubble needs to be contracted to measure the kinetic exchange parameters. However through our experiments we found out that at an average compression rate of O(100) $mm^2/s$, hydrodynamic effects start to alter the shape of the bubble formed in a 70:30 glycerol/water mixture and Young-Laplace's equation cannot be used to measure the surface tension from the pendant bubble profiles. However at an average compression rate of O(10) $mm^2/s$, hydrodynamic effects don't effect the shape of the contracting bubble. As described in chapter 3, at these slow compression rates, the absolute value of the kinetic rates constants cannot be measured and only bounds can be measured. To measure the absolute value of kinetic

rate constants, dynamic surface tension needs to measured at compression rates of the order of O(100) $mm^2/s$ or higher.

Another study that can be carried to out is to experimentally visualize the micelle and micelle-free zones predicted for $C_o < C_{CMC}$ by using fluorescence microscopy. This technique is based on the concept of using a surfactant dye molecule with a long hydrophobic chain and a chromophore attached to one end of the chain which is weakly polar. The chromophore fluoresces upon excitation when it is in a hydrophobic environment, but the fluorescence is quenched when the chromophore is immersed in an aqueous environment. This property can be used to visualize the micelle-free zone in the following way. When the surfactant dye molecule is dissolved into a miceller solution, the long hydrocarbon chain of the molecule allows it to partition into the hydrophobic cores of the micelles. When the solution is illuminated at the excitation wavelength of chromphore, the chromophore fluoresces and illuminates the solution. If the surfactant solution does not contain micelles, then the dye molecule solubility in the solution is much reduced relative to micellar solutions since the dye must adsorb into the phase and the long hydrocarbon chain of the dye limits its dissolution in water. The limited amount of dye, which adsorbs into the surfactant solutions below the CMC does not fluoresce in any case because the chromophore is in an aqueous environment. These experiments can be conducted in a micro-fluidic cell. Train of alternating air and aqueous solution (with a remobilizing surfactant) segments can be made to pass through the channels in the micro-fluidic cell. If the aqueous solution preferentially wets the surface of the channels, the air slugs would move in these channels without touching the surface. The rate of surface convection of surfactant at the air/water interface can be controlled by controlling the

drawn velocity of the slugs. This rate can be kept small enough, such that the long time scale of the break-up of the micelles is greater than the time scale of surface convection. Confocal microscope can be used to observe the micelle zone formed at the rear end of these slugs.

In chapter 4, we have presented our theoretical study to predict the remobilization of interface of bubbles rising at bulk surfactant concentrations just below to greater than the critical micelle concentration. This study is carried out for the case when the bubble is moving in creeping flow limits, for Peclet number of 0.1 and Marangoni number of 0.1 and 1.0. It would be interesting to extend the study, to the case of higher Peclet numbers and Marangoni numbers.

# APPENDIX A

## Analytical Solution for Creeping

## Flow around a Partially Remobilized Bubble

Axsymmetric creeping flow around a spherical particle can be given in terms of stream function $\psi$, satisfying the following equation.

$$E^4\psi = 0 \qquad \text{A.1}$$

The general solution to the above equation is

$$\psi = \sum_{n=0}^{\infty}\left(A_n r^{-n+3} + B_n r^{-n+1} + C_n r^{n+2} + D_n r^{n}\right)C_n^{-1/2}(\cos\theta) \qquad \text{A.2}$$

Where $C_n^{-1/2}(\cos\theta)$ is the Gegenbauer polynomials of degree -1/2.

Thus Velocity in radial direction ($V_r$) and in azimuthal direction ($V_\theta$) is given by:

$$V_r = -\frac{1}{r^2\sin\theta}\frac{\partial\Psi}{\partial\theta} = -\frac{1}{r^2}\sum_{n=2}^{\infty}(A_n r^n + B_n r^{1-n} + \frac{C_n}{2(2n+1)}r^{n+2} + \frac{D_n}{2(3-2n)}r^{3-n})P_{n-1}(\cos\theta)$$

A.3

$$V_\theta = \frac{1}{r\sin\theta}\frac{\partial\Psi}{\partial r} = \frac{1}{r}\sum_{n=2}^{\infty}(nA_n r^{n-1} + B_n(1-n)r^{-n} + \frac{C_n(n+2)}{2(2n+1)}r^{n+1} + \frac{D_n(3-n)}{2(3-2n)}r^{2-n})\frac{C_n^{-1/2}(\cos\theta)}{\sin\theta} +$$
$$\frac{1}{r\sin\theta}\left[B_0 + C_0 r + \frac{3D_0}{6}r^2\right]C_0^{-1/2}(\cos\theta) + \frac{1}{r\sin\theta}\left[A_1 + \frac{C_1}{2}r^2 + D_1 r\right]C_1^{-1/2}(\cos\theta)$$

A.4

Where $P_{n-1}(\cos\theta)$ is the Legendre Polynomial of order n.

Shear stress is given by

$$\tau_{r\theta} = r\frac{d}{dr}\left(\frac{V_\theta}{r}\right) + \frac{1}{r}\frac{dV_r}{d\theta} = -\frac{1}{r}V_\theta + \frac{dV_\theta}{dr} + \frac{1}{r}\frac{\partial V_r}{\partial\theta} \qquad \text{A.5}$$

$$\tau_{r\theta}\big|_{r=1} = \left(\frac{dV_\theta}{dr} - \frac{1}{r}V_\theta\right)\Bigg|_{r=1} \qquad \text{A.6}$$

The following set of boundary conditions

$$\psi = 0 \qquad \text{for } \theta = 0, \pi \qquad \text{A.7a}$$

$$\psi\big|_{r=1} = 0 \qquad \text{for all } \theta \qquad \text{A.7b}$$

$$\psi\big|_{r\to\infty} = \frac{1}{2}\mathrm{r}^2\sin^2\theta \qquad \text{for all } \theta \qquad \text{A.7c}$$

reduces equations A.2, A.3, A.4 and A.6 to

$$\psi = \frac{1}{2}\left\{r^2 - r\right\}\sin^2\theta + \sum_{n=2}^{\infty} B_n\left[r^{-n+1} - r^{-n+3}\right]C_n^{-1/2}\cos(\theta) \qquad \text{A.8}$$

$$V_{\mathrm{r}} = -(1-\frac{1}{r})\cos\theta - \sum_{n=2}^{\infty} B_n(r^{-1-n} - r^{1-n})P_{n-1}(\cos\theta) \qquad \text{A.9}$$

$$V_\theta = (1-\frac{1}{2r})\sin\theta + \sum_{n=2}^{\infty} B_n\left\{(1-n)r^{-1-n} - (3-n)r^{1-n}\right\}C_n^{-1/2}(\cos\theta) \qquad \text{A.10}$$

$$\tau_{r\theta}\big|_{r=1} = \sum_{n=2}^{\infty} 2B_n(2n-1)\frac{C_n^{-1/2}(\cos\theta)}{\sin\theta} \qquad \text{A.11}$$

If the adsorbed surfactant molecules are distributed onto the surface of the bubble such that there is a surfactant concentration gradient, then Marangoni stresses are generated on the surface.

By the condition of tangential stress balance, we get

$$\tau'_{r\theta}\big|_{r=a} + \frac{1}{a}\frac{\partial\gamma'(\theta)}{\partial\theta}\Bigg|_{r=a} = 0 \qquad \text{A.12}$$

where $\tau'_{r\theta}$ is the dimensional stress, a is the radius of the bubble and $\left.\frac{\partial\gamma'(\theta)}{\partial\theta}\right|_{r=a}$ is the dimensional surface tension gradient on the surface of the bubble.

Tthe equation of state obtained from Langmuir isotherm and Gibbs Duhmen equation (refer equations 3.12 and 3.14 in chapter 3) is

$$\gamma^{'} = \gamma_0 + RT\Gamma_\infty \ln(1 - \frac{\Gamma^{'}}{\Gamma_\infty}) \qquad \text{A.13}$$

Where T is the temperature, $\Gamma_\infty$ is maximum packing concentration, Γ' is the surface concentration and $\gamma_0$ is the surface tension of clean interface (with no adsorbed surfactant molecules)

Non-dimensionalizing shear stress ( $\tau_{r\theta}$ ) by viscous scale (μU/a) and surface tension (γ) by $\gamma_0$, where μ is the viscosity of the bulk liquid and U is the far field velocity of the translating bubble, we get

$$\gamma = 1 + \frac{RT\Gamma_\infty}{\gamma_0} \ln(1 - \Gamma) \qquad \text{A.14}$$

and

$$\sum_{n=2}^{\infty} 2B_n (2n-1) \frac{C_n^{-1/2}(\cos\theta)}{\sin\theta} - \frac{Ma}{1-\Gamma} \frac{\partial \Gamma}{\partial \theta} = 0 \qquad \text{A.15}$$

γ(θ) can be computed numerically, with the help of Legendre polynomial, $P_n$ as interpolating functions.

Let, $$\gamma(\theta) = \sum_{n=0}^{\infty} \omega_n P_n \qquad \text{A16}$$

Using the condition of orthogonality on Legendre Polynomials $P_n(\cos\theta)$, we get

$$\omega_n = \frac{2n+1}{2} \int_0^{\pi} \gamma(\theta) P_n(\cos\theta) \sin\theta \, d\theta \qquad \text{A17}$$

Therefore

$$\frac{\partial \gamma}{\partial \theta} = -\sum_{n=1}^{\infty} \omega_n \frac{n(n+1)}{\sin\theta} C_{n+1}^{-1/2}(\cos\theta) \qquad \text{A18}$$

Putting n+1= k in equation A.17, we get

$$\frac{\partial \gamma}{\partial \theta} = -\sum_{k=2}^{\infty} \omega_{k-1} \frac{k(k-1)}{\sin\theta} C_{k}^{-1/2}(\cos\theta) \qquad \text{A.19}$$

From equation A.16, we get

$$\omega_n = \frac{2k+1}{2} \int_0^{\pi} \left\{ 1 + \frac{RT\Gamma_{\infty}}{\gamma_0} \ln(1-\Gamma) \right\} P_k(\cos\theta) \sin\theta \, d\theta \qquad \text{for } k \geq 1 \qquad \text{A.20}$$

$$\omega_n = \left(\frac{2k+1}{2}\right) \frac{RT\Gamma_{\infty}}{\gamma_0} \int_0^{\pi} \ln(1-\Gamma) P_k(\cos\theta) \sin\theta \, d\theta \qquad \text{for } k \geq 1 \qquad \text{A.21}$$

Using equation A.14 and A.15, we get

$$B_k = \frac{(k-1)k}{2(2k-1)} \left(\frac{\gamma_0}{\mu U}\right) \omega_{k-1} \qquad \text{A.22}$$

Using equations A.21 and A.22, we get

$$B_k = \left(\frac{Ma \cdot k}{2}\right) \int_0^{\pi} \ln(1-\Gamma) P_{k-1}(\cos\theta) \sin\theta \, d\theta \qquad \text{for } k \geq 1 \qquad \text{A.23}$$

# BIBLOGRAPHY

[Acrivos & Goddard (1965)] ACRIVOS, A., GODDARD, J.D. *J. Fluid Mech.* 1965, **23**, 273-291.

[Aniansson & Wall (1974)] ANIANSSON, E.A.G., WALL, S. N., *The Journal of Physical Chemistry*,1974, **78**(10), 1024.

[Balasubramaniam, R. & Lavery (1989)]BALASUBRAMANIAM, R. & LAVERY, *J.*, *Numerical J. Heat Transfer A*, 1989, **16**, 175.

[Barton & Subramanian (1989)] BARTON, K.D., SUBRAMANIAN, R. S. *Journal of Colloid and Interface Science*, 1989, **133**, 211-222.

[Beard & Pruppacher (1969)] BEARD K.V., PRUPPACHER H.R. *Journal of The Atmospheric Sciences*,1969**, 26**, 1066-1072.

[Beitel & Heideger (1971)] BEITEL, A., HEIDEGER, W.J. *Chemical Engineering Science* 1971, **26**, 711-717.

[Bel Fdhila & Duineveld (1996)] BEL FDHILA, R., DUINEVELD, P. C. *Phys. Fluids* 1996**, 8**, 310-321.

[Bird et al (2001)] Bird, R.B., Stewart, W.E., Lightfoot, E.N, *Transport Phenomena*; Wiley, New York, 2001.

[Bond & Newton (1928)] BOND, W.N. AND NEWTON D.A., *Phil. Mag., 7th Series*, 1928, **5**, 794

[Chang et al (1998)] CHANG,C.H., HSU, C.T., LIN S.Y., *Langmuir*,1998,**14**,2476

[Chen & Stebe (1996)] CHEN, J., STEBE, K. *J. Colloid Interfacial Sci.* 1996, **178**, 144-155.

[Chen & Stebe (1997)] CHEN, J., STEBE, K. *J. Fluid Mech.* 1997, **340**, 35-60.

[Clift, Grace & Weber (1978)] CLIFT, R., GRACE, J.R., WEBER, M.E. *Bubbles, Drops and Particles*; Academic Press: New York, 1978.

[Coe & Godfrey (1944)] COE, J.R,GODFREY T.B, *Journal of Applied Physics*, 1944;**15**, 625.

[Colegate & Bain (2005)] D. COLEGATE,D., BAIN,C., *Phys. Rev. Lett*. 2005**, 95**, 198302.

[Danov et al (1996)] DANOV K.B., VLAHOSVSKA P.M., HOROZOV T, DUSHKIN C.D., KRALCHEVSKY, P.A., MEHRETEAB A, BROZE G, *Journal of Colloid and Interface Science*, 1996, **183**, 223-235.

[Davis & Acrivos (1966)] DAVIS, R. E., ACRIVOS, A. *Chemical Engineering Science* 1966, **21**, 681-685.

[Defay & Hommelen (1959)] DEFAY, R., HOMMELEN, J.R., *Journal of Colloid Science*,1959, **160**, 411-418.

[Deryagin, Dukhin & Lisichenko(1959)] DERYAGIN, B. V., DUKHIN, S.S., LISICHENKO, V.A. *Russ. J. Phys. Chem* 1959, **33**, 389-393.

[Duineveld(1994)] DUINEVELD, P. C. *Bouncing and Coalescence of Two Bubbles in Water*; University of Twente, 1994.

[Dunkin & Buikov (1965)] DUNKIN,S.& BUIKOV, M., *Russian Journal of Physical Chemistry*,1965,**39**,482-485

[Elzinga & Banchero (1961)] ELZINGA, E. R., BANCHERO, J. T. *AIChE J.* 1961, **7**, 394-399.

[Fainerman (1981)] FAINERMAN V.B., *Kolloidn. Zh.* 1981, **43**, 94–100.

[Frössling (1938)] Frössling, N., *Gerlands Beitage zur Geophysik.* 1938, **52**, 170–216

[Frumkin & Levich (1947)] FRUMKIN, A.; LEVICH, V. *Zhur. Fiz. Khim.* 1947, **21**, 1183.

[Griffith (1962)] GRIFFITH, R. M. *Chemical Engineering Science* 1962, **17**, 1057-1070.

[Haberman & Morton (1954)] HABERMAN, W. L., MORTON, R.K. *Proc. Am. Soc. Civ. Eng* 1954, **387**, 227-252.

[Hadamard (1911)] HADAMARD, J., Compr. Rend. Acad. Sci., 1911, **152**, 1735

[Harper (1972)] HARPER,J., *Adv* Appl. *Mech.*,1972,**12**,59-129

[Harper (1973)] HARPER, J. F. *J. Fluid Mech.* 1973, **58**, 539-545.

[Harper (1974)] HARPER, J. F. *Q. J Mech. Appl. Math.* 1974, **27**, 87-100.

[Harper (1982)] HARPER, J. F. *Sci. Res.* 1982, **38**, 343-351.

[He, Maldarelli & Dagan (1991)] HE, Z., MALDARELLI, C., DAGAN, Z. *Journal of Colloid and Interfacial Science* 1991, **146**, 442-451.

[Holbrook & Levan (1983a)] HOLBROOK, J. A., LEVAN, M. D. *Chem. Engr. Commun.* 1983a, **20**, 191-207.

[ Holbrook & Levan (1983b)] HOLBROOK, J. A., LEVAN, M. D. *Chem. Engr. Commun.* 1983b, **20**, 273-290.

[Horton, Fritsch & Kintner(1965)] HORTON, T. J., FRITSCH, T. R, KINTNER, R. C. *Can. J. Chem. Engr.* 1965, **43**, 143-146.

[Jennings & Pallas (1988)] JENNINGS, J.W.,JR.; PALLAS, N.R., *Langmuir,* 1988;**4**, 959.

[Joos & Serrien (1989)] JOOS, P., SERRIEN, G., *Journal of Colloids and Interface Science*,1989, **127**, 97-103.

[Kim & Subramanian (1989a)]KIM, H., SUBRAMANIAN, R. *J. Colloid and Int. Sci.* 1989a, **127**, 417-430.

[Kim & Subramanian (1989b)] KIM, H., SUBRAMANIAN, R. *J. Colloid and Int. Sci.* 1989b, **130**, 112-125.

[Korosi & Fabuss (1968)] KOROSI,A., FABUSS, B.M., *Analytical Chemistry*, 1968;**40**, 157.

[Korson, Hansen & Millero (1969)] KORSON,L., HANSEN, W.D., MILLERO,F.J., *The Journal of Physical Chemistry*, 1969;**73**, 34-39.

[Levan & Newman (1976)] LEVAN, M., NEWMAN, J *AIChE J.* 1976, **22**, 695-701.

[Levich (1962)] LEVICH *Physicochemical Hydrodynamics.*; Prentice Hall:, 1962.

[Lin et al (1995)] LIN S.Y, CHEN L.J, XYU J.W, WANG W.J, *Langmuir*, 1995;**11**, 4159-4166.

[Lin et al (1996)] LIN SY., WANG W.J, LIN L.W, CHEN L.J., *Colloids and Surfaces A: Physicochemical and Engineering Aspects*, 1996;**114**,31-39

[Lin (1997)] LIN, S.Y. ET. AL. *Langmuir,*1997, **13**, 6211-6218.

[Lucassen (1968)] LUCASSEN, J, *Trans. Faraday Soc.* 1968, **64**,2221-2230.

[Lucassen (1976)] LUCASSEN J., *Faraday Discuss. Chem. Soc.* 1976, **59**,76.

[Lucassen & Barnes (1972)] LUCASSEN, J AND BARNES, G.T., *J. Chem. Soc. Faraday I* 1972, **68**,2129.

[Lucassen & Giles (1975)] LUCASSEN, J AND GILES, D., *ibid* 1975, **71**,217.

[Magnaudet, Rivero & Fabre (1995)] MAGNAUDET, J., RIVERO, M., FABRE, J. *J. Fluid Mech.* 1995, **284**, 97-135.

[Merritt & Subramanian (1988)] MERRITT, R.M., SUBRAMANIAN, R. S. *Journal of Colloid and Interface Science*, 1989, **125(1)**, 333-339.

[Miller (1981)] MILLER R., Adsorption kinetics of surfactants from micellar solutions, Colloid Polymer Science, 1981, **259,** 1124–1128.

[Nallani & Subramanian (1993)] NALLANI, M., SUBRAMANIAN, R. S. *Journal of Colloid and Interface Science*, 1993, **157(1)**, 24-31.

[Nikolov & Wasan (1995)] NIKOLOV, A.D. AND WASAN, D.T., *Ind. Eng. Res.* 1995, **34**, 3653-3661

[Palaparthi (2001)] PALAPARTHI,R, *Effect of Surfactant Transport on the Mobility of Bubbles in Liquids-An Experimental and Computational Study*, The City University of New York, 2001

[Palaparthi et al (2005)] PALAPARTHI, R.,PAPAGEORGIOU,D.T.,BALASUBRAMANIAN, R,MALDARELLI,C, "Experimental Verification of the Remobilization of Surfactant Retarded Interfaces",*Journal of Colloid andInterface Science*, 2005 (*Submitted*)

[Palaparthi et al (2006)] PALAPARTHI, R.,PAPAGEORGIOU,D.T.,BALASUBRAMANIAN, R,MALDARELLI,C, *Journal of Fluid Mechanics*, 2006;**559**, 1-44

[Pan, Green & Maldarelli (1998)] PAN, R., GREEN, J., MALDARELLI, C. *Journal of Colloid and Interfacial Science* 1998, **205**, 213-230.

[Papazian & Wilcox (1978)] PAPAZIAN, J.M., WILCOX, W.R. *AIAA J.* 1978, **16,** 447-45.

[Patankar (1980)] PATANKAR S.V. ,*Numerical Heat Transfer and Fluid Flow*, Hemisphere Publishers,1980

[Payne & Pell (1960)] Payne, L.E. AND PELL, W.H. *J. Fluid Mech.* 1960, **7**, 529-549.

[Pruppacher & Steinberger (1968)] PRUPPACHER H.R., STEINBERGER E.H. *Journal of Applied Physics*,1968, **39**, 4129-4132.

[Peyret & Taylor (1983)] PEYRET, R.; TAYLOR, T. D. *Computational methods for fluid flow.*, 1983.

[Raymond & Zieminski (1971)] RAYMOND, D. R.; ZIEMINSKI, S. A. *AIChEJ* 1971, **17**, 57-65.

[Rybczynski (1911)] RYBCZYNSKI, W., *Polska Akademja Umiejetnosci Krakow Wydzial Matemyczno-Przetroniczy, Series A*, 1911, **40**, 403

[Sadhal & Johnson (1982)] SADHAL, S., JOHNSON, R. *J. Fluid Mech.* 1982, **126**, 237-250.

[Savic (1953)] SAVIC, P. *Nat. Res. Counc. Can. Div. Mech. Engng Rep.* **MT-22** 1953. 36- 37)

[Saville (1973)] SAVILLE, D. *Chem. Engr. J.* 1973, **5**, 251-259.

[Stebe, Lin & Maldarelli (1991)] STEBE, K. J., LIN, S. Y., MALDARELLI, C *Phys. Fluids A.* 1991, **3**, 3-20.

[Stebe & Maldarelli (1994)] STEBE, K. J., MALDARELLI, C. *Journal Of Colloid and Interface Science* 1994, **163**, 177-189.

[Subramanian, Chabra & DeKee (1992)] SUBRAMANIAN, R. S. ; CHABRA, R. P. and DEKEE, D., Ed.; Hemisphere Publishing: New York, 1992, pp 1-42.

[Song et al (2006)] SONG, Q., COUZIS, A., SOMASUNDARAN, P. AND MALDARELLI, C., Colloids and Surfaces A: Physicochem. Eng. Aspects 2006, **282–283**, 162–18

[Takemura & Yabe (1999)] TAKEMURA, F., YABE, A. *J. Fluid Mech.* 1999, **378**, 319-334.

[Wang, Papageorgiou, & Maldarelli (1999)] WANG, Y., PAPAGEORGIOU, D. T., MALDARELLI, C. *J. Fluid Mech.* 1999, **390**, 251-270.

[Takemura (2005)] TAKEMURA, F.,*Phys. of Fluids.*2005, **17**, 048104.

[Wang, Papageorgiou, & Maldarelli (1999)] WANG, Y., PAPAGEORGIOU, D. T., MALDARELLI, C. *J. Fluid Mech.* 1999, **390**, 251-270.

[Wang, Papageorgiou, & Maldarelli (2001)] WANG, Y., PAPAGEORGIOU, D., MALDARELLI, C. *J. Fluid Mech.* 2001, **453**, 1-19.

[Wasserman & Slattery (1969)] WASSERMAN, M.L. AND SLATTERY, J.C., *AICHE J.*1969,**15**, 533

[Ybert & Megilo (2000)] YBERT, C. & MEGILO, J.D., *Eur. Phys.J.* 2000, **3**, 143-148

[Zhang, McLaughlin, & Finch (2001)] ZHANG, Y., MCLAUGHLIN,J.B., FINCH, J.A.*Chem. Engng. Sci* 2001, **56,** 6605-6616.